Sediment Profile Imaging Report

June 2014

Characterization of the Lower Willamette River with Sediment Profile Imaging: Changes in Space & Time



Prepared for

de maximis, inc.
2203 Timberloch Place, Suite 213
The Woodlands, TX 37919

Project Number 3190J
P.O Number 3190J112713

Prepared by

Germano & Associates, Inc.
12100 SE 46th Place
Bellevue, WA 98006

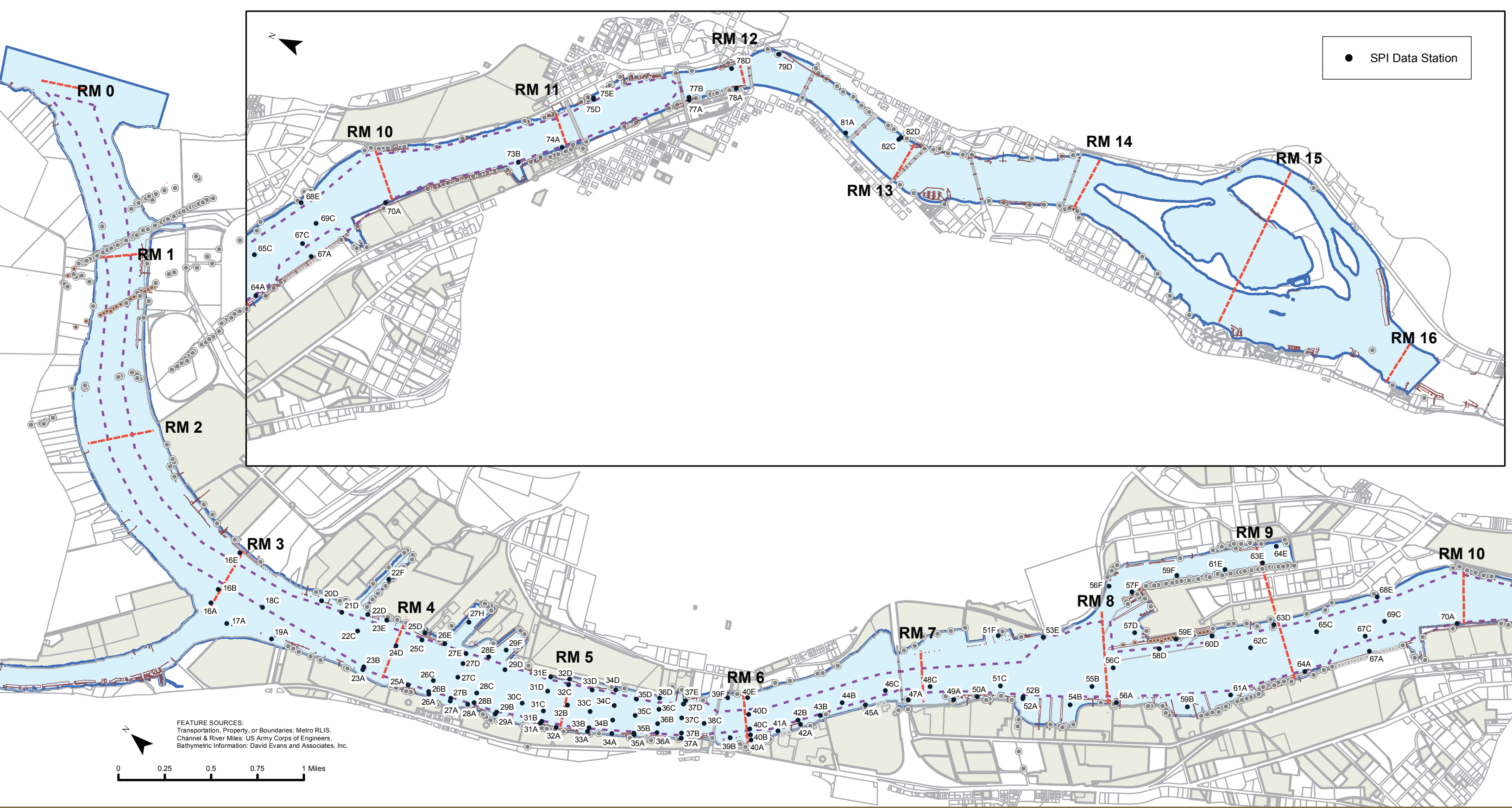

Sediment Profile Imaging Report

CHARACTERIZATION OF THE LOWER WILLAMETTE RIVER WITH SEDIMENT PROFILE IMAGING: CHANGES IN SPACE & TIME

Prepared for

de maximis, inc.
2203 Timberloch Place, Suite 213
The Woodlands, TX 37919

Project Number 3190J
P.O Number 3190J112713

Prepared by

Germano & Associates, Inc.
12100 SE 46th Place
Bellevue, WA 98006

July, 2014

TABLE OF CONTENTS

LIST OF FIGURES

1.0 INTRODUCTION

In December, 2001, a Sediment Profile Imaging (SPI) survey was conducted by Germano & Associates (G&A) in the Lower Willamette River (LWR) under contract to Striplin Environmental Associates (SEA) as part of the preliminary investigations for the Portland Harbor Remedial Investigation/Feasibility Study (RI/FS) for the Lower Willamette Group (LWG). The purpose of that initial reconnaissance survey in 2001 was to provide information on the physical and biological features of the surface sediments in the river from Ross Island to the Columbia River; a total of 478 stations were sampled from river mile (RM) 0 (the Willamette's confluence with the Columbia River) upstream to RM 15.7 (the upstream edge of Ross Island). The results of this 2001 SPI survey (SEA, 2002) were combined with other Phase 1 sampling efforts in order to develop an effective approach for the RI/FS for sediments in the LWR.

In December, 2013, some of the original reconnaissance survey locations were re-sampled with SPI technology along a 10 mile stretch of the LWR to characterize current conditions in the river sediments and to document what changes had occurred at these locations in the ensuing 12 years since the initial characterization; of particular interest for this survey were any changes in conditions at stations covering River Miles 4 and 5. While the 2001 survey sampled stations between RM 0 to RM 15.7, the 2013 survey sampled a subset (128) of these same stations between RM 3 to RM 13. The 2013 objectives were to characterize current sediment conditions in the LWR by collecting the following quantitative and qualitative information and comparing these results to those from 2001:

- Indications of aerobic and/or anaerobic conditions in surface sediments
- Indications of sediment physical conditions: sediment grain-size major mode and range, and relative shear strength
- Indications of sediment chemical and biological conditions: depth of the mean apparent redox potential discontinuity (aRPD), evidence of excess organic enrichment and the presence of sedimentary methane, the composition of the benthic community and evidence (if any) of disturbance gradients in the community

From a standpoint of benthic habitat quality, the key parameters of interest were signs of excess organic enrichment (a negative indication), depth of the aRPD from biological mixing (a positive indication), and any dramatic change in infaunal successional stage as compared with conditions that existed in 2001.

2.0
MATERIALS AND METHODS

Between December 2-7, 2013, under contract to de maximis, inc., scientists from G&A performed an SPI survey in the LWR aboard the R/V Nancy Ann, owned and operated by Marine Sampling Services of Burley, WA. An Ocean Imaging Systems Model 3731 sediment profile camera was used for this survey; a total of 561 sediment profile images were collected at 128 stations during the course of the week (Figure 1).

The sediment profile camera works like an inverted periscope. A Nikon D7000 16.2-megapixel SLR camera with two 16-gigabyte secure digital (SD) memory cards is mounted horizontally inside a watertight housing on top of a wedge-shaped prism. The prism has a Plexiglas® faceplate at the front with a mirror placed at a 45° angle at the back. The camera lens looks down at the mirror, which is reflecting the image from the faceplate. The prism has an internal strobe mounted inside at the back of the wedge to provide illumination for the image; this chamber is filled with distilled water, so the camera always has an optically clear path. This wedge assembly is mounted on a moveable carriage within a stainless steel frame. The frame is lowered to the seafloor on a winch wire, and the tension on the wire keeps the prism in its “up” position. When the frame comes to rest on the seafloor, the winch wire goes slack and the camera prism descends into the sediment at a slow, controlled rate by the dampening action of a hydraulic piston so as not to disturb the sediment-water interface. On the way down, it trips a trigger that activates a time-delay circuit of variable length (operator-selected) to allow the camera to penetrate the seafloor before any image is taken (Figure 2). The knife-sharp edge of the prism transects the sediment, and the prism penetrates the bottom. The strobe is discharged after an appropriate time delay to obtain a cross-sectional image of the upper 20 cm of the sediment column. The resulting images give the viewer the same perspective as looking through the side of an aquarium half-filled with sediment. After the first image is obtained at the first location, the camera is then raised up about 2 to 3 meters off the bottom to allow the strobe to recharge; a wiper blade mounted on the frame removes any mud adhering to the faceplate. The strobe recharges within 5 seconds, and the camera is ready to be lowered again for a replicate image. Surveys can be accomplished rapidly by “pogo-sticking” the camera across an area of seafloor while recording positional fixes on the surface vessel.

Two types of adjustments to the SPI system are typically made in the field: physical adjustments to the chassis stop collars or adding/subtracting lead weights to the chassis to control penetration in harder or softer sediments, and electronic software adjustments to the Nikon D7000 to control camera settings. Camera settings (f-stop, shutter speed, ISO equivalents, digital file format, color balance, etc.) are selectable through a water-tight USB port on the camera housing and Nikon Control Pro® software. At the beginning of the survey, the time on the sediment profile camera's internal data logger was synchronized with the internal clock on the computerized navigation system to local time.

Details of the camera settings for each digital image are available in the associated parameters file embedded in the electronic image file; for this survey, the ISO-equivalent was set at 640. The additional camera settings used were as follows: shutter speed was 1/250, f9, white balance set to flash, color mode to Adobe RGB, sharpening to none, noise reduction off, and storage in compressed raw Nikon Electronic Format (NEF) files (approximately 20 MB each). Electronic files were converted to high-resolution jpeg (8-bit) format files (3264 x 4928 pixels) using Nikon Capture NX2® software (Version 2.2.7).

A minimum of four replicate images were taken at each station; each SPI replicate is identified by the time recorded on the digital image file in the camera and on disk along with vessel position on the navigation computer. The unique time stamp on the digital image was then cross-checked with the time stamp in the navigational system's computer data file. The field crew kept redundant written sample logs. Images were downloaded periodically (sometimes after each station) to verify successful sample acquisition or to assess what type of sediment/depositional layer was present at a particular station. Digital image files were re-named with the appropriate station name immediately after downloading on deck as a further quality assurance step.

Test exposures of the Kodak® Color Separation Guide (Publication No. Q-13) were made on deck at the beginning and end of each survey to verify that all internal electronic systems were working to design specifications and to provide a color standard against which final images could be checked for proper color balance. A spare camera and charged battery were carried in the field at all times to insure uninterrupted sample acquisition. After deployment of the camera at each station, the frame counter was checked to make sure that the requisite number of replicates had been taken. In addition, a prism penetration depth indicator on the camera frame was checked to verify that the optical prism had actually penetrated the bottom to a sufficient depth. If images were missed (frame counter indicator or verification from digital download) or the penetration depth was insufficient (penetration indicator), chassis stops were adjusted and/or weights were added or removed, and additional replicate images were taken. Changes in prism weight amounts, the presence or absence of mud doors, and chassis stop positions were recorded for each replicate image. Images were inspected at high magnification to determine whether any stations needed resampling with different stop collar or weight settings.

Following completion of the field operations, the raw NEF image files were converted to high-resolution Joint Photographic Experts Group (jpeg) format files using the minimal amount of image file compression. Once converted to jpeg format, the intensity histogram (RGB channel) for each image was adjusted in Adobe Photoshop® to maximize contrast without distortion. The jpeg images were then imported to Sigmascan Pro® (Aspire Software International) for image calibration and analysis. Calibration information was determined by measuring 1-cm gradations from the Kodak® Color Separation Guide.

This calibration information was applied to all SPI images analyzed. Linear and area measurements were recorded as number of pixels and converted to scientific units using the calibration information.

Measured parameters were recorded on a Microsoft® Excel© spreadsheet. G&A's senior scientist (Dr. J. Germano) subsequently checked all these data as an independent quality assurance/quality control review of the measurements before final interpretation was performed.

2.1 MEASURING, INTERPRETING, AND MAPPING SPI PARAMETERS

2.1.1 Sediment Type

The sediment grain-size major mode and range were visually estimated from the color images by overlaying a grain-size comparator that was at the same scale. This comparator was prepared by photographing a series of Udden-Wentworth size classes (equal to or less than coarse silt up to granule and larger sizes) with the SPI camera. Seven grain-size classes were on this comparator: >4 ϕ (silt-clay), 4 - 3 ϕ (very fine sand), 3-2 ϕ (fine sand), 2 - 1 ϕ (medium sand), 1-0 ϕ (coarse sand), 0 - (-1) ϕ (very coarse sand), < -1 ϕ (granule and larger). The lower limit of optical resolution of the photographic system was about 62 microns, allowing recognition of grain sizes equal to or greater than coarse silt (≥ 4 ϕ). The accuracy of this method has been documented by comparing SPI estimates with grain-size statistics determined from laboratory sieve analyses (Germano et al. 2011).

The comparison of the SPI images with Udden-Wentworth sediment standards photographed through the SPI optical system was also used to map near-surface stratigraphy such as sand-over-mud and mud-over-sand. When mapped on a local scale, this stratigraphy can provide information on relative transport magnitude and frequency.

2.1.2 Prism Penetration Depth

The SPI prism penetration depth was measured from the bottom of the image to the sediment-water interface. The area of the entire cross-sectional sedimentary portion of the image was digitized, and this number was divided by the calibrated linear width of the image to determine the average penetration depth. Linear maximum and minimum depths of penetration were also measured. All three measurements (maximum, minimum, and average penetration depths) were recorded in the data file.

Prism penetration is a noteworthy parameter; if the number of weights used in the camera is held constant throughout a survey, the camera functions as a static-load penetrometer.

Comparative penetration values from sites of similar grain size give an indication of the relative water content of the sediment. Highly bioturbated sediments and rapidly accumulating sediments tend to have the highest water contents and greatest prism penetration depths.

The depth of penetration also reflects the bearing capacity and shear strength of the sediments. Over consolidated or relic sediments and shell-bearing sands resist camera penetration. Highly bioturbated, sulfitic, or methanogenic muds are the least consolidated, and deep penetration is typical. Seasonal changes in camera prism penetration have been observed at the same station in other studies and are related to the control of sediment geotechnical properties by bioturbation (Rhoads and Boyer 1982). The effect of water temperature on bioturbation rates appears to be important in controlling both biogenic surface relief and prism penetration depth (Rhoads and Germano 1982).

2.1.3 Small-Scale Surface Boundary Roughness

Surface boundary roughness was determined by measuring the vertical distance between the highest and lowest points of the sediment-water interface. The surface boundary roughness (sediment surface relief) measured over the width of sediment profile images typically ranges from 0.02 to 3.8 cm, and may be related to either physical structures (ripples, rip-up structures, mud clasts) or biogenic features (burrow openings, fecal mounds, foraging depressions). Biogenic roughness typically changes seasonally and is related to the interaction of bottom turbulence and bioturbational activities.

The camera must be level in order to take accurate boundary roughness measurements. In sandy sediments, boundary roughness can be a measure of sand wave height. On silt-clay bottoms, boundary roughness values often reflect biogenic features such as fecal mounds or surface burrows. The size and scale of boundary roughness values can have dramatic effects on both sediment erodibility and localized oxygen penetration into the bottom (Huettel et al., 1996).

2.1.4 Mud Clasts

When fine-grained, cohesive sediments are disturbed, either by physical bottom scour or faunal activity, e.g., decapod foraging, intact clumps of sediment are often scattered about the seafloor. These mud clasts can be seen at the sediment-water interface in SPI images. During analysis, the number of clasts can be counted, the diameter of a typical clast was measured, and their oxidation state assessed. The abundance, distribution, oxidation state, and angularity of mud clasts also can be used to make inferences about the recent pattern of sedimentary disturbance in an area.

Depending on their place of origin and the depth of disturbance of the sediment column, mud clasts can be reduced or oxidized. In SPI images, the oxidation state is apparent from the reflectance; see Section 2.1.5. Also, once at the sediment-water interface, these mud clasts are subject to bottom-water oxygen concentrations and currents. Evidence from laboratory microcosm observations of reduced sediments placed within an aerobic environment indicates that oxidation of reduced surface layers by diffusion alone is quite rapid, occurring within 6 to 12 hours (Germano 1983). Consequently, the detection of reduced mud clasts in an obviously aerobic setting suggests a recent origin. The size and shape of the mud clasts are also revealing; some clasts seen in the profile images are artifacts caused by the camera deployment (mud clots falling off the back of the prism or the wiper blade). Naturally-occurring mud clasts may be moved and broken by bottom currents and animals (macro- or meiofauna; Germano 1983). Over time, these naturally-occurring, large angular clasts become small and rounded.

2.1.5 Apparent Redox Potential Discontinuity Depth

Aerobic near-surface freshwater sediments typically have higher reflectance relative to underlying hypoxic or anoxic sediments. Surface sands washed free of mud also have higher optical reflectance than underlying muddy sands. These differences in optical reflectance are readily apparent in SPI images; the oxidized surface sediment contains particles coated with ferric hydroxide (an olive or tan color when associated with particles), while reduced and muddy sediments below this oxygenated layer are darker, generally gray to black. The boundary between the colored ferric hydroxide surface sediment and underlying gray to black sediment is called the apparent redox potential discontinuity (RPD).

The depth of the apparent RPD in the sediment column is an important time-integrator of dissolved oxygen conditions within sediment pore waters. In quiescent freshwater systems such as lakes, the absence of bioturbating organisms will limit the depth of this high reflectance layer in fine-grained silt/clays to a thickness of 2 mm below the sediment-water interface (Rhoads 1974). This depth is related to the supply rate of molecular oxygen by diffusion into the bottom and the consumption of that oxygen by the sediment and associated micro flora. In sediments that have very high sediment oxygen demand (SOD), the sediment may lack a high reflectance layer even when the overlying water column is aerobic.

This vertical zonation of redox stratification results from the oxidation of organic matter by a series of increasingly less energetically-favorable terminal electron acceptors, e.g., O_2, NO_3, Mn(IV), Fe (III), and SO_4^{-2} (Froelich et al., 1979). Typically, zones of Mn and Fe oxide (FMO) enrichment are present just below the oxic surface layers of sediment; Mn(IV) and Fe(III) form sparingly soluble oxides, which reductively dissolve to produce much more soluble Mn(II) and Fe(II). Therefore, accumulation of FMO just below the oxic zone is caused by Mn(II) and Fe(II) diffusing upwards from deeper, more reduced sediment zones and reacting with oxygen or nitrate diffusing downward from overlying oxic lake or pore waters (Koretsky et al., 2006). Redox zonation is influenced by many things besides this transport via diffusion of dissolved solutes, including macrophyte activity and transport of solutes and particles via bio-irrigation and bioturbation. The relative sizes of these redox zones are affected by the interaction of numerous factors, including temperature, hydrology, lake turnover, mixing by river currents, and macrophytes and macrofaunal activity, all of which can vary on a seasonal basis and influence the balance between organic matter and terminal electron acceptor availability (Davison, 1993; Sherman et al., 1994; Urban et al, 1997).

The relationship between the thickness of this high reflectance layer and the presence or absence of free molecular oxygen in the associated pore waters must be considered with caution. The actual RPD is the boundary or horizon that separates the positive Eh region of the sediment column from the underlying negative Eh region. The exact location of this Eh = 0 boundary can be determined accurately only with microelectrodes; hence, the relationship between the change in optical reflectance, as imaged with the SPI camera, and the actual RPD can be determined only by making the appropriate *in situ* Eh measurements. For this reason, the optical reflectance boundary, as imaged, was described in this study as the “apparent” RPD (aRPD) and it was mapped as a mean value. In general, the depth of the actual Eh = 0 horizon will be either equal to or slightly shallower than the depth of the optical reflectance boundary (Rosenberg et al., 2001). This is because bioturbating organisms can mix ferric hydroxide-coated particles downward into the bottom below the Eh = 0 horizon. Depending on hydrodynamics, the apparent mean RPD depth can be used either as an estimate of the depth of pore water exchange, usually through pore water irrigation from hydraulic flow or bio-irrigation, or an indication of sediment accumulation from rapid deposition of re-suspended, oxidized particles in fluvial systems.

Measurable changes in the aRPD depth using the SPI optical technique can be used effectively to document changes (or gradients) that develop over a seasonal or yearly cycle in river or lake systems related to changes in flow regime (rivers), water stratification/mixing (lakes), temperature effects on bioturbation rates, seasonal hypoxia, SOD, and infaunal recruitment. Time-series aRPD measurements following a disturbance can be a critical diagnostic element in monitoring the degree of recolonization in an area by the ambient benthos (Rhoads and Germano 1986).

The apparent mean RPD depth also can be affected by local erosion; scouring around curves in rivers can wash away fines and form shell or gravel lag deposits, resulting in very thin surface oxidized layer. Storm energy or heavy winds in shallow areas of lakes or rivers can cause erosion of the oxidized surface layers, effectively removing any evidence of an aRPD.

Another important characteristic of the aRPD is the contrast in reflectance at this boundary. This contrast is related to the interactions among the degree of organic loading, the physical or biological mixing depth of the sediment, the concentrations of bottom-water dissolved oxygen in an area, and localized sediment geochemistry. High inputs of labile organic material increase SOD and, subsequently, sulfate reduction rates and the associated abundance of sulfide end products. This results in more highly reduced, lower-reflectance sediments at depth and higher aRPD contrasts. In a region of generally low aRPD contrasts, images with high aRPD contrasts indicate localized sites of relatively large inputs of organic-rich material such as phytoplankton, other naturally-occurring organic detritus, or anthropogenic impacts (industrial or sewage run-off or discharge).

Because the determination of the aRPD requires discrimination of optical contrast between oxidized and reduced particles, it is difficult, if not impossible, to determine the depth of the aRPD in well-sorted sands of any size that have little to no silt or organic matter in them (Painter et al, 2007). When using SPI technology on sand bottoms, little information other than grain-size, prism penetration depth, and boundary roughness values can be measured; while oxygen has no doubt penetrated the sand beneath the sediment-water interface just due to physical forcing factors acting on surface roughness elements (Ziebis et al., 1996; Huettel et al., 1998), estimates of the mean aRPD depths in these types of sediments are indeterminate with conventional white light photography.

2.1.6 Sedimentary Methane

Free gases in sediments (typically hydrogen sulfide or methane, and sometimes carbon dioxide or traces of nitrogen or ammonia) are formed from either diagenetic bacterial reactions or migration of thermally-derived gases from greater depths. All of these gases are formed by microbial communities metabolizing organic substrates; therefore, presence of gas is an indicator of organic-rich sediments. If oxygen is available in the overlying waters and pore waters, an aerobic bacterial community dominates and carbon dioxide is the end product of their metabolism; generally, carbon dioxide will diffuse upward into the water column and rarely reaches concentrations high enough for a free gas phase to develop (Middleton, 2003). If organic loading is extremely high and pore water sulfate is depleted, then methanogenesis will occur. Because sulfate concentrations are low in freshwater sediments (in contrast to marine or alkaline waters), methanogenesis is a much more common occurrence in freshwater sediments. Two competing bacterial reactions generate free methane gas in sediments, one for anaerobic acetate (or similar) fermentation ($CH_3COOH \rightarrow CH_4 + CO_2$) and the other from carbon dioxide reduction ($CO_2 + 4H_2 \rightarrow CH_4 + 2H_2O$). In general, CO_2 reduction is dominant in marine sediments while fermentation reactions are the dominant ones in freshwater environments, although in all cases both reactions operate to some extent (Clayton, 1995).

The process of methanogenesis is indicated by the appearance of methane bubbles in the sediment column. These gas-filled voids are readily discernable in SPI images because of their irregular, generally circular aspect and glassy texture (due to the reflection of the strobe off the gas bubble).

2.1.7 Infaunal Successional Stage

The mapping of infaunal successional stages is readily accomplished in marine environments with SPI technology (Rhoads and Germano, 1982, 1986; Germano et al. 2011). While there are relatively few applications of SPI technology in freshwater environments (Boyer and Hedrick 1989; Boyer and Shen, 1988; Boyer and Whitlatch 1989) as compared with those in marine (Solan et al. 2003), there have been sufficient studies on benthic recolonization in freshwater (Tevesz, 1985; Soster and McCall, 1990a, b) to provide a basis for biological community interpretation of sediment profile images in freshwater systems.

While an early study by Moon (1935) in Lake Windemere (UK) was not focused specifically on recolonization patterns, he did show that the fauna collected in trays of what initially was defaunated sediment were similar to those found on the natural bottom after 4 weeks' time. Soster and McCall (1990a) performed a series of tray recolonization experiments in western Lake Erie during different seasons of two successive years to examine recolonization patterns in freshwater benthos following a mortality-producing disturbance. Benthic communities in the trays remained different from the surrounding bottom anywhere from 2-14 months after the start of the experiment; recovery in the first year happened much quicker than in the second year of the experiment, in part due to differences in a high abundance of the oligochaete *Vejdovskyella intermedia* on the natural bottom the first year and its lack of abundance the second year of the experiment. Three species of opportunists (*Physocrypia globula* [an ostracod], *V. intermedia* [a tubificid oligochaete], and a *Chironomus plumosus* [chironomid larvae]) colonized sediments quite rapidly and in disproportionately high numbers, but then suffered population declines later in the year. A second group of chironomids (*Procladius* sp. and *Coelotanypus* sp.) and naidid oligochaetes (*Specaria josinae*, *Dero digitata*, *Arcteonais lomondi*, and *Pristina acuminata*) colonized the tray sediments in approximate proportion to their abundances on the natural bottom. This group was followed by the late successional group of species consisting of pisidiid bivalves and the tubificid oligochaetes *Limnodrilus* spp., *Ilyodrilus templetoni*, and to some extent, *Aulodrilus piqueti*; this group gradually increased in abundance during the experiments and eventually dominated the tray communities.

The general pattern that emerged showed a characteristic response of the benthic community following a major disturbance on the lake floor during the spring or summer (Figure 3). The disturbed area is colonized by many of the same species present in undisturbed habitats on the natural bottom, but only one or a few species dominate the first few months; even though the taxonomic composition varied annually and seasonally, the opportunistic species mentioned earlier (*P. globula, V. intermedia,* and *C. plumosus*) were characteristic of this early assemblage. Over time, the assemblage gradually changed as slower colonizers increase in abundance and early colonizers decline. Some naidid oligochaetes, predatory chrinomids, and pididiid bivalves were also present in these late successional assemblages. Similar to recolonization patterns found in soft-bottom marine environments responding to disturbance (McCall, 1977; Rhoads et al., 1978; Pearson and Rosenberg, 1978), the life history characteristics of the early opportunists include small, mobile surface deposit feeders or suspension feeders that live at or near the sediment-water interface; their reproductive rate is high, and each species is capable of producing several generations a year, either because of short generation time (*P. globula*) or rapid asexual reproduction (*V. intermedia*). Late successional species were relatively deep infaunal dwellers that either deposit feed (tubificid oligochaetes) or filter feed (pisidiid bivalves) which grow slowly, mature later in life, and have generation times of at least one year (Soster and McCall, 1990a). Their adult body size is generally several times larger than that of early colonizers, they have infaunal life positions, and most of them reproduce sexually. The differences between these early and late successional assemblages are visible in sediment profile images.

While it may be that the response to disturbance by Lake Erie benthic communities is typical of sub littoral lacustrine benthos, there are relatively few additional studies with which to compare these results. Reviews of freshwater successional literature by Tevesz (1985) and Lopez (1988) describe similar characteristics of early and late successional stages during colonization of new lakes. Early successional stages are characterized by small, rapidly growing, suspension and surface deposit feeding taxa (*Chironomus*, naidid oligochaetes, and amphipods), and late successional stages are characterized by longer-lived, subsurface deposit-feeding tubificid oligochaetes. So, despite profound taxonomic differences between freshwater and marine benthos (freshwater muddy bottoms are dominated by chironomid insect larvae, amphipods, tubificid oligochaetes, and bivalves [McCall and Tevesz 1982] whereas marine muddy bottoms are dominated by polychaetes, amphipods, and different families of bivalves [Sanders 1968; Rhoads, 1974]), the successional patterns are functionally similar.

While the successional dynamics of invertebrate communities in freshwater lacustrine fine-grained sediments have been documented, the successional dynamics of invertebrate communities in sand and coarser sediments are not well-known. Subsequently, the insights gained from sediment profile imaging technology regarding biological community structure and dynamics in sandy and coarse-grained bottoms are fairly limited.

2.1.8 Biological Mixing Depth

During the past two decades, there has been a considerable emphasis on studying the effects of bioturbation on sediment geotechnical properties as well as sediment diagenesis (Ekman et al., 1981; Nowell et al., 1981; Rhoads and Boyer, 1982; Grant et al., 1982; Boudreau, 1986; 1994; 1998). However, an increasing focus of research is centering on the rates of contaminant flux in sediments (Reible and Thibodeaux, 1999; François et al., 2002; Gilbert et al., 2003), and the two parameters that affect the time rate of contaminant flux the greatest are erosion and bioturbation (Reible and Thibodeaux, 1999). The depth to which sediments are bioturbated, or the biological mixing depth, can be an important parameter for studying either nutrient or contaminant flux in sediments. While the apparent RPD is one potential measure of biological mixing depth, it is quite common in profile images to see evidence of biological activity (burrows, voids, or actual animals) well below the mean apparent RPD. Both the minimum and maximum linear distance from the sediment surface to both the shallowest and deepest feature of biological activity can be measured along with a notation of the type of biogenic structure measured. For this survey, the maximum biological mixing depth was measured.

2.2 DATA ANALYSIS METHODS

A variety of exploratory data analysis techniques were used to examine patterns in the SPI data in addition to simple scatter plots.

2.2.1 Box and Whisker plots

Box and whisker plots (a.k.a. boxplots) were used to illustrate the distribution of the data, providing information about the location and spread of the data as well as skewness. They are especially useful when several boxplots are placed side-by-side. Each boxplot has a shaded/colored rectangle that shows the spread of values between the 1st and 3rd quartiles (i.e., the 25th and 75th percentiles). The height of this box is the inter-quartile range (IQR) which is simply the value of the 3rd quartile minus the value of the 1st quartile. The line inside the box indicates the median; the outer brackets (the “whiskers”) are drawn to the nearest value not beyond a standard span from the quartiles; points outside the whiskers are possible extreme values and are shown as single lines. The standard span is 1.5 times the IQR from the nearest quartile. This standard span is a reasonable boundary to contain most (at least 90 percent) of the data from a Normal (Gaussian) distribution.

2.2.2 Data Transformations

The recorded SPI results contain data recorded on a variety of measurement scales: nominal, ordinal, interval, and ratio. Because different operational tests are allowable on different measurement scales, some of these data needed to be transformed so that stations could be compared either by box and whisker plots, scatter plots, or non-metric multi-dimensional scaling (see next section). The sediment grain size major mode category was converted to a rank according to Table 1. If there was a mixture of sediment types (noted in the final SPI data matrix with a "/") indicating a layered sediment, then the first class (the top layer of sediment) was used in the analysis and the dominant sediment major mode class interval reported among all replicate images was used as the station value.

Table 1. Rank Conversion for Sediment Grain-size

Assigned Rank	Grain Size major mode (phi units	Size Class Description
1	>4	silt-clay
2	4-3	very fine sand
3	3-2	fine sand
4	2-1	Medium sand
5	1-0	coarse sand
6	0 to -1	very coarse sand
7	< -1	granule and larger

Methane was not quantified comparably in the two surveys, so methane was incorporated as simply present or absent. Infaunal successional stage was converted to a rank according to Table 2.

Table 2. Rank Conversion for Successional Stage

Assigned Rank	Successional Stage
1	1
1.5	1->2
2	2
2.5	2->3
3	3
3	1 on 3
3	2 on 3
--	Indeterminate

2.2.3 Multi-dimensional Scaling

Non-metric multi-dimensional scaling (N-MDS) was also used to depict the similarities among stations based on a subset of the measured SPI parameters at each station. MDS is a method for creating a low dimensional picture of the relationships among stations in a complex, multi-dimensional situation. In N-MDS, only the rank order of entries in the distance matrix is assumed to contain the significant information. So the distances of the final configuration in the N-MDS plot should be in the same rank order as the original distances. Thus, the purpose of the N-MDS algorithm is to find a configuration of points whose rank ordered distances in k-dimensions reflect as closely as possible the rank order of the distances on the original data. Because the SPI data included a variety of data types (continuous as well as interval data), the Gower coefficient (Gower 1971) was used. For the Gower coefficient, ordinal categorical variables are replaced by their integer codes, and all of the variables are standardized by subtracting the minimum value and dividing by the range of the shifted values to produce a set of rescaled variables each with a new range [0, 1]. Without the normalizing effect of the standardization, the variables with the widest range and largest variability will automatically dominate the ordination results. The Gower coefficient of dissimilarity between two stations is calculated on the rescaled variables as the average of the variable-specific distances, each calculated as the absolute difference in values between two stations. For a given pairwise distance, all variables that have missing values (indeterminate values) for one or both stations are omitted from the average Gower coefficient. The Gower coefficient is averaged over all variables without missing values on a pairwise basis. The resulting coefficients are all within the interval [0,1].

The algorithm used to create the 2-dimensional configuration is Kruskal's N-MDS which attempts to find the ordination that minimizes stress. The stress formula used was Kruskal's f-stress (or stress formula 1; Kruskal and Wish 1978) and is equal to the square root of the ratio of the sum of squared differences between a monotonic transformation of the input distances and the plotted distances to the sum of the plotted distances squared. Essentially, the algorithm tries to maximize the rank correlation between the input distances and the plotted distances. The smaller the stress, the better the fit; rule of thumb values for Kruskal's f-stress consider values under 10 percent as "good" and values over 15 percent as "poor." (McCune and Grace 2002 after Kruskal 1964).

The nMDS configurations were generated using the *metaMDS* function in the *vegan* package (Oksanen et al. 2013) in R (R Core Team 2013). The Gower coefficients were calculated using the *daisy* function in the *cluster* package (Maechler et al. 2013).

2.3 USING SPI DATA TO ASSESS BENTHIC QUALITY & HABITAT CONDITIONS

While various measurements of water quality such as dissolved oxygen, contaminants, or nutrients are often used to assess regional ecological quality, interpretation is difficult because of the transient nature of water-column phenomena. Measurement of a particular value of any water-column variable represents an instantaneous "snapshot" that can change within minutes after the measurement is taken. By the time an adverse signal in the water column such as a low dissolved oxygen concentration is persistent, the system may have degraded to the point where resource managers can do little but map the spatial extent of the phenomenon while gaining a minimal understanding of factors contributing to the overall degradation.

The sediment column, on the other hand, is a long-term time integrator of sediment and overlying water quality; values for any variable measured are the result of physical, chemical, and biological interactions on time scales much longer than those present in a rapidly moving fluid. Sediments are therefore an excellent indicator of environmental quality, both in terms of historical impacts and of future trends for any particular variable.

Physical measurements made with the SPI system from profile images provide background information about gradients in physical disturbance (caused by dredging, disposal, oil platform cuttings and drilling muds discharge, ship prop wash in channels or in berthing areas, trawling, or storm resuspension and transport) in the form of maps of sediment grain size, boundary roughness, sediment textural fabrics, and structures. The concentration of organic matter and the SOD can be inferred from the optical reflectance of the sediment column and the apparent RPD depth. Organic matter is an important indicator of the relative value of the sediment as a carbon source for both bacteria and infaunal deposit feeders. SOD is an important measure of ecological quality; oxygen can be depleted quickly in sediment by the accumulation of organic matter and by bacterial respiration, both of which place an oxygen demand on the porewater and compete with animals for a potentially limited oxygen resource (Kennish 1986).

The apparent RPD depth is useful in assessing the quality of a habitat for epifauna and infauna from both physical and biological points of view. The apparent RPD depth in profile images has been shown to be directly correlated to the quality of the benthic habitat in polyhaline and mesohaline estuarine zones (Rhoads and Germano 1986; Revelas et al. 1987; Valente et al. 1992). Controlling for differences in sediment type and physical disturbance factors, apparent RPD depths < 1 cm can indicate chronic benthic environmental stress or recent catastrophic disturbance.

Soster and McCall (1990b) found that the spatial and temporal distributions of many of the infaunal macrobenthos in western Lake Erie were correlated with disturbance levels; species that were abundant late in the colonization sequence were more evenly distributed in the area surveyed, while early colonizers were usually more abundant in the more severely disturbed parts of the basin. These small, shallow-dwelling opportunists appeared to have suffered a higher mortality than larger, deeper-dwelling, late colonizers during unusually windy/high stress periods, but they are quick to recolonize the area after the disturbance abates. While comparing the fauna of mud bottom lakes created by water supply dams on the Sangamon River and its tributaries in Illinois, Gersbacher (1937) found that the taxa identified as early successional stages in the Soster and McCall (1990a) study were more frequently found in disturbed parts of the river, while the more stable areas contained faunas resembling those from older pools. Studies done in Lake George (Ganf and Viner 1973) found that chironomids and ostracods recovered most rapidly from disturbances; they were most abundant in the top 5 cm of disturbed sediment, while tubificids were more abundant in the 5-35 cm layer than in the 0-5 cm layer. If early and late successional assemblages are recognizable in freshwater sediment profile images, then inferences can be made about disturbance patterns affecting different regions of the area surveyed.

SPI has been shown to be a powerful reconnaissance tool that can efficiently map gradients in sediment type, biological communities, or disturbances from physical forces or organic enrichment. The conclusions reached at the end of this report are about dynamic processes that have been deduced from imaged structures; as such, they should be considered hypotheses available for further testing/confirmation.

3.0 RESULTS

A complete set of all the summary data measured from each image is presented in Appendix A; station coordinates from the navigation log are in Appendix B. Thumbnails of each image are available in the electronic version of the station map (Figure 1) in this report by putting the computer cursor over each station location; a DVD with high-resolution jpeg files of all sediment profile images collected was provided to the client soon after completion of the survey. While data measured from each image are shown in the appendix, the plotted values shown in the figures (maps) referenced in the sections below are station average values.

Parameters such as boundary roughness and mud clast data (number, size) provide supplemental information pertaining to the physical regime and bottom sediment transport activity at a site. Even though mud clasts are definitive characteristics whose presence can indicate physical disturbance of some form, the mud clasts seen in the profile images from this survey (Appendix A) were in the replicate images subsequent to the first camera lowering and were primarily sampling artifacts (mud shavings from the wiper blade, mud clots falling off the base frame, or clasts created from the frame impact on the bottom during the first camera lowering). Therefore, mud clast data are not discussed in any detail in the sections that follow.

The study area was originally divided into three different subareas in 2001 with different sampling densities:

- **Upper Willamette River (RM 9.7 to RM 15.7)**: A total of 24 cross-river transects were spaced 400 meters apart in 2001; in 2013, only 9 of these transects were re-occupied with a total of 13 stations sampled (Stations 70A – 82 D; Figure 1)
- **Portland Harbor Area (RM 3 to RM 9.7):** A total of 54 cross-river transects were spaced 200 meters apart in 2001; in 2013, 52 of these transects were re-occupied with a total of 115 stations sampled (Stations 16A – 69C; Figure 1)
- **Lower Willamette River (RM 0 to RM 3)**: A total of 16 cross-river transects were spaced 300 meters apart in 2001; none of these transects were re-sampled in 2013.

3.1 LWR Spatial Variation: Conditions in 2013

Results for each of the measured parameters will be presented starting with the survey area farthest upstream (RM 13) and proceeding downstream to the last transect sampled in the Portland Harbor area (RM 3); the results for each parameter are mapped over the entire stretch of the river surveyed in five panels (an overview followed by four close-up detailed panels) along with representative profile images to illustrate some of the descriptions in the text.

3.1.1 Grain Size

The spatial variation in sediment grain size major mode is shown in Figures 4a-e. The upper Willamette River naturally subdivides into two separate zones based on grain size results and river morphology (Figures 4b-c); between miles 11 and 13, the sediments were primarily silty very fine to fine sands, with some of the near shore locations being on cobble or rocky bottoms (Figure 5). Downstream of the Fremont Bridge, from miles 11 to 9.7, the river widens and the deeper areas of the main channel become more depositional (Figure 6), with silt-clay sediments predominating; however, some of the near shore areas showed alternating episodes of quiescent depositional periods of silt accumulation followed by bed load transport of sands (Figure 7).

Most of the locations in upper Portland Harbor (Figures 4c-d; RM 9.7 to RM 7) were fine grained, depositional areas dominated by silt-clays admixed with some very fine sands (Figure 8); more consolidated, sandier sediments could be found along the northern shore of the river in the shallow areas (Figure 9). Sediments were much more variable in middle Portland Harbor between RM 7 to 5, with near shore locations alternating between silt-clay (Stations 39A – 41A; Figure 4d) to layered sands (Stations 32A, 34D, and 45A; Figure 10) to hard pebble and rocky bottom (Station 36A, 37A, 36D, and 37E; Figure 11). Unlike the channel stations above RM7, those between RM5 to RM7 were mostly medium to fine sands (Figures 4d-e), with one channel station (46C) showing hard bottom (Figure 12).

Between RM 3 – RM5 in middle Portland Harbor, the channel widens and becomes depositional once more, with fine-grained sediments predominant at most stations in the channel (Figure 4e); as the river starts to bend to the north at Transect 19, flows increase and sandier sediments are dominant major mode (Figure 13).

3.1.2 Surface Boundary Roughness

Small-scale boundary roughness ranged from 0.38 – 4.16 cm throughout the 10 mile stretch of river surveyed (Figure 14 a-e), with an overall average site value of 1.31 cm. Not surprisingly, the greatest variation in boundary roughness values corresponded with the stretch of the river with the most variable sediment size distribution (RM5 – RM7;

Figure 14d); 78% of the roughness elements measured were due to biogenic alteration of the sediment surface (Appendix A). While some of the larger boundary roughness values were measured at locations where bottom currents had influenced the river bed, it was equally likely that stations experiencing strong bottom currents had been “flattened out” by erosive forces and therefore had relatively low boundary roughness values (Figure 15).

3.1.3 Prism Penetration Depth

Prism penetration varied throughout the site with a strong correlation to sediment grain size major mode (Figure 16a-e); greater penetration values were usually achieved at stations with finer sediments. The stop collars and weights were frequently adjusted to compensate for changes in sediment type (see Appendix A), and prism penetration values ranged from 0 (hard bottom/rocky stations) to 21.1 cm (over penetration in some of the softer sediments) with an overall site average value of 13.2 cm. Sediments in the upper Willamette River (Figure 16b) were bimodal in relative bearing strength, with about half the stations, e.g., 75D, 75E, 78D, 79D, 81A, on hard bottom allowing little to no penetration while the other half had relatively low bearing strength with both high water and methane content so that penetration values exceeded 15 cm (Figure 17).

The sediments below of the Fremont Bridge (RM 11) had higher water content smaller particle sizes, so prism penetration generally exceeded 10 cm (Figure 16c). Sediments and penetration depths were much more variable as one moves south of RM 7 (Figure 16d), with the area between Transects 48 and 35 showing the greatest variability in prism penetration depth over the whole survey area. Softer sediments appear in the main channel below RM5 except along some of the near shore areas, with transitions to sandy, harder bottoms and lower penetration values in the arc of stations starting with 19A and continuing along the western bank of the river up through Station 16E (Figure 16e).

3.1.4 Apparent Redox Potential Discontinuity Depth

The distribution of mean apparent RPD depths is shown in Figure 18(a-e); values throughout the site ranged from 0.4 – 4.6 cm, with an overall site average of 2.7 cm. In the near shore areas between RM 13 to RM 11 at those locations where the camera could penetrate the sediments sufficiently, aRPD depths were higher than the overall site average (Figure 18b), with a well-developed surface oxidized layer due to the bioturbational activities of the resident deposit-feeding infauna (Figure 19).

Below the Fremont Bridge, aRPD values continue to be above the overall site average with resident infauna actively reworking the upper sediment column (Figure 18c). Moving below RM7, aRPD values decrease slightly and increase in spatial variability given the heterogeneity in sediment type and corresponding infaunal community (Figure

18 d). Between RM 5 – RM 3, aRPD values fluctuate around the overall site average value, with surface oxidized layers developed from a combination of infaunal reworking, deposition of oxidized particles, and hydraulically-driven oxidation as a result of surface roughness elements (Figure 20).

3.1.5 Sedimentary Methane

Evidence of excess organic loading was found in the form of methanogenesis at 52 of the 128 stations (Figure 21 a-e), less than half the stations surveyed. In the upper Willamette River between RM 13 and 11, subsurface methane was only observed at 2 of the nearshore locations (Stations 77B and 78A; see Figure 17). In the upper Portland Harbor area below the Fremont Bridge (Figure 21c) where fine grained sediments were more common, methane was only found at a handful of stations (about evenly split between the deeper channel stations and near shore depositional areas). Below RM 8, methane was found only at selected near shore stations (Figure 21 D); it was not until around RM 5 (Transect 33) where methane started to appear in the deeper stations in the channel, and the highest percentage of stations with methane was between RM 5 and 4 (Figure 21e), both in the deeper channel and the shallow near shore areas. As flows increase and sediments got coarser, the presence of methane tapered off below Transect 20 (Figure 21e).

3.1.6 Infaunal Successional Stage

The spatial distribution of infaunal successional stages throughout the 10 miles of the LWR surveyed is shown in Figure 22 a-e. What is notable is the presence of Stage 3 taxa in almost all of the near shore stations with fine-grained sediment in RM 11 – RM 13 of the upper Willamette River (Figure 23); the only near shore station with fine-grained sediments in this reach without any evidence of Stage 3 taxa was Station 78A (Figure 22b).

The distribution of infaunal successional stages in upper Portland Harbor is shown in Figure 22c; Stage 3 taxa are present at every station except two (Stations 69C and 60D). Head-down deposit feeders were also detected at all stations in the Swan Island Lagoon. Stage 3 taxa continued to be present at both channel and near shore stations below RM 8 until Station 41A and 40D, where only Stage 1 opportunists were detected (Figure 22d). Despite the wide variation in disturbance regime and sediment type, Stage 3 taxa continued to be present at the majority of stations sampled in middle Portland Harbor between RM 5.5 to RM 3 (Figure 22e). Even in locations where it was obvious that deposition was occurring at a fairly constant rate, Stage 3 taxa continued to exist and appeared to be able to cope with this level of disturbance (Figure 24). Out of the 128 stations surveyed, there were only 5 locations (Stations 26E, 27A, 28E, 40D, and 41A) where only Stage 1 taxa were found.

3.1.7 *Feeding Void Depth*

The spatial distribution of maximum station infaunal feeding void depth is shown in Figure 25a-e; even though the distribution of Stage 3 infauna was quite widespread throughout the site, given the relatively high water content of many of the fine-grained stations and geotechnical properties of the silt-clay (and the frequent occurrence of methane gas), the subsurface sediments did not have the structural competence to support subsurface void chambers at every location where Stage 3 infauna were present. Very often, either the presence of portions of worms against the faceplate and transected edges of burrows were the only visible signs that Stage 3 taxa were indeed present at a particular location (Figure 26). The maximum station feeding void depths ranged from 3.1 - 20.9 cm, with an overall site average maximum depth of 12.2 cm.

3.2 LWR Temporal Variation: Changes from 2001 to 2013

Even though 128 stations were sampled in 2013, three of these stations (27D, 40D, and 61E) had no usable data from 2001, so there were only 125 stations for comparison. For these stations, temporal changes were calculated using the difference in values between the two surveys. Temporal differences were calculated as the 2013 survey value minus the 2001 survey value, so a positive temporal difference indicated higher values in 2013. The data for camera penetration depth, aRPD depth, maximum void depth, successional stage rank, and methane are summarized in Table 3 and Figure 27.

Table 3. Summary statistics of the temporal changes observed at stations surveyed in both 2001 and 2013 (n=125)

	Minimum	Maximum	Mean	Bootstrap 95% CI of the Mean[1]	Pearson's Correlation coefficient
Average penetration depth (cm)	-10.1	16.0	0.40	[-0.36, 1.24]	0.73 (p<<0.01)
Average aRPD depth (cm)	-13.1	2.18	-0.58	[-1.17, -0.23]	0.39 (p<<0.01)
Maximum void depth (cm)	-7.96	13.6	0.67	[-1.15, 3.05]	0.07 (p=0.8)
Maximum Successional Stage Rank	-2	2	0.8	[0.6, 1.0]	0.18 (p=0.08)

1Bias-corrected and accelerated (BCA) bootstrap confidence intervals

3.2.1 Prism Penetration Depth

The prism penetration depths from the two years covaried (Pearson's correlation coefficient was 0.73, n=119). Approximately half the temporal differences were within the range of +/- 3 cm. The largest differences (a difference in penetration depth of more than 6 cm between the two years) were found between RM 4.6 and RM 9.2 (Table 4).

Table 4. Stations in the LWR exhibiting the greatest temporal change in prism penetration depth between 2001 and 2013

Station	Water depth (mllw, ft)	River Mile	2013 Penetration depth (cm)	2001 Penetration depth (cm)	Delta
29B	20	4.625	19.13	12.39	6.74
33D	51.2	5.125	18.37	2.42	15.95
34A	15.8	5.25	7.88	0.16	7.72
35A	23.9	5.375	18.51	4.66	13.85
37A	12.5	5.625	1.1	10.15	-9.05
37B	49.5	5.625	3.37	12.73	-9.36
37D	30.5	5.625	15.01	7.67	7.34
40E	32.6	6.00	1.69	11.76	-10.07
41A	8.3	6.125	1.96	8.33	-6.37
42B	44.9	6.25	9.69	18.83	-9.14
49A	7.4	7.175	21.06	12.04	9.02
51F	15.6	7.425	19.33	10.69	8.64
57F	38.6	8.175	16.29	8.34	7.95
59B	19	8.425	19.22	8.06	11.16
65C	51.8	9.175	6.14	12.2	-6.06

The mean temporal difference among the stations for which prism penetration depth was available in both surveys (n=119) was 0.40 cm, with a 95% confidence interval of [-0.4 cm, 1.2 cm], meaning they are not statistically distinct. While the changes in penetration depth between the two years were related to changes in the sediment type in the river bed due to shifting hydraulic energy regimes (at some locations, what was a sandy bottom in 2001 had a higher percentage of fines in 2013, and vice versa; see Figure 28[2]), the variation was great enough in both directions that effectively there was no overall difference in this parameter between the two years.

[2] In the figures where the profile images from the two surveys are compared, there is a very obvious difference in the color balance between these 2 sets of images because of the difference in camera technology between the 2001 (film) and 2013 (digital) survey. The 2001 survey used Ektachrome film, which is heavily biased in the blue color range, so all the sediments have a blue-green tint to them; the 2013 images are captured with a digital image sensor (Nikon D7000 camera) that more accurately represents the true color of the sediments. However, all images from the 2 different surveys are at comparable scales

3.2.2 Apparent Redox Potential Discontinuity Depth

The aRPD depths from the two years weakly co-varied (Pearson's correlation coefficient was 0.39, n=99). The aRPD depths in the 2013 survey ranged from 0.4 to 4.5 cm; these same stations had aRPD depths in the 2001 survey that ranged from 0.1 cm to 16.4 cm. More than sixty percent (63 out of 99) of the temporal differences were within the range of +/-1 cm. The distribution of temporal differences was strongly skewed to the negative due to extremely deep aRPD values at 5 of the stations in 2001; stations 74A, 67C, 73B, 70A, and 82D (between RM 9.4 and RM 12.9) had aRPD depths that ranged from 4 cm to 13 cm shallower in 2013 (Figure 29). The mean temporal difference among the stations for which aRPD values could be measured in both surveys (n=99) was -0.6 cm, with a 95% confidence interval for the mean of [-1.2 cm, -0.2 cm], which is significantly different from zero using a 2-tailed alpha = 0.05. If the five stations with the depositional (extremely deep) aRPD values in 2001 were excluded (n=94), then the temporal differences had a range of [-2.9 cm, 2.2 cm], with a mean of -0.16 cm, and a 95% confidence interval of [-0.38 cm, 0.05 cm], which is not significantly different than zero.

3.2.3 Sedimentary Methane

Subsurface methane (an indicator of organic enrichment) was present at 57 of the stations sampled in common in 2001 and at 51 of the stations sampled in 2013. A contingency table (Table 5) showing the numbers of stations with methane present or absent (or indeterminate) in the two surveys indicated that there were 17 stations where methane was absent in 2001 and present in 2013. Thirteen of these stations were located between RM 3.9 and RM 6. Within this same segment of the river, there were 8 stations where methane was present in 2001 and absent in 2013. There were 23 stations in total where methane was present in 2001 and absent in 2013, spanning nearly the full surveyed length of the river (i.e., RM 3.9 to RM 11.7).

Table 5. Numbers of stations with methane present/absent for the 2001 and 2013 surveys

	2001 Survey			
2013 Survey	Absent	Present	Ind	Totals (Including Ind)
Absent	44	23	(5)	67 (72)
Present	17	34	(1)	51 (52)
Ind	(1)	(1)	(2)	(4)
Totals (Including Ind)	61 (62)	57 (58)	(8)	118 (128)

3.2.4 Infaunal Successional Stage

The successional stage ranks were predominantly Stage 3 equivalent in 2013 (72 out of 101 stations), while in 2001 only 46 out of 101 stations had Stage 3 communities apparent. A contingency table (Table 6) shows the number of stations that moved from one successional stage to another between the two survey dates. Nine stations that were Stage 3 in 2001 moved to a lower stage in the 2013 survey; but 52 stations moved up in successional stage status, from a Stage 1 in 2001 to a higher successional stage in 2013. The mean temporal difference in successional stage rank among the stations for which successional stage could be determined in both surveys (n=101) was 0.8, with a 95% confidence interval of [0.6, 1.0]; this positive difference is a statistically significant improvement in benthic community status.

Table 6. Numbers of stations in each successional stage category for the 2001 and 2013 surveys

	2001 Survey			
2013 Survey	Stage 1	Stage 3	Ind	Totals (including Ind)
Stage 1	3	1	(1)	4 (5)
Stage 2	6	2	(0)	8 (8)
Stage 2->3	11	6	(3)	17 (20)
Stage 3	35	37	(8)	72 (80)
Ind	(8)	(0)	(7)	(15)
Totals (including Ind)	55 (63)	46 (46)	(19)	101 (128)

3.2.5 Feeding Void Depth

The maximum void depths from the two years did not covary (Pearson's correlation coefficient was 0.07, n=23), which is highly indicative of the spatial variability of this measurement. The void depths can only be quantified when a void is captured in an image; even replicate drops of the camera at a single station varied substantially number and depth of feeding voids. The number of voids was often zero at stations in each survey, but even within a single station, the void count could vary greatly among the 3 replicate images (voids ranged from 0 to 4 at Station 31B in 2013; see Appendix A). Within-station variability for void depth also was common; for example, at Station 51C, a single void was present in each replicate, but the maximum void depths ranged from 3.1 to 16 cm among the images (Appendix A). Any station-specific changes between the 2001 and 2013 surveys were more likely due to spatial heterogeneity than to temporal effects.

3.2.6 Summary of Temporal Changes in Individual SPI variables

Evaluation of the station-specific temporal differences in the individual SPI variables as summarized above indicated that strong temporal trends did not exist for the survey area as a whole, with the exception of the increase in stations with Stage 3 infauna. Overall, the aRPD depths significantly declined between 2001 and 2013, but this was primarily driven by five stations with extremely deep aRPD values in 2001 that were caused by hydraulic (depositional) effects, not bioturbational effects. When these stations were omitted from the evaluation, the resulting mean temporal shift in aRPD values was not significantly different from zero. The methane results showed comparable numbers of stations that shifted from methane present (in 2001) to absent (in 2013) as the reverse. The successional stage rank results indicated the greatest improvement between the two surveys, with more than a 50% increase in the number of stations with Stage 3 equivalent infauna (46 in 2001 and 72 in 2013).

3.2.7 Multivariate Ordination of Patterns in the Data

The presence of a spatial component to any trends observed in the data was investigated using multivariate ordination techniques. An ordination was conducted using three biological and one chemical response variables (aRPD depth, maximum void depth, successional stage rank, and methane presence/absence). The results of this ordination were evaluated with respect to several criteria:

1. How well did the ordination describe the patterns in the data?
2. Which response variables distinguished the ordination?
3. Are the ordination axes correlated with spatial or temporal variables?
4. Are the ordination axes correlated with structuring habitat variables?

The stress for the two dimensional nMDS ordination plot (Figure 30) was 9.8%, considered to be a ‘good’ representation of the multivariate data set (McCune and Grace 2002 after Kruskal 1964). The primary drivers were successional stage rank (Spearman rank correlation of 0.85 with MDS1) and methane presence/absence (Spearman correlation of -0.84 with MDS2), identified on Figure 30. Both feeding void depth and aRPD depths had weak associations with these two primary ordination axes (Spearman rank correlations ranged from -0.11 to 0.44; see also Figure 31)

The nMDS ordination axes were slightly correlated with survey year because of the association between successional stage and year (Figure 32, top row); but there was no association between the patterns observed in the ordination and River Mile (Figure 32, bottom row).

Among the physical habitat variables, the variable with the strongest association with the nMDS ordination axes was prism penetration depth (Figure 33). The Spearman rank correlation between MDS1 and prism penetration depth was 0.56

The ordination investigation of the other response variables indicated that there was little correlation among the four response variables (Figure 31). Stage 3 infauna were observed regardless of the presence of methane, and the highest aRPD depths co-occurred at stations with Stage 1 infauna. There was no spatial component to the observed patterns, at least in relation to river mile (Figure 32). Prism penetration depth was moderately associated with successional stage (and therefore with the primary ordination axis, MDS1). The remaining physical habitat variables did not contribute much to explain the patterns observed in the variable biological responses among stations.

4.0 DISCUSSION

Rivers are naturally dynamic systems, continually changing their position and shape as a result of hydraulic forces acting on their beds and banks, so it is not too surprising that the results from the SPI survey revealed a spatially and temporally complex, dynamic fluvial system, with both hydraulic flow and sediment transport varying in both time and space. These two dominant physical forces (hydraulic volume/flow rate and sediment transport dynamics) are having a definite influence on both sediment organic carbon diagenesis and biological community structure in the LWR.

It is precisely these fluvial system dynamics that must be kept in mind at all times to provide the context for interpreting the processes reflected by the structures seen in the sediment profile images. In alluvial river systems, it is the rule (rather than the exception) that sediments will be deposited, banks will erode, and floodplains, islands, and side channels will undergo either very slow or dramatically rapid changes over time (Simons and Sentürk, 1992). The morphology of any river is related to the sediment dynamics of the system, and there are a wide variety of both natural and anthropogenic factors that affect spatial variation in morphology. The natural factors include the river valley gradient, valley width, stream discharge rate, bank and bed resistance to flow, and sediment supply (as well as type of sediment). In an urban river such as the LWR, there are additional anthropogenic factors that can affect river morphology directly or indirectly, including dams and water extraction, dykes and embankments, channelization and dredging activities, CSO discharges, bridges, water inflow, groundwater level, and phreatophyte[3] growth. All of these factors will have an influence on the geological, biological, or chemical characteristics found at any point in the river and must be considered when trying to understand spatial patterns in any of these measurements.

It is important to remember that there was considerable variability even within the two different reaches of the river that were surveyed (Upper Willamette River and Portland Harbor Area); while fine-grained deposits were found in both areas, depositional regimes with silt-clays as the dominant sediment type (and associated organic loading with subsurface methane generation) were more commonly found at locations in the Portland Harbor area (Figures 4 [d-e] and 21 [d-e]).

Because of the dynamic nature of alluvial river systems, it is not uncommon to find the whole range of sediment types and kinetic regimes that you would find in different river reaches within a single transect. While the initial characterization survey in 2001 had a much more comprehensive sampling array (both nearshore and channel stations were surveyed in each transect sampled; SEA 2002), the reduced sampling array in the 2013

3 A deep-rooted plant that obtains water from a permanent ground supply or from the water table.

survey with more focus on the variable near shore areas did not result in the same pattern of "benthic zones" outlined from the 2001 results (SEA 2002). While the infaunal community did vary quite a bit with sediment type in the near shore stations (Figure 22 a-e), the majority of stations had evidence of Stage 3 taxa present.

Aside from providing a general description of physical and biological characteristics along the length of the river that was surveyed, the four primary objectives of this study were to discover:

- Indications of aerobic and/or anaerobic conditions in surface sediments
- Indications of sediment physical conditions (e.g., relative shear strength, density, and grain size)
- Indications of sediment chemical and biological conditions
- What, if any, significant differences were there in the results from 2001 as compared with those obtained in 2013, especially the River Mile 4 and 5 reach?

Even though only about one-fourth of the stations sampled in 2001 were re-occupied in 2013, there were still a sufficient number of stations sampled to achieve all of the survey objectives:

- There was no evidence of anaerobic conditions at the sediment surface anywhere in the river; all surface sediments appeared to be well-oxygenated at every location sampled
- Sediment geophysical conditions were shown in both the grain-size major mode maps and example profile images (Figures 4-13) and prism penetration maps (Figures 16 a-e)
- While there was plenty of evidence of physical disturbance gradients (change in sediment transport patterns; see Figures 7, 9, and 10), it was difficult to discriminate any broad-scale disturbance gradients in the benthic community. Early successional stages indicative of recent disturbance were most commonly encountered at near shore stations (Figure 22 a-e). The most common fauna seen in the images were either oligochaetes or insect larvae; because biogenic structures do not last long in such a hydraulically-active transport regime (both fluid and sediment), we could not find feeding voids at many of the locations (see Figure 25 a-e).
- Other than grain size and penetration depth shifts at individual scattered locations (Figure 28), there were only two parameters that were noticeably different in the overall results from 2001 and 2013: aRPD depth and infaunal

successional stage. While overall aRPD depths appear to have decreased between 2001 and 2013 (indicating increased stress to the benthic environment), upon closer examination, the detected difference was due to abnormally high aRPD values measured in 2001 at 5 stations where oxygenated fine particles had settled out in low-energy locations. These "depositional aRPD layers" are not due to biological reworking from larger organisms or higher densities of infaunal deposit feeders and so are not necessarily correlated with improvements in benthic community status. If the values from these 5 outliers were ignored in the 2001 data set, there was no detectable difference in aRPD depths between the two surveys. The one measured and important difference was a definite improvement in benthic community status, with a more than 50% increase in the number of stations that had Stage 3 fauna present.

- As far as changes in the River Mile 4 and 5 reach (west of the St. Johns Bridge to the Multnomah Channel), there were no signs of increased organic enrichment between 2001 and 2013, and the aRPD depths were essentially equivalent between these two surveys. The one substantial change was a dramatic improvement in benthic infaunal successional stage at all stations located on Transects 31-35. In 2001, the only location on the western bank of the river that showed any signs of Stage 3 infauna was Station 32A (SEA 2002). In 2013, all of the stations on the western bank in the area of interest (Station 31A, 32A, 33A, 34A, and 35A) had at least one or more replicate images with evidence of Stage 3 taxa present. In fact, these 4 transects had all but one of the Stations (35E) sampled in both 2001 and 2013; in 2001, only 6 stations among the remaining 21 locations sampled in these 4 transects had any evidence of Stage 3 taxa (SEA 2002, Figure 3-4). In 2013, 19 of these 21 stations had images with evidence of Stage 3 taxa present (Figures 22d-e), a clear improvement in benthic habitat conditions.

It appears that the general pattern of benthic community recovery in freshwater is similar whether it is in response to physical disturbance or a pollution event; once the source of stress to the community has abated, recovery happens quite quickly by fast growing, rapidly dispersing opportunistic taxa (oligochaetes and chrionomids). Downes and Keough (1998) documented colonization in streams through a variety of avenues; streams and rivers are dominated by macroinvertebrates, the majority of which are insects, and most of these have an aquatic larval form and a terrestrial, flying adult. Both eggs and larvae can be transported downstream in the drift, larvae can walk or crawl to new patches, and adult insects can be transported by wind or actively fly to lay eggs in new areas. Matthaei et al. (1996) showed that disturbed patches in rapid flow environments recover extremely rapidly, with populations recovering to undisturbed levels within 1-14 days following disturbance. There were seasonal differences, with recovery happening quickly in the summer (8-12 days) and more slowly in the winter (71 days). The resilience of the benthic community in environments that are frequently disturbed by physical forces (not contaminant impacts) is, not surprisingly, exceedingly high. Therefore, one would expect recolonization of any disturbed area in the higher-energy regimes of the LWR to occur quite rapidly. The marked improvement in benthic community structure between 2001 and 2013 also lends support to the argument that natural recovery is occurring since the original site investigations started more than a decade ago.

5.0
REFERENCES CITED

Boudreau, B.P. 1986. Mathematics of tracer mixing in sediment. I-Spatially-dependent, diffusive mixing. II: Non-local mixing and biological conveyor-belt phenomena. Am. Jour. Sci. 286: 161-238.

Boudreau, B.P. 1994. Is burial velocity a master parameter for bioturbation? Geochimica et Cosmochemica Acta 58: 1243-1249.

Boudreau, B. P. 1998. Mean mixed depth of sediments: The wherefore and the why. Limnol. Oceanogr. 43: 524-526.

Boyer, L.F. and Hedrick, J.D. (1989) Submersible deployed video sediment profile camera system for benthic studies. Journal of Great Lakes Research, 15(1), 34 – 45.

Boyer, L.F. and Shen, E.J. (1988) Sediment profile camera study of Milwaukee harbour sediments. Journal of Great Lakes Research, 14(4): 444 – 465.

Boyer, L.F. and Whitlatch, R.B. (1989) In situ studies of organism-sediment relationships in the Caribou Island Basin, Lake Superior. Journal of Great Lakes Research, 15(1), 147 – 155.

Charbonneau, P. and L. Hare. 1998. Burrowing behavior and biogenic structures of mud-dwelling insects. Journal of the North American Benthological Society 17: 239-249.

Charbonneau, P., L. Hare, and R. Carignan. 1997 Use of X-ray images and a contrasting agent to study the behavior of animals in soft sediments. Limnology and Oceanography 42: 1823-1828.

Clayton, C.J. 1995. Microbial and Organic Processes. In Parker, A. and B. W. Sellwood (eds). Quantitative Diagenesis: Recent Developments and Applications to Reservoir Geology. Kluwer Academic Publishers, pp. 125-160.

Davison, W. 1993. Iron and manganese in lakes. Earth Science Reviews 34: 119-163.

Diaz, R. J. and L. C. Schaffner. 1988. Comparison of sediment landscapes in the Chesapeake Bay as seen by surface and profile imaging, p. 222-240 In M. P. Lynch and E. C. Krome (eds.), Understanding the Estuary: Advances in Chesapeake Bay Research, Chesapeake Bay Research Consortium Publication 129, Chesapeake Bay Program 24/88.

Downes, B.J. and M.J. Keough. 1998. Scaling of colonization processes in streams: Parallels and lessons from marine hard substrata. Australian Journal of Ecology 23: 8-26.

Ekman, J.E., Nowell, A.R.M., and P.A. Jumars. 1981. Sediment destabilization by animal tubes. J. Mar. Res. 39: 361-374.

François, F., Gerino, M., Stora, G., Durbec, J.P., and J.C. Poggiale. 2002. Functional approach to sediment reworking by gallery-forming macrobenthic organisms: modeling and application with the polychaete *Nereis diversicolor.* Marine Ecology Progress Series 229: 127–136.

Froelich, P. N., G.P. Klinkhammer, M.L. Bender, N. A. Luedtke, G. R. Heath, D. Cullen, P. Dauphin, D. Hammond, B. Hartman, and V. Maynard. 1979. Early oxidation of organic matter in pelagic sediments of the eastern equatorial Atlantic: suboxic diagenesis. Geochimica et Cosmochimica Acta 43: 1075-1090.

Ganf, G.G. and A.B. Viner. 1973. Ecological stability in shallow equatorial Lake George, Uganda. Proceedings of the Royal Society of London B 184: 235-270.

Germano, J.D. 1983. Infaunal succession in Long Island Sound: Animal-sediment interactions and the effects of predation. Ph.D. dissertation. Yale University, New Haven, CT. 206 pp.

Germano, J.D., D.C. Rhoads, R.M. Valente, D.A. Carey, and M. Solan. 2011. The use of Sediment Profile Imaging (SPI) for environmental impact assessments and monitoring studies – lessons learned from the past four decades. Oceanography and Marine Biology: An Annual Review 49: 247-310.

Gersbacher, W.M. 1937. Development of stream bottom communities in Illinois. Ecology 18: 359-390.

Gilbert, F. S. Hulth, N. Strömberg, K. Ringdahl, and J.-C. Poggiale. 2003. 2-D optical quantification of particle reworking activities in marine surface sediments. Jour. Exp. Mar. Biol. Ecol. 285-286: 251-264.

Gower, J.C. 1971. A general coefficient of similarity and some of its properties. *Biometrics* 27: 857–874.

Grant, W.D., Jr., Boyer, L.F., and Sanford, L.P. 1982. The effects of bioturbation on the initiation of motion of intertidal sands: Jour. Mar. Res., Vol. 40, pp. 659-677.

Huettel, M., W. Ziebis, and S. Forster. 1996. Flow-induced uptake of particulate matter in permeable sediments. Limnol. Oceanogr. 41: 309-322.

Huettel, M., Ziebis, W., Forster., S., and G.W. Luther III. 1998. Advective transport affecting metal and nutrient distributions and interfacial fluxes in permeable sediments. Geochimica et Cosmochemica Acta 62: 613-631.

Kennish, M.J. 1986. Ecology of estuaries. Vol. I: Physical and chemical aspects. CRC Press, Boca Raton, FL.

Koretsky, C.M., J.R. Haas, D. Miller, and N.T. Ndenga. 2006. Seasonal variations in pore water and sediment geochemistry of littoral lake sediments (Asylum Lake, MI, USA). Geochemical Transactions 7: 11 pages (published online).

Kruskal, J.B. 1964. Multidimensional scaling by optimizing goodness of fit to a nonmetric hypothesis. *Psychometrika* 29: 1-27.

Lopez, G.R. 1988. Comparative ecology of the macrofauna of freshwater and marine muds. Limnology and Oceanography 33: 946-962.

Maechler, M., P. Rousseeuw, A. Struyf, M. Hubert, and K. Hornik. 2013. cluster: Cluster Analysis Basics and Extensions. R package version 1.14.4.

Matthaei, C.D., U. Uehlinger, E. I. Meyer, and A. Frutiger. 1996. Recolonization by benthic invertebrates after experimental disturbance in a Swiss prealpine river. Freshwater Biology 35: 233-248.

McCall, P.L. 1977. Community patterns and adaptive strategies of the infaunal benthos of Long Island Sound. Journal of Marine Research 35: 221-266.

McCall, P.L. and M.J.S. Tevesz. 1982. The effects of benthos on physical properties of freshwater sediments, pp. 105-176. IN P.L. McCall and M.J.S. Tevesz (eds). Animal-Sediment Relations. Plenum Press, New York.

McCune, B., and J.B. Grace. 2002. Analysis of Ecological Communities. MjM Software Design, Gleneden Beach, OR. 283 pp.

Metcalfe, T.L., C.D. Metcalfe, E.R. Bennett, and G.D. Haffner. 2000. Distribution of toxic organic contaminants in water and sediments of the Detroit River. Journal of Great Lakes Research 26: 55-64.

Middleton, G.V. 2003. Encyclopedia of Sediments and Sedimentary Rocks. Springer, New York.

Miller, M.F., and C.C. Labandeira. Slow crawl across the salinity divide: Delayed colonization of freshwater ecosystems by invertebrates. GSA Today 12: 4-10.

Moon, H.P. 1935. Methods and apparatus suitable for an investigation of the littoral region of oligotrophic lakes. Internationale Revue Gesamten Hdyrobiologie and Hydrographie 32: 319-333.

Nowell, A.R.M., P.A. Jumars, and J.E. Ekman. 1981. Effects of biological activity on the entrainment of marine sediments. Mar. Geol. 42: 133-153.

Oksanen, J., F.G. Blanchet, R. Kindt, P. Legendre, P.R. Minchin, R. . O'Hara, G.L. Simpson, P. Solymos, M.H.H. Stevens, and H. Wagner. 2013. vegan: Community Ecology Package. R package version 2.0-7. http://CRAN.R-project.org/package=vegan

Painter, T.H., M. E. Schaepman, W. Schweizer, and J. Brazile. 2007. Spectroscopic discrimination of shit from shinola. Annals of Improbable Research 13: 22-23.

Pearson, T.H. and R. Rosenberg. 1978. Macrobenthic succession in relation to organic enrichment and pollution of the marine environment. Oceanogr. Mar. Biol. Ann. Rev. 16:229-311.

Poff, N.L. and J.D. Allan. 1995. Functional organization of stream fish assemblages in relation to hydrological variability. Ecology 76: 606-627.

R Core Team. 2013. R: A language and environment for statistical computing. R Foundation for Statistical Computing, Vienna, Austria. http://www.R-project.org/

Reible, D and Thibodeaux, L. 1999. Using Natural Processes to Define Exposure From Sediments., in Sediment Management Work Group; Contaminated Sediment Management Technical Papers, Sediment Management Work Group, http://www.smwg.org/index.htm.

Revelas, E.C., J.D. Germano, and D.C. Rhoads. 1987. REMOTS reconnaissance of benthic environments. pp. 2069-2083. In: Coastal Zone ‘87 Proceedings, ASCE, WW Division, May 26-29, Seattle, WA.

Rhoads, D.C. 1974. Organism-sediment relations on the muddy seafloor. Oceanogr. Mar. Biol. Ann. Rev. 12: 263-300.

Rhoads, D.C. and L.F. Boyer. 1982. The effects of marine benthos on physical properties of sediments. pp. 3-52. In: Animal-Sediment Relations. McCall, P.L. and M.J.S. Tevesz (eds). Plenum Press, New York, NY.

Rhoads, D.C. and J.D. Germano. 1982. Characterization of benthic processes using sediment profile imaging: An efficient method of remote ecological monitoring of the seafloor (REMOTS™ System). Mar. Ecol. Prog. Ser. 8:115-128.

Rhoads, D.C. and J.D. Germano. 1986. Interpreting long-term changes in benthic community structure: A new protocol. Hydrobiologia. 142:291-308.

Rhoads, D.C. and J.D. Germano. 1990. The use of REMOTS® imaging technology for disposal site selection and monitoring. pp. 50-64. In: Geotechnical Engineering of Ocean Waste Disposal, K. Demars and R. Chaney (eds). ASTM Symposium Volume, January, 1989. Orlando, FL.

Rhoads, D.C., P.L. McCall, and J.Y. Yingst. 1978. Disturbance and production on the estuarine seafloor. American Scientist 66: 577-586.

Rosenberg, R., H.C. Nilsson, and R.J. Diaz. 2001. Response of benthic fauna and changing sediment redox profiles over a hypoxic gradient. Estuarine, Coastal and Shelf Science 53: 343-350.

Sanders, H.L. 1968. Marine benthic diversity: a comparative study. American Naturalist 102: 224-282.

SEA. 2002. Sediment Profile Image Survey of the Lower Willamette River. Report prepared for Lower Willamette Group by Striplin Environmental Associates. April 26, 2002.

Sherman, L. A., L. A. Baker, E. P. Weir, and P. L. Brezonik. 1994. Sediment pore-water dynamics of Little Rock Lake, Wisconsin: Geochemical processes and seasonal and spatial variability. Limnology and Oceanography 39: 1155-1171.

Simons, D.B. and F. Sentürk. 1992. Sediment Transport Technology: Water and Sediment Dynamics. Water Resources Publ, LLC, Highlands Ranch, CO. 897 pages.

Solan, M., J.D. Germano, D.C. Rhoads, C. Smith, E. Michaud, D. Parry, F. Wenzhöfer, B. Kennedy, C. Henriques, E. Battle, D. Carey, L. Iocco, R. Valente, J. Watson, and R. Rosenberg. 2003. Towards a greater understanding of pattern, scale, and process in marine benthic systems: a picture is worth a thousand worms. Journal of Experimental Marine Biology and Ecology 285-286: 313-338.

Soster, F.M. and P.L. McCall. 1990a. Benthos response to disturbance in western Lake Erie: field experiments. Canadian Journal of Fisheries and Aquatic Sciences 47: 1970-1985.

Soster, F.M. and P.L. McCall. 1990b. Benthos response to disturbance in western Lake Erie: regional faunal surveys. Canadian Journal of Fisheries and Aquatic Sciences 47: 1996-2009.

Tevesz, M.J.S. 1985. Benthic colonization in fresh water: a synthesis. Kirtlandia 41: 3-14.

Urban, N.R., C. Dinkel, and B. Wherli. 1997. Solute transfer across the sediment surface of a eutrophic lake: I. Porewater profiles from dialysis samplers. Aquatic Sciences 59: 1-25.

Valente, R.M., D.C. Rhoads, J.D. Germano, and V.J. Cabelli. 1992. Mapping of benthic enrichment patterns in Narragansett Bay, RI. Estuaries 15:1-17.

Ziebis, W., Huettel, M., and S. Forster. 1996. Impact of biogenic sediment topography on oxygen fluxes in permeable seabeds. Mar. Ecol. Prog. Ser. 1409: 227-237.

FIGURES

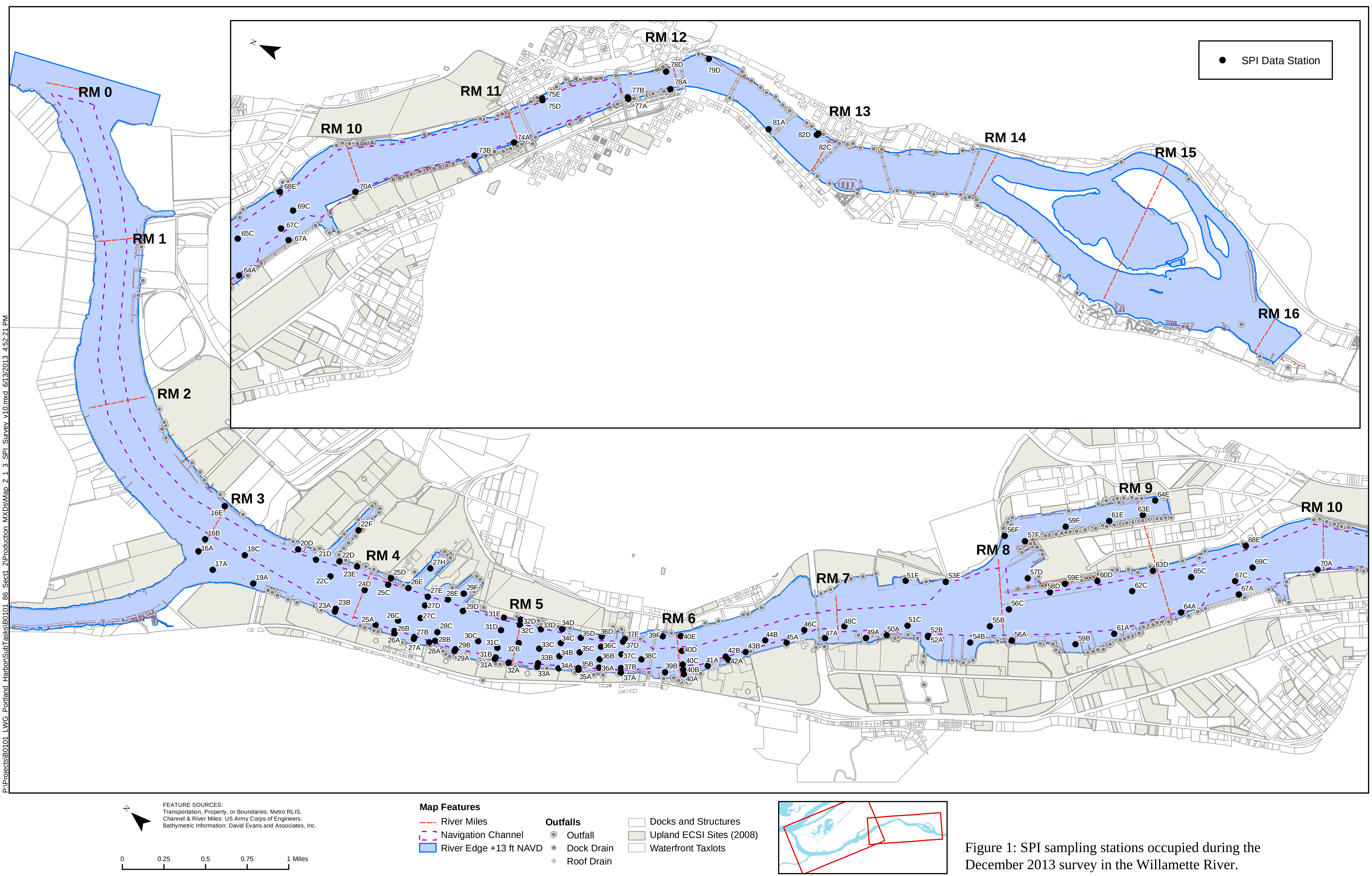

Figure 1: SPI sampling stations occupied during the December 2013 survey in the Willamette River.

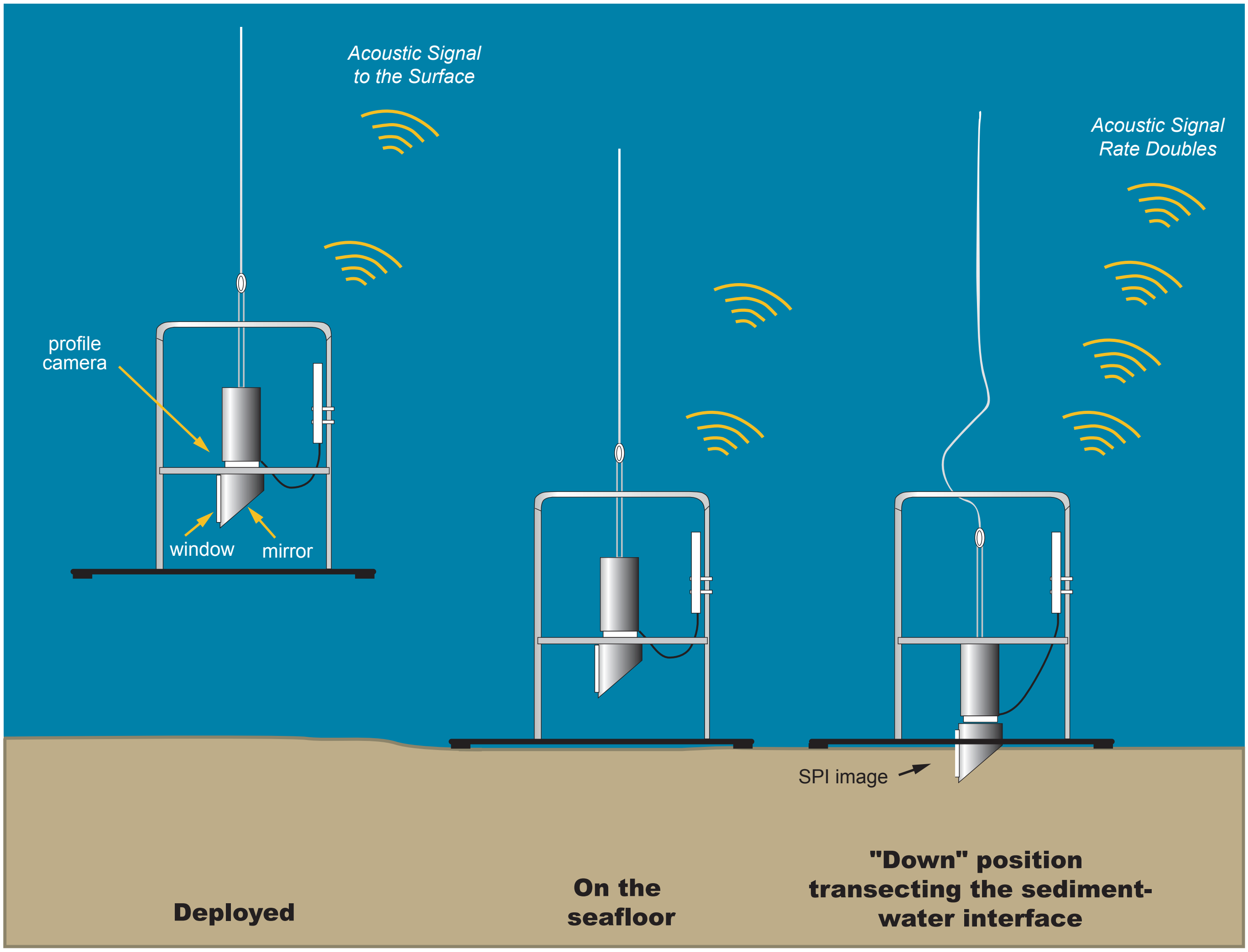

Figure 2: Schematic showing the deployment and operation of the Ocean Imaging 3731 Sediment Profile Camera.

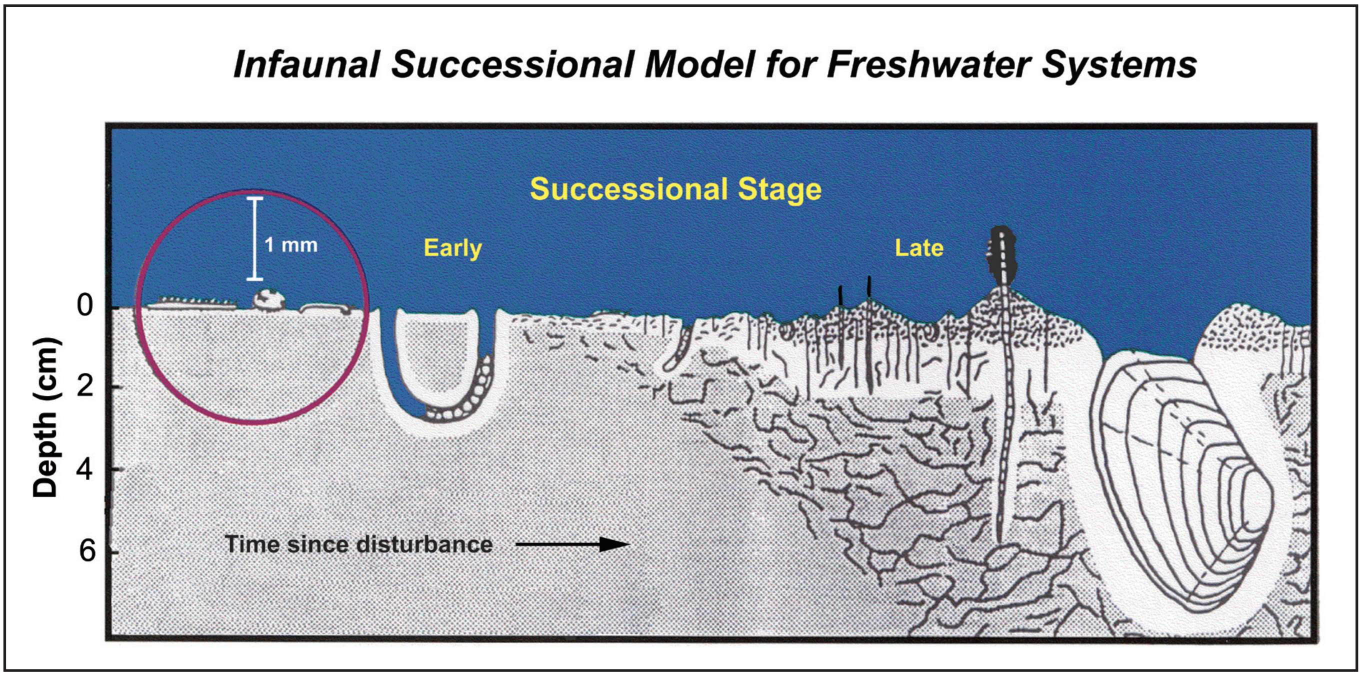

Figure 3: Freshwater muddy bottom successional model for western Lake Erie macrobenthos following a disturbance of the lakefloor which eliminates the ambient fauna (from Soster and McCall, 1990a).

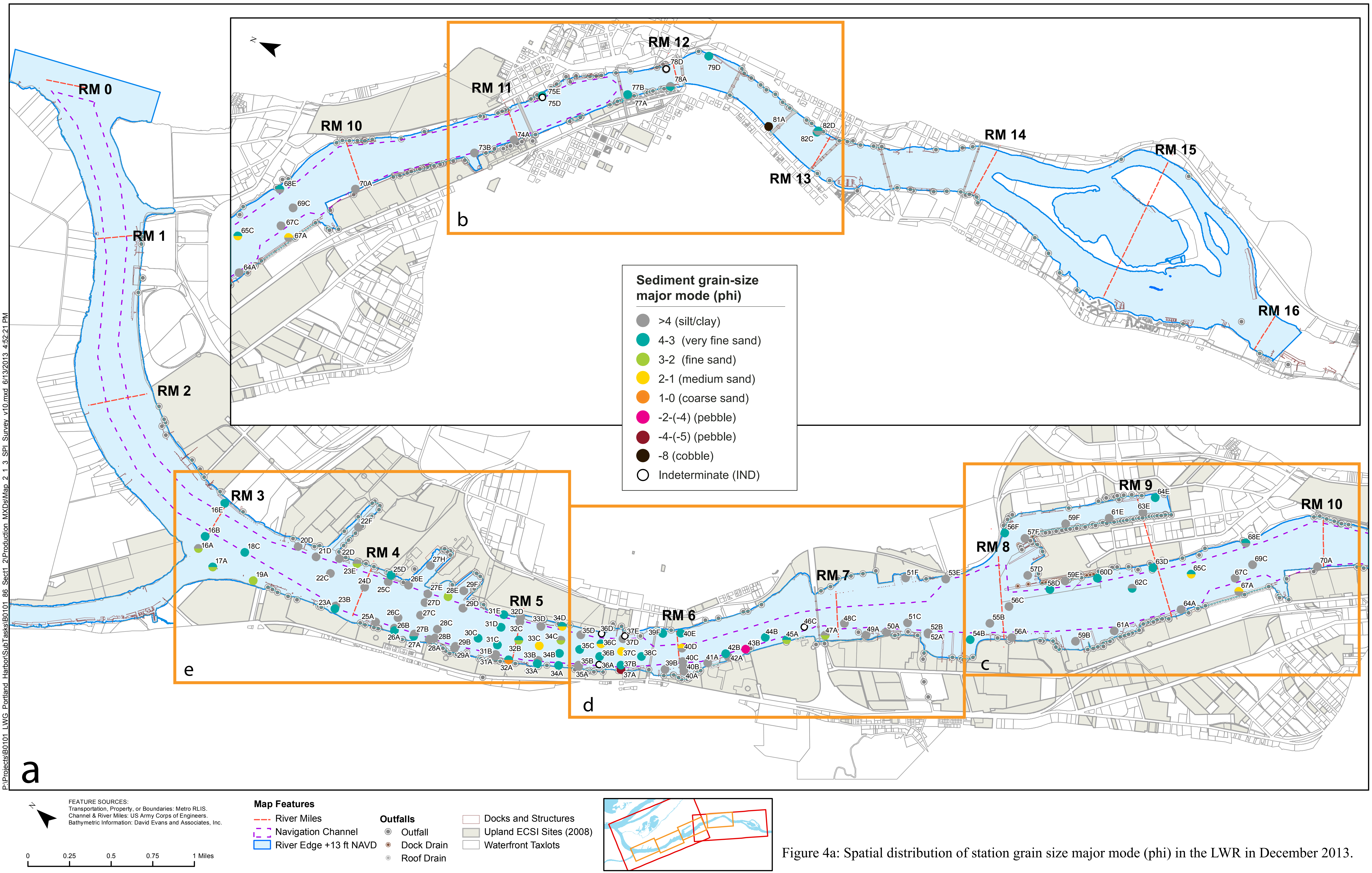

Figure 4a: Spatial distribution of station grain size major mode (phi) in the LWR in December 2013.

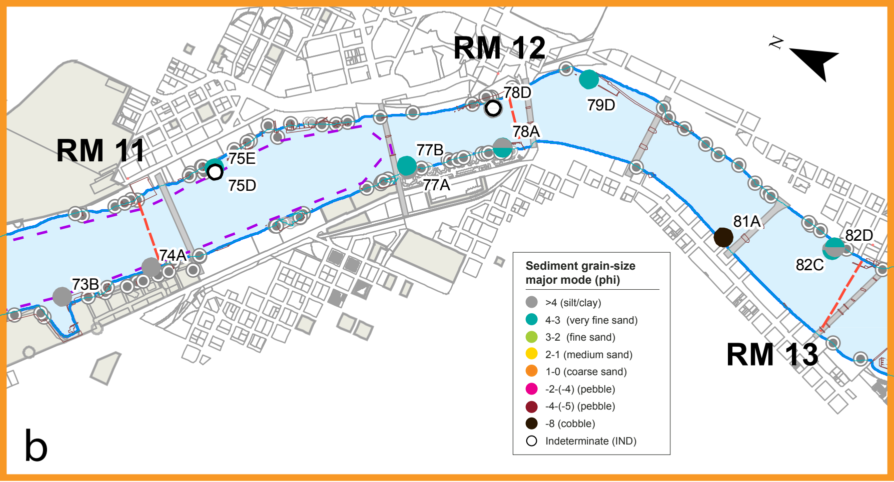

Figure 4b: Spatial distribution of station grain size major mode (phi) in the LWR in December 2013.

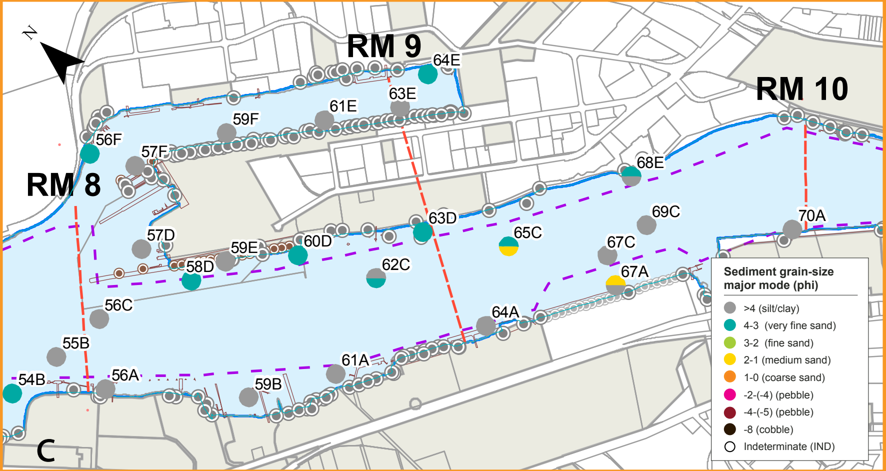

Figure 4c: Spatial distribution of station grain size major mode (phi) in the LWR in December 2013.

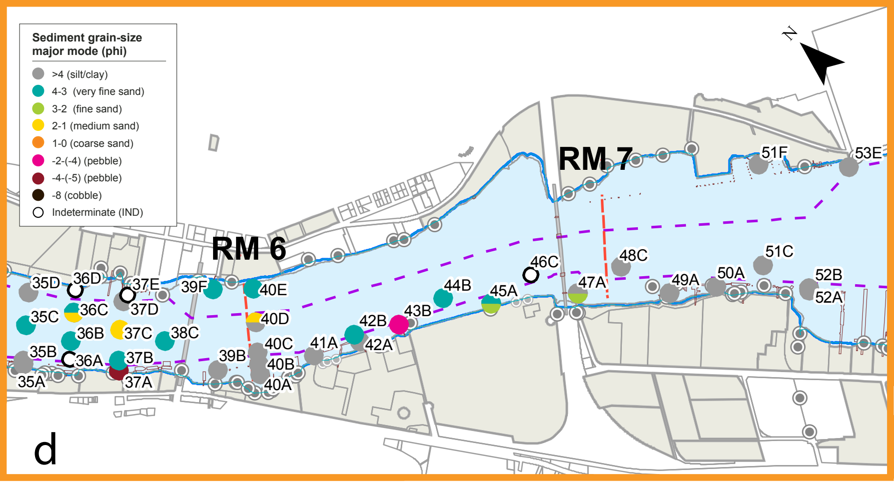

Figure 4d: Spatial distribution of station grain size major mode (phi) in the LWR in December 2013.

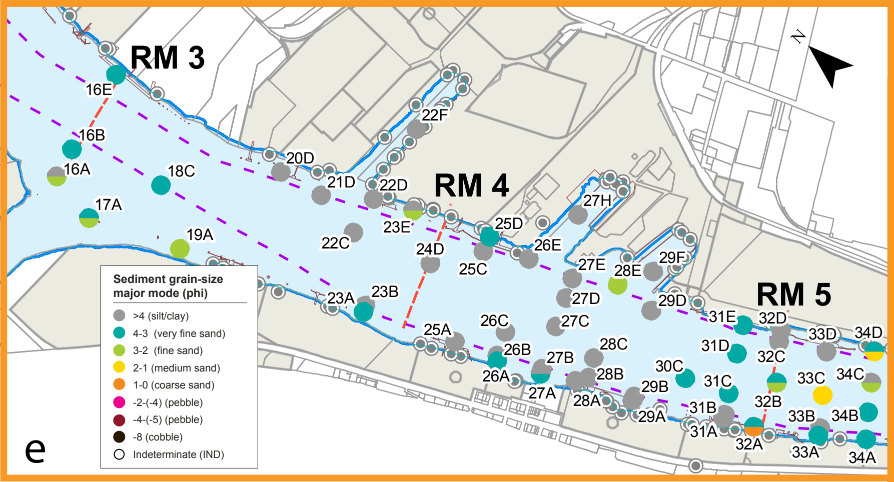

Figure 4e: Spatial distribution of station grain size major mode (phi) in the LWR in December 2013.

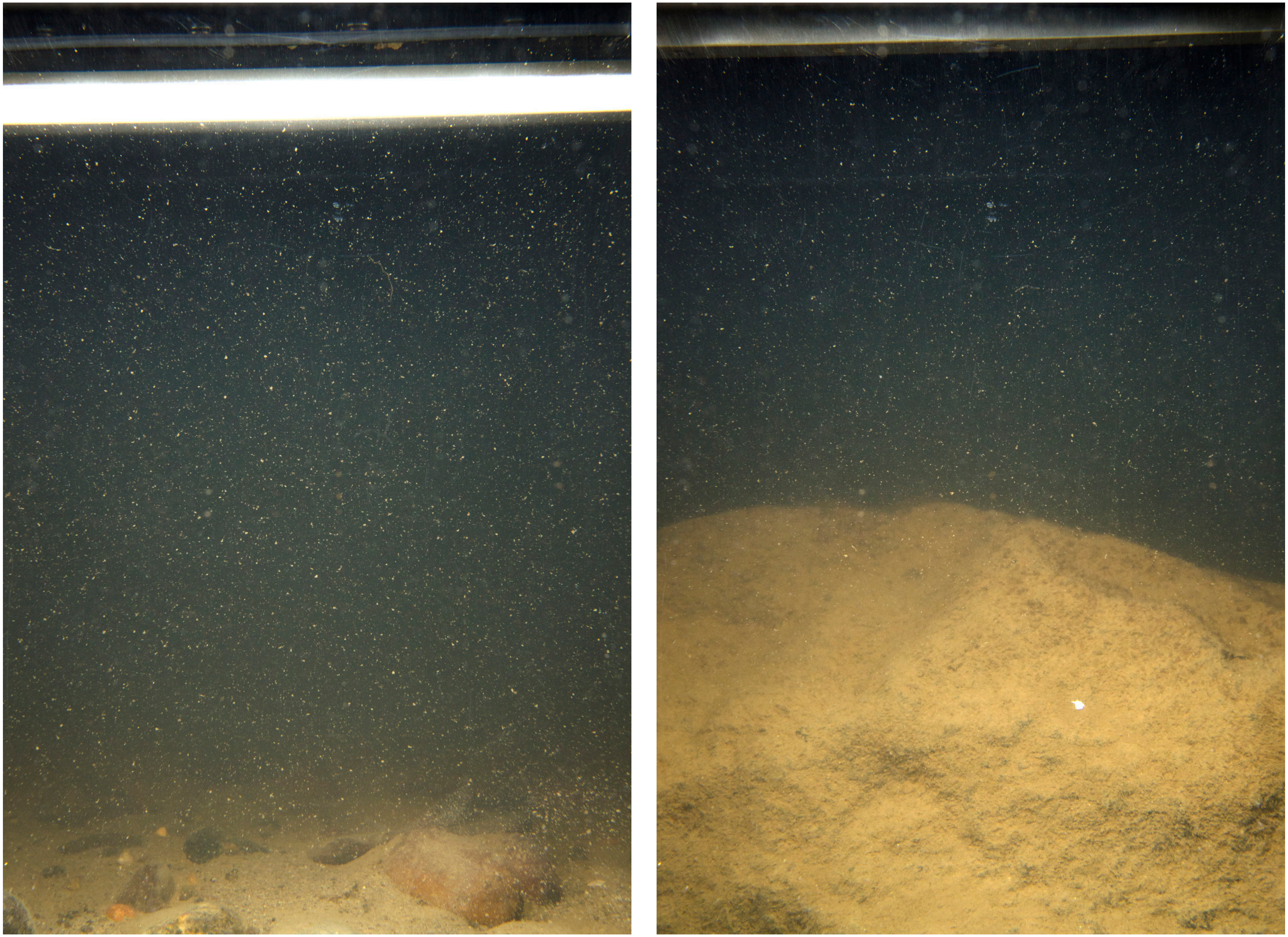

78D

81A

Figure 5: These profile images from Station 78D (left) and Station 81A (right) show a sandy cobble bottom (left) and a large rock (right) as part of the hard bottom substratum in this stretch of the river. Scale: width of each profile image = 14.5 cm.

Figure 6: This profile image from Station 67C in the deeper area of the main channel shows a thick silt-clay deposit over a very fine sandy silt layer at depth. Scale: width of profile image = 14.5 cm.

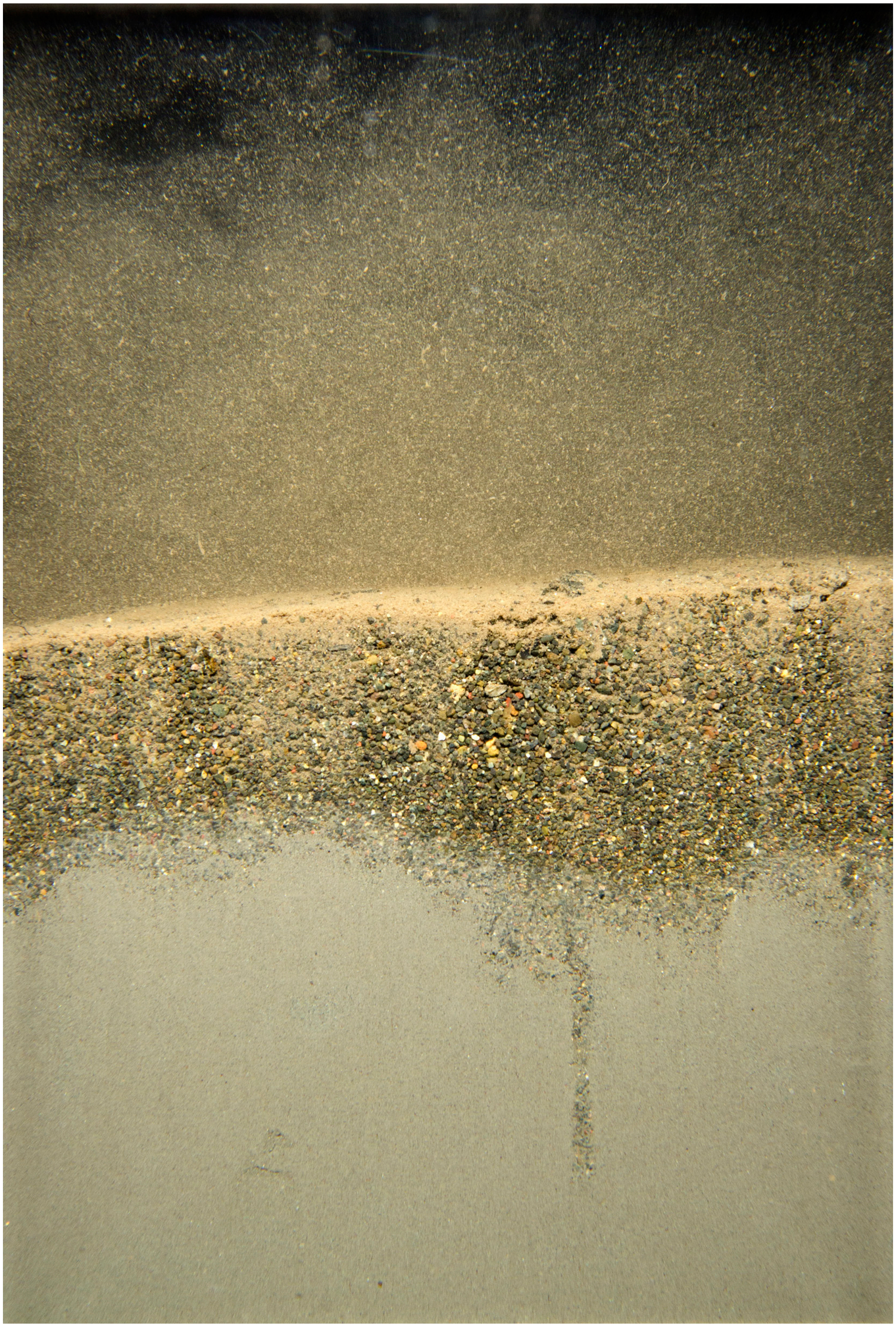

Figure 7: This profile image from Station 67A in the nearshore area shows a layer of sand that has been transported by currents over a layer of silt-clay. Scale: width of profile image = 14.5 cm.

Figure 8: The silt-clay sediments in this profile image from Station 51C in the main river channel is typical of the depositional areas found throughout the upper portion of Portland Harbor. Scale: width of image = 14.5 cm.

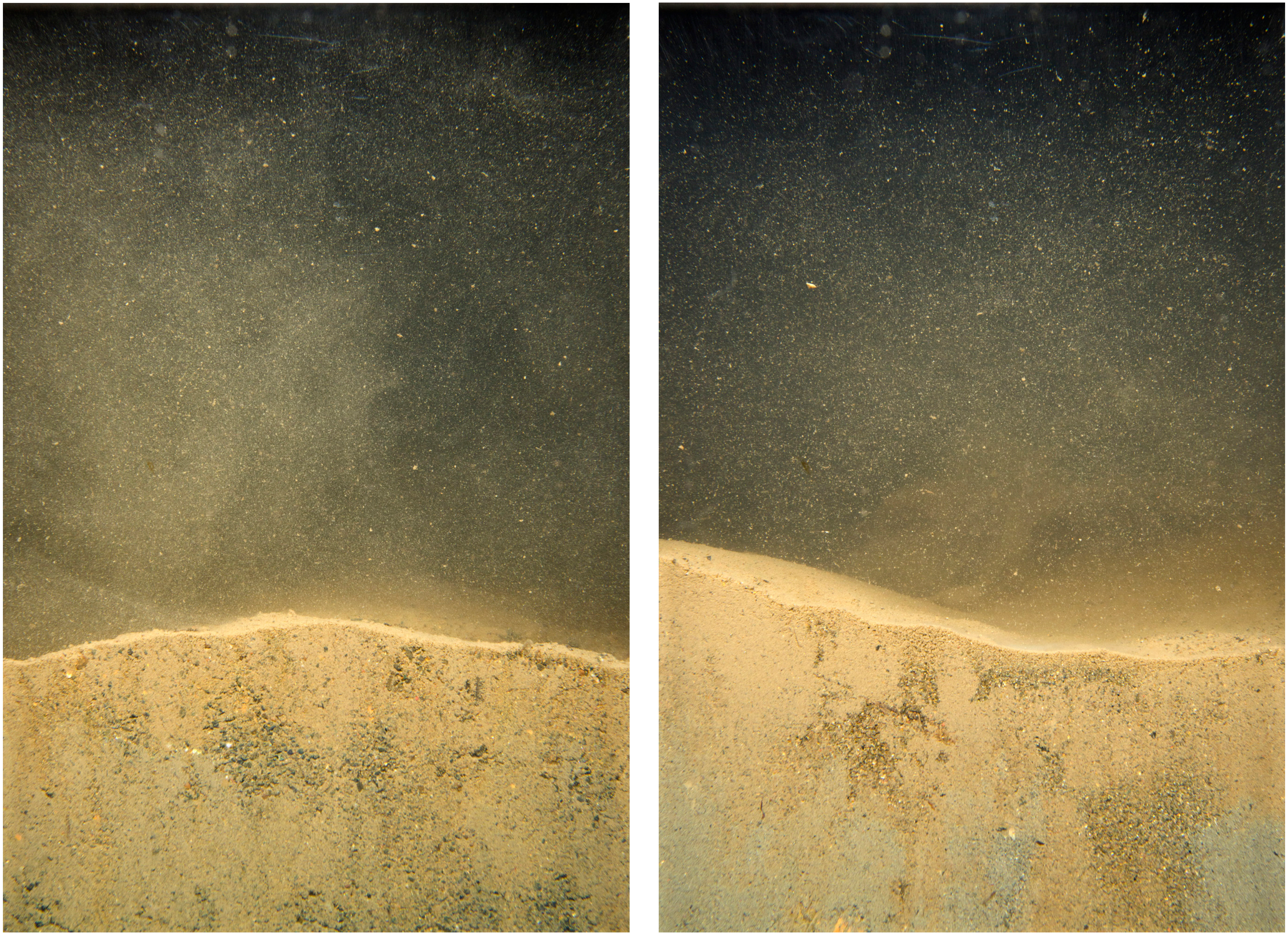

56F **53D**

Figure 9: These profile images from Stations 56F (left) and 53D (right) are typical of the sandy bottoms found along the northern bank of the river in the shallow areas between RM 7 and 9.7. Scale: width of each profile image = 14.5 cm.

Figure 10: This profile image from Station 32B of mud over sand shows a switch in hydraulic regimes from erosional to more recently depositional. Scale: width of image = 14.5 cm.

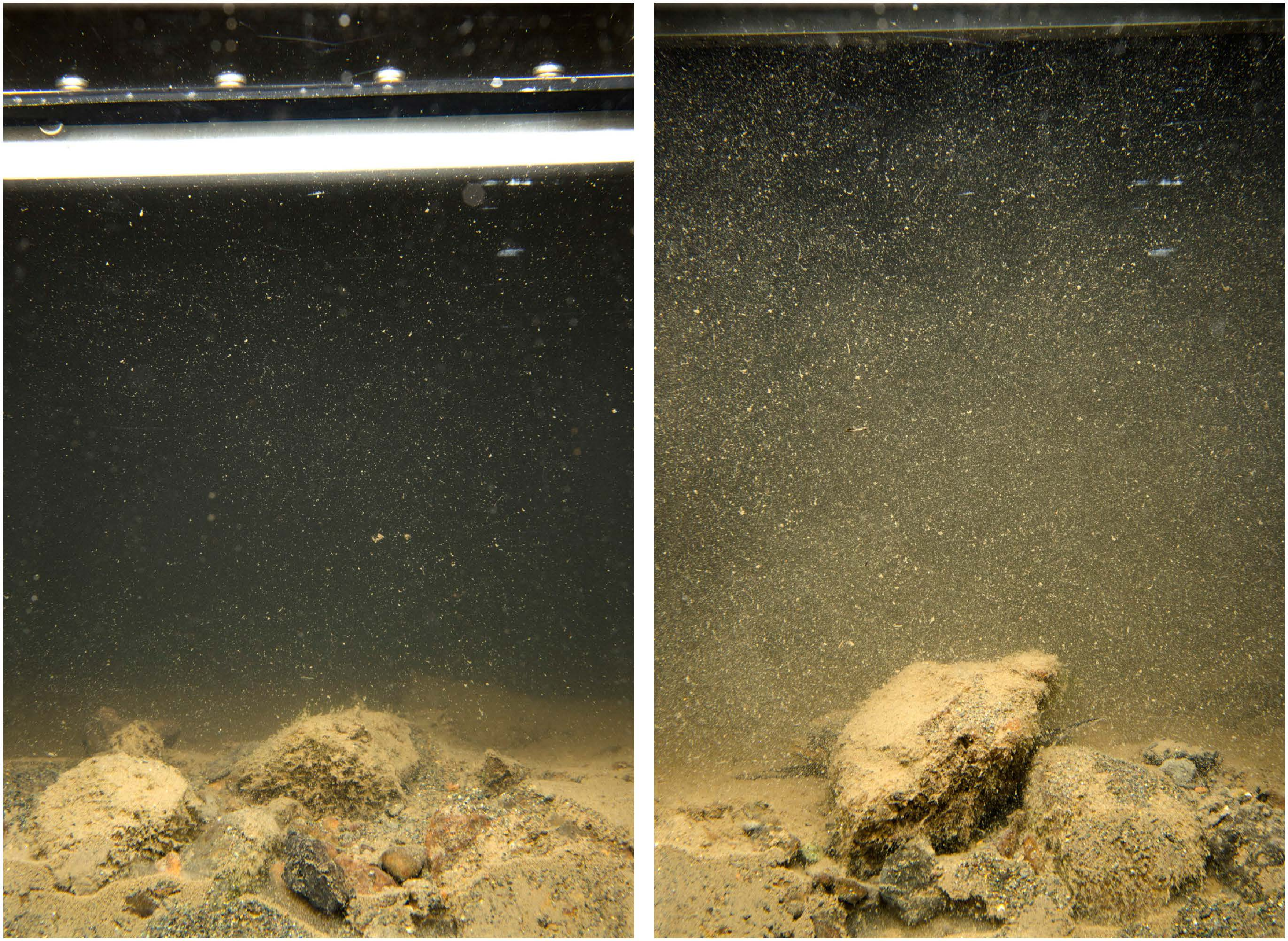

Figure 11: These profile images from nearshore Station 37A show a rocky bottom with a mantle of fine detritus covering the sediment. Scale: width of each profile image = 14.5 cm.

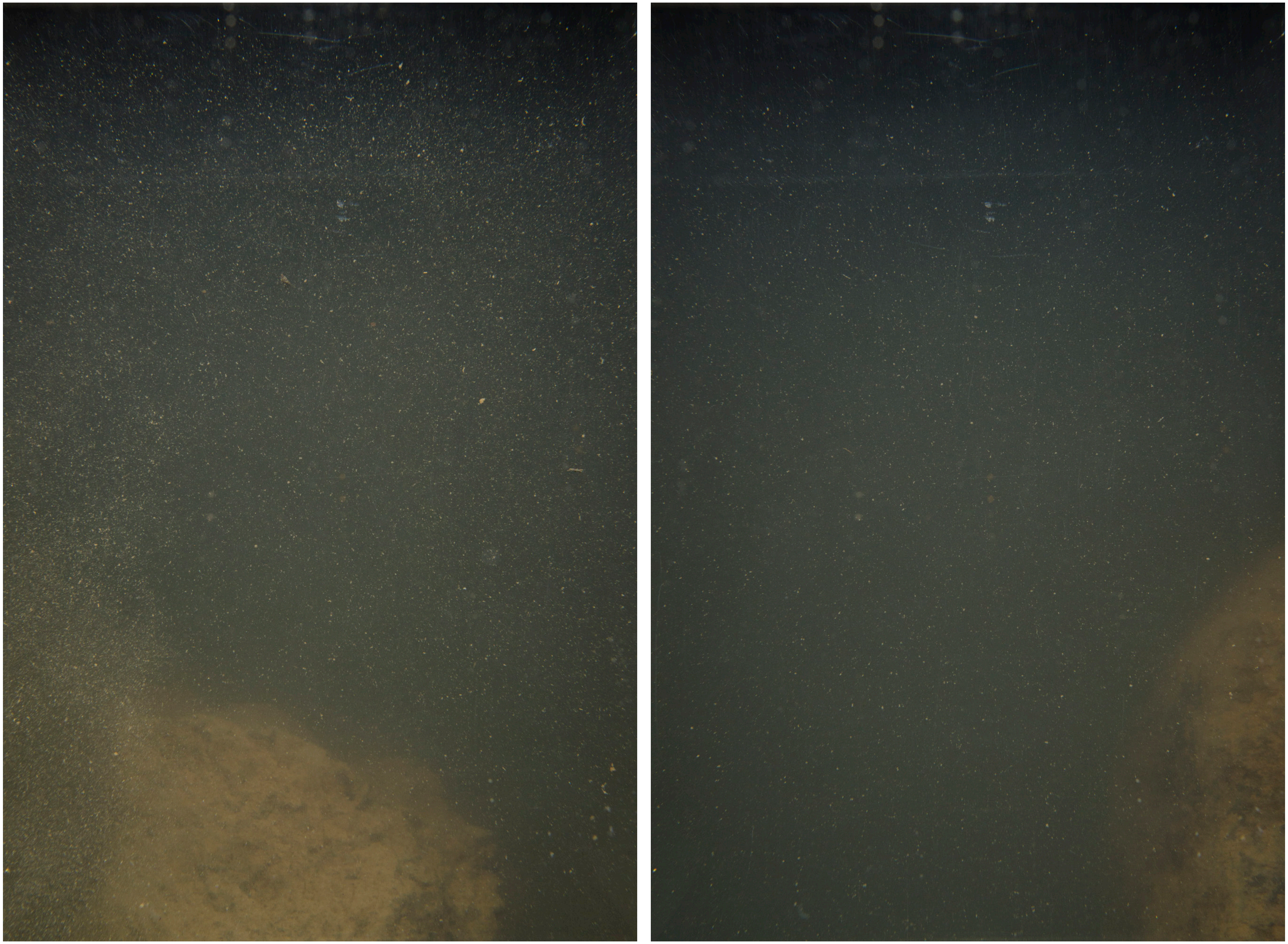

Figure 12: Portions of large rocks can be seen in the background in these two replicate images from Station 46C in the main channel. Scale: width of each profile image = 14.5 cm.

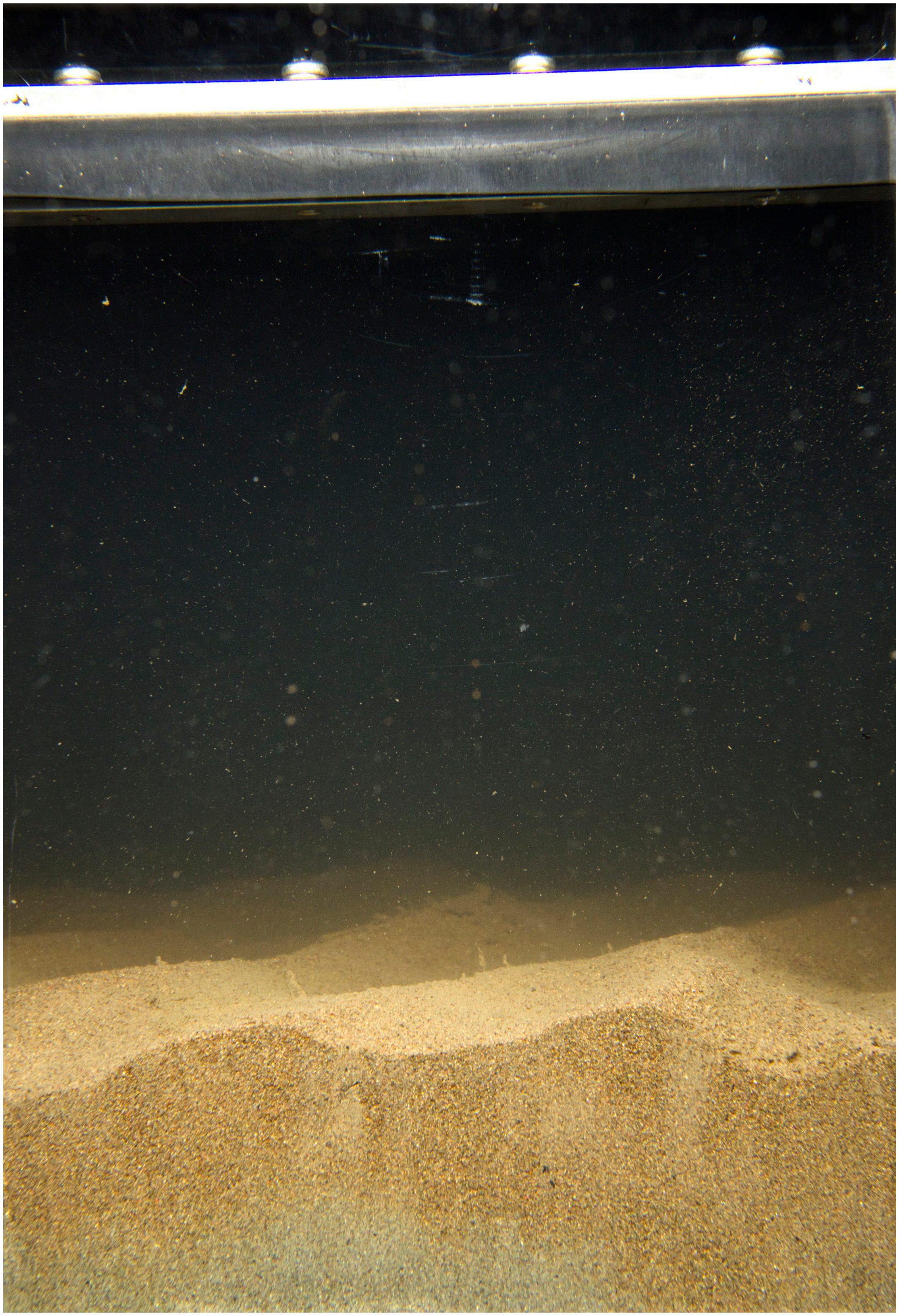

Figure 13: Rippled fine to medium sands can be seen in this profile image from Station 19A. Scale: width of image = 14.5 cm.

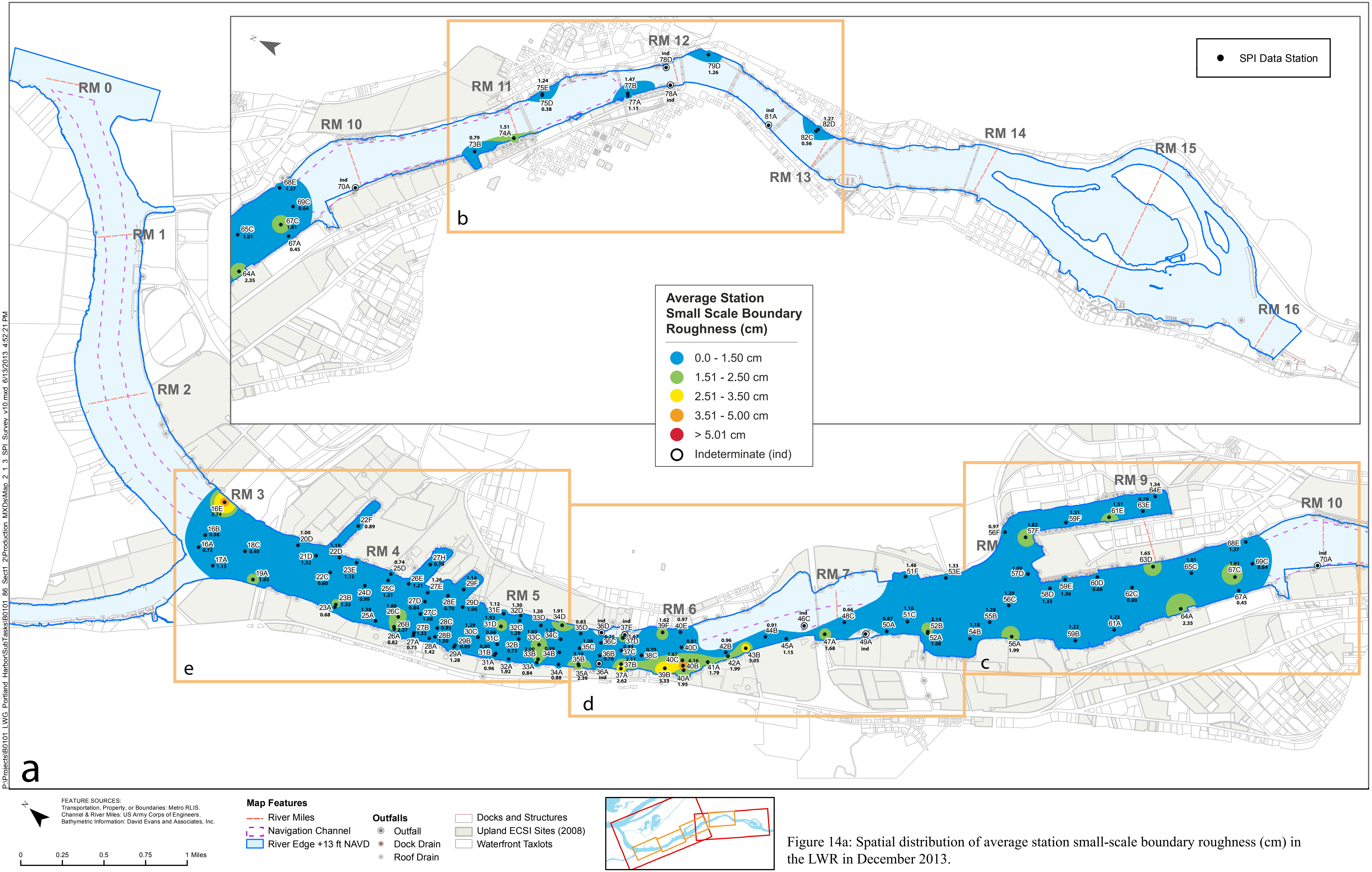

Figure 14a: Spatial distribution of average station small-scale boundary roughness (cm) in the LWR in December 2013.

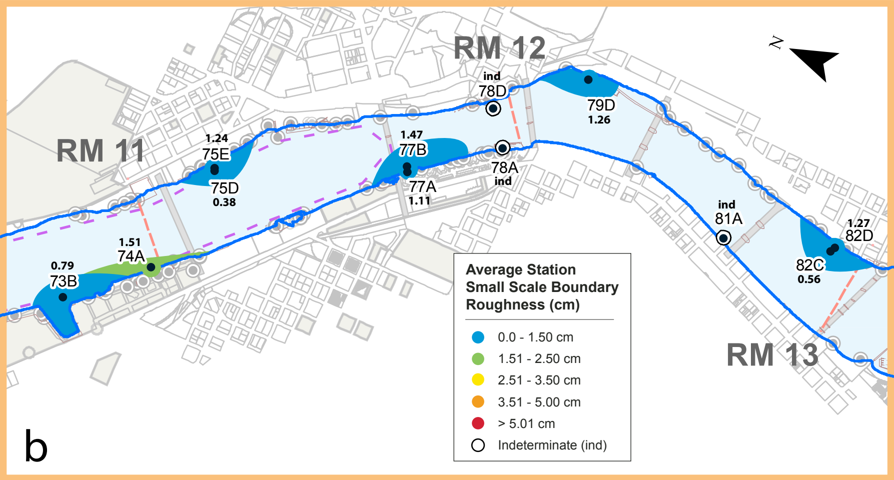

Figure 14b: Spatial distribution of average station small-scale boundary roughness (cm) in the LWR in December 2013.

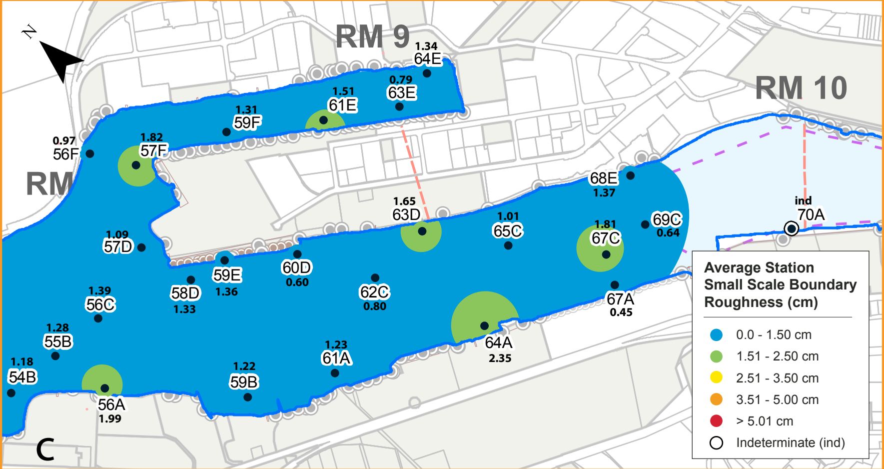

Figure 14c: Spatial distribution of average station small-scale boundary roughness (cm) in the LWR in December 2013.

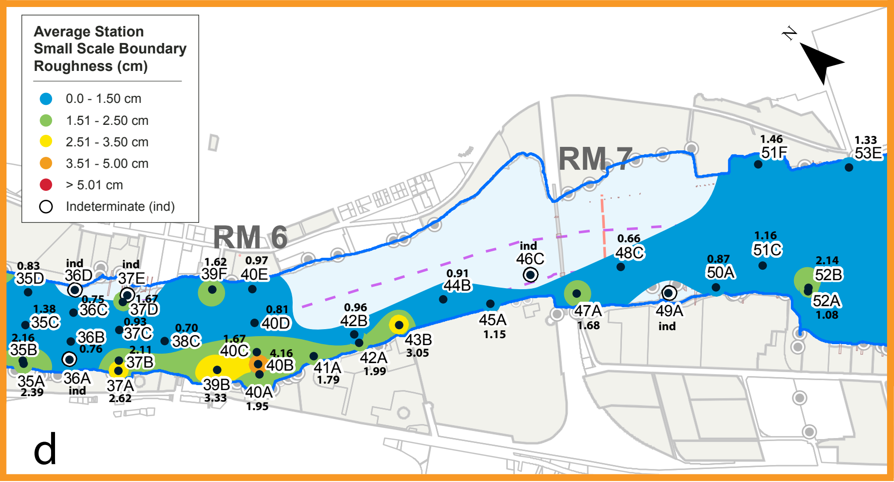

Figure 14d: Spatial distribution of average station small-scale boundary roughness (cm) in the LWR in December 2013.

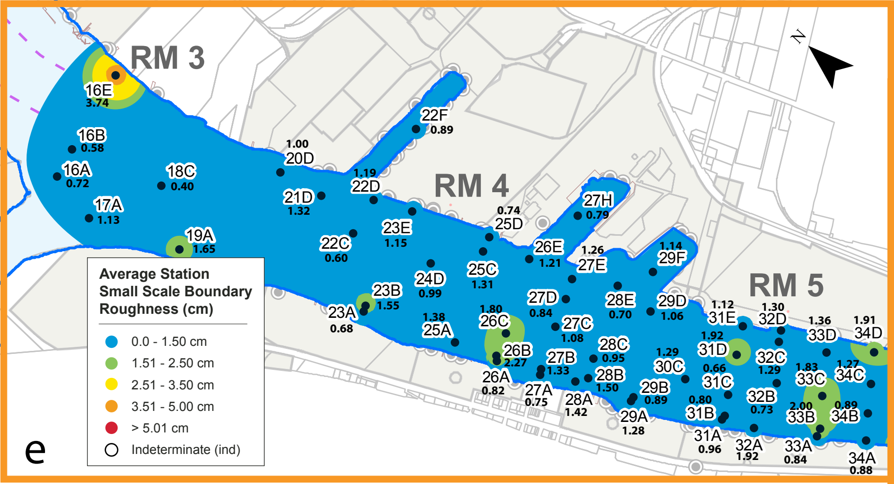

Figure 14e: Spatial distribution of average station small-scale boundary roughness (cm) in the LWR in December 2013.

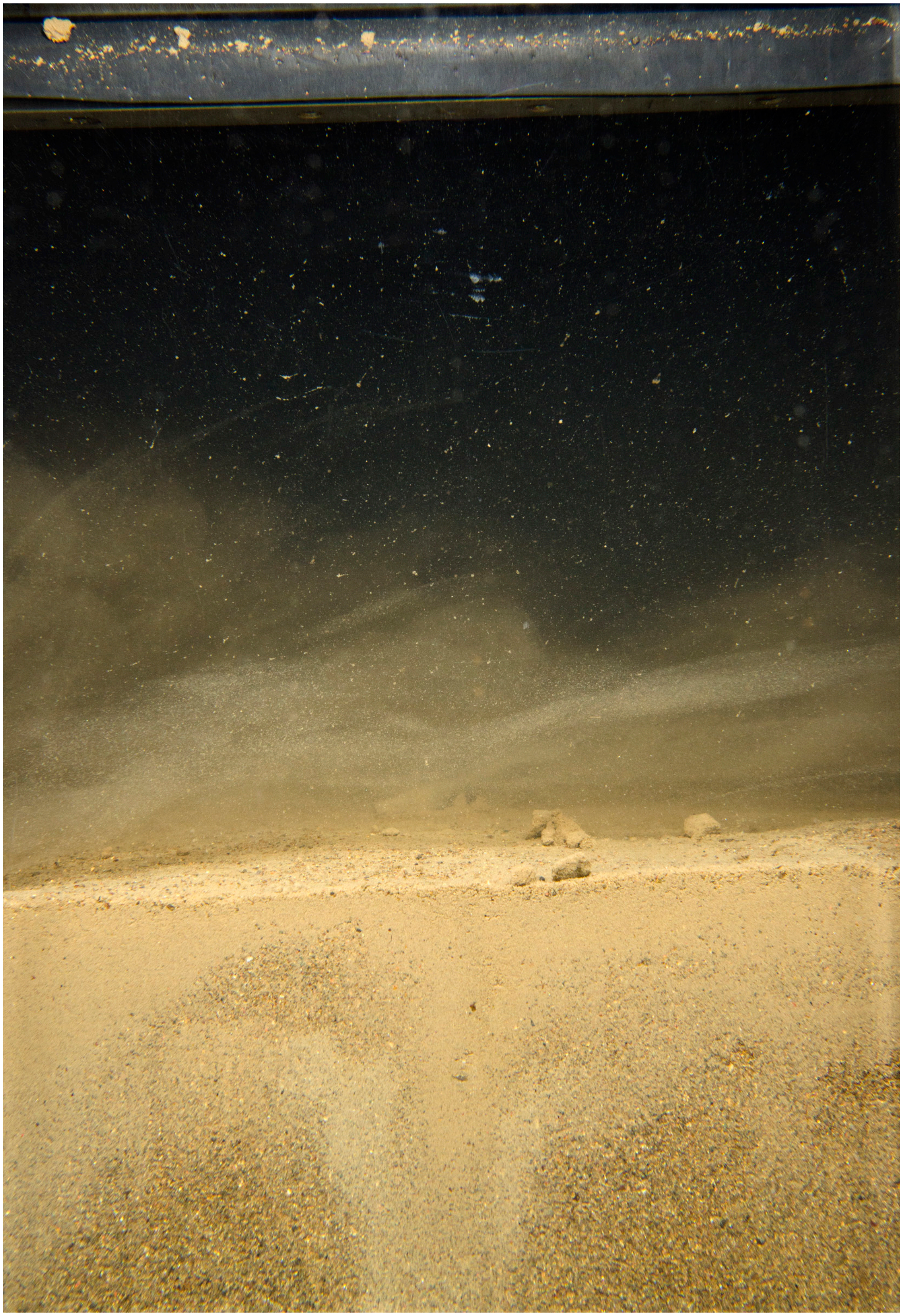

Figure 15: Even though sediment particles can be seen being transported above the bed by apparently strong river currents in this profile image from Station 16A, the surface boundary roughness value (0.56 cm) is well below the overall site average value. Scale: width of image = 14.5 cm.

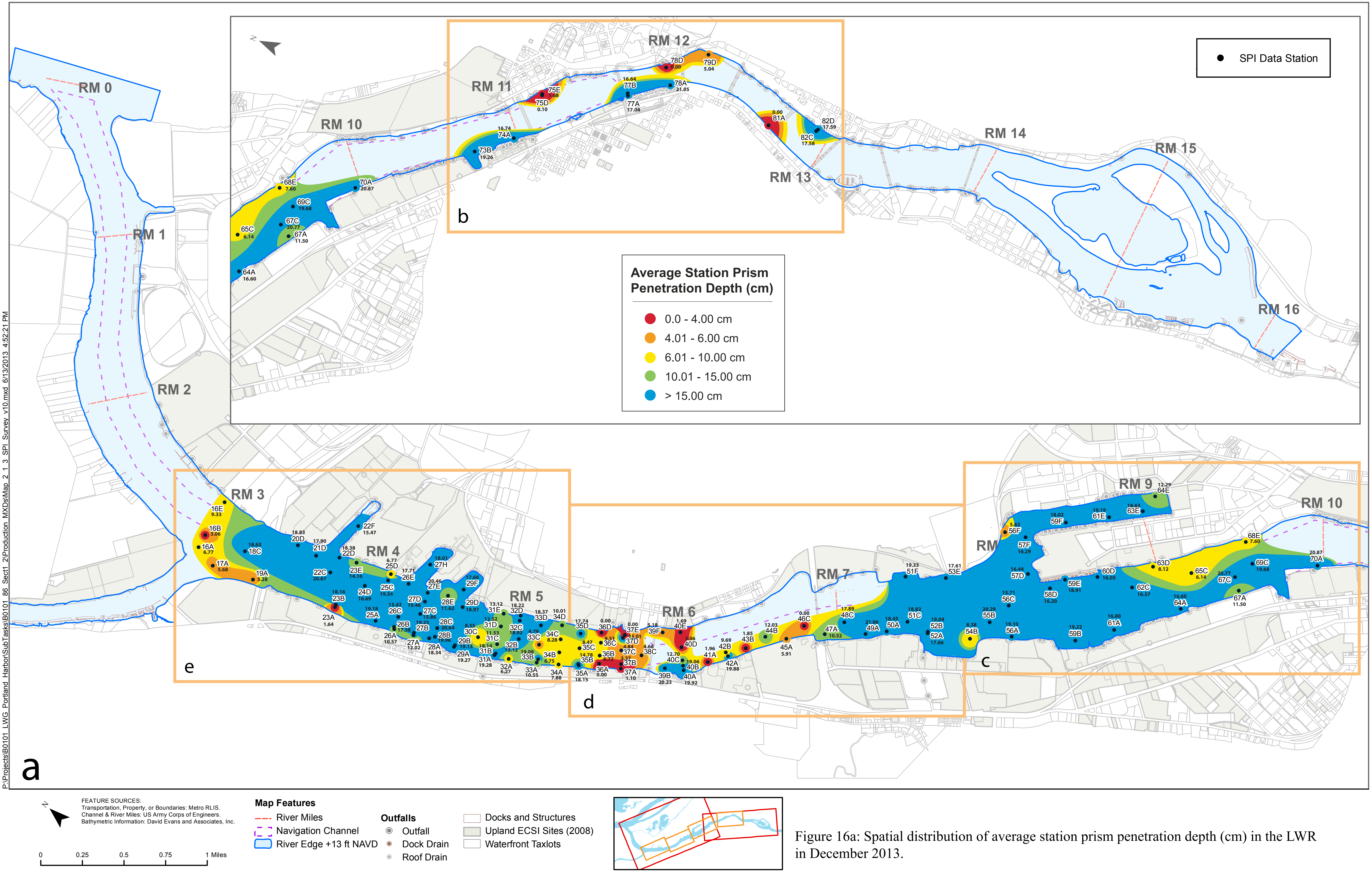

Figure 16a: Spatial distribution of average station prism penetration depth (cm) in the LWR in December 2013.

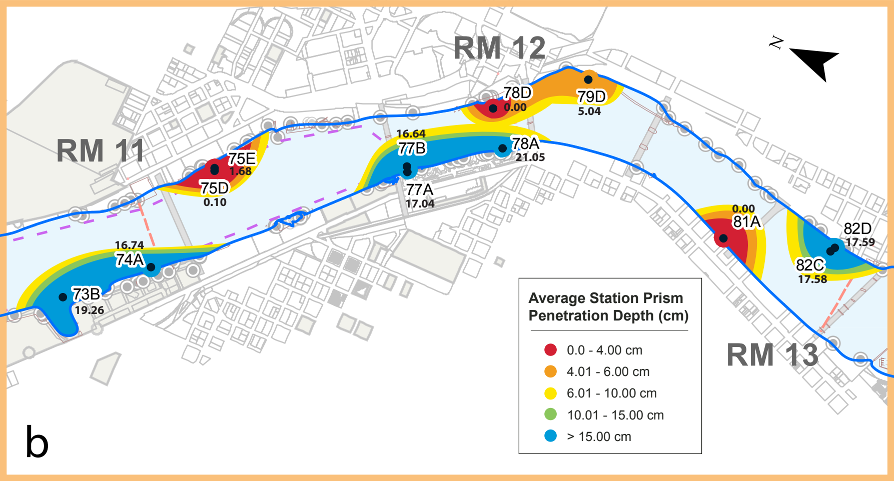

Figure 16b: Spatial distribution of average station prism penetration depth (cm) in the LWR in December 2013.

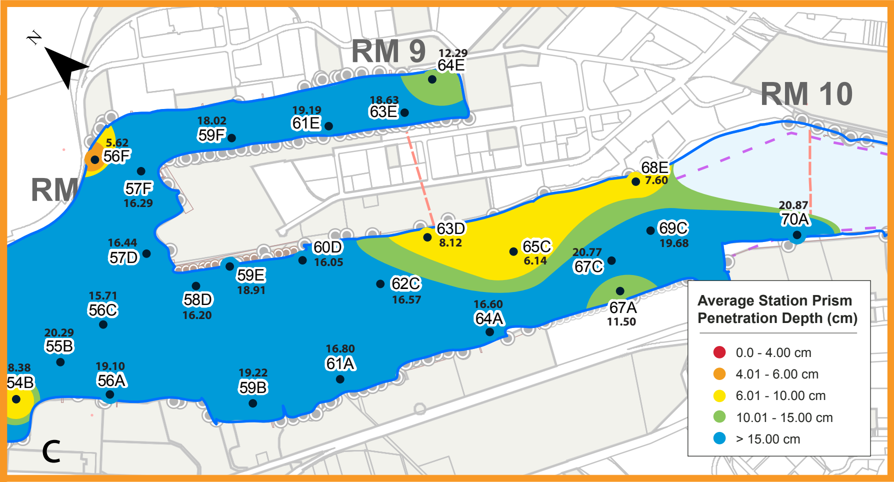

Figure 16c: Spatial distribution of average station prism penetration depth (cm) in the LWR in December 2013.

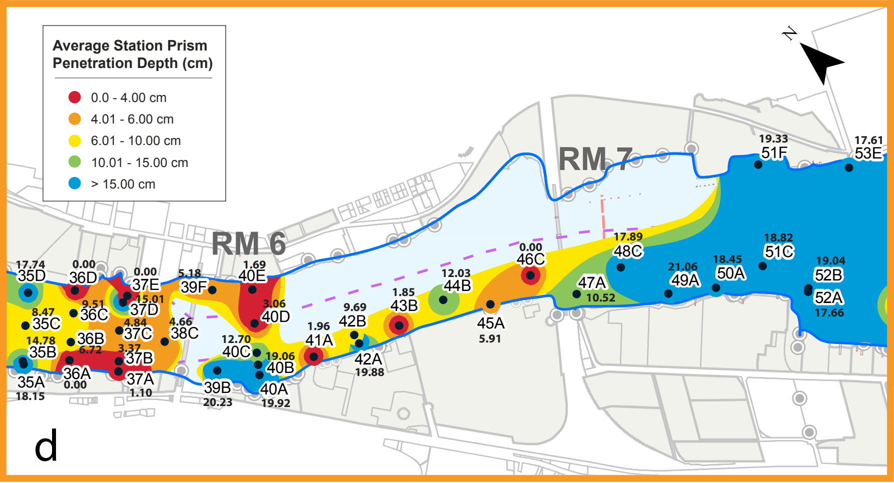

Figure 16d: Spatial distribution of average station prism penetration depth (cm) in the LWR in December 2013.

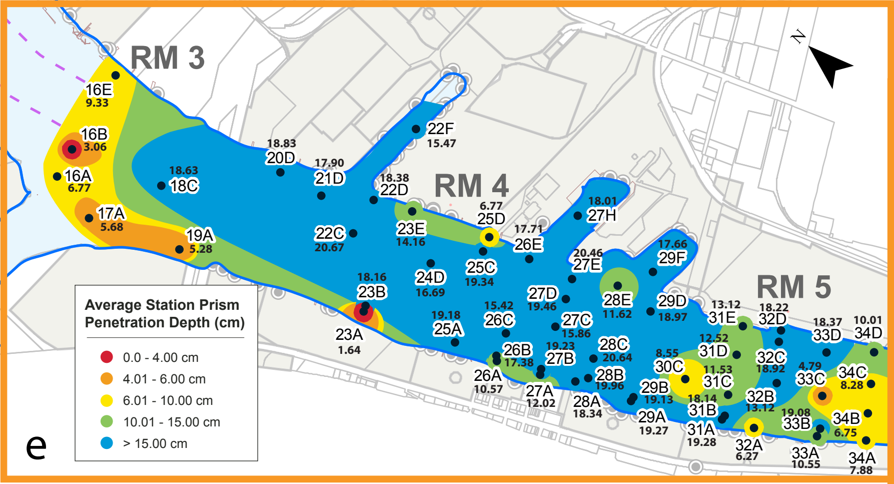

Figure 16e: Spatial distribution of average station prism penetration depth (cm) in the LWR in December 2013.

Figure 17: The relatively high volume of subsurface methane gas in this profile image from Station 78A contributed to the low bearing strength and high prism penetration values at this location. Scale: width of image = 14.5 cm

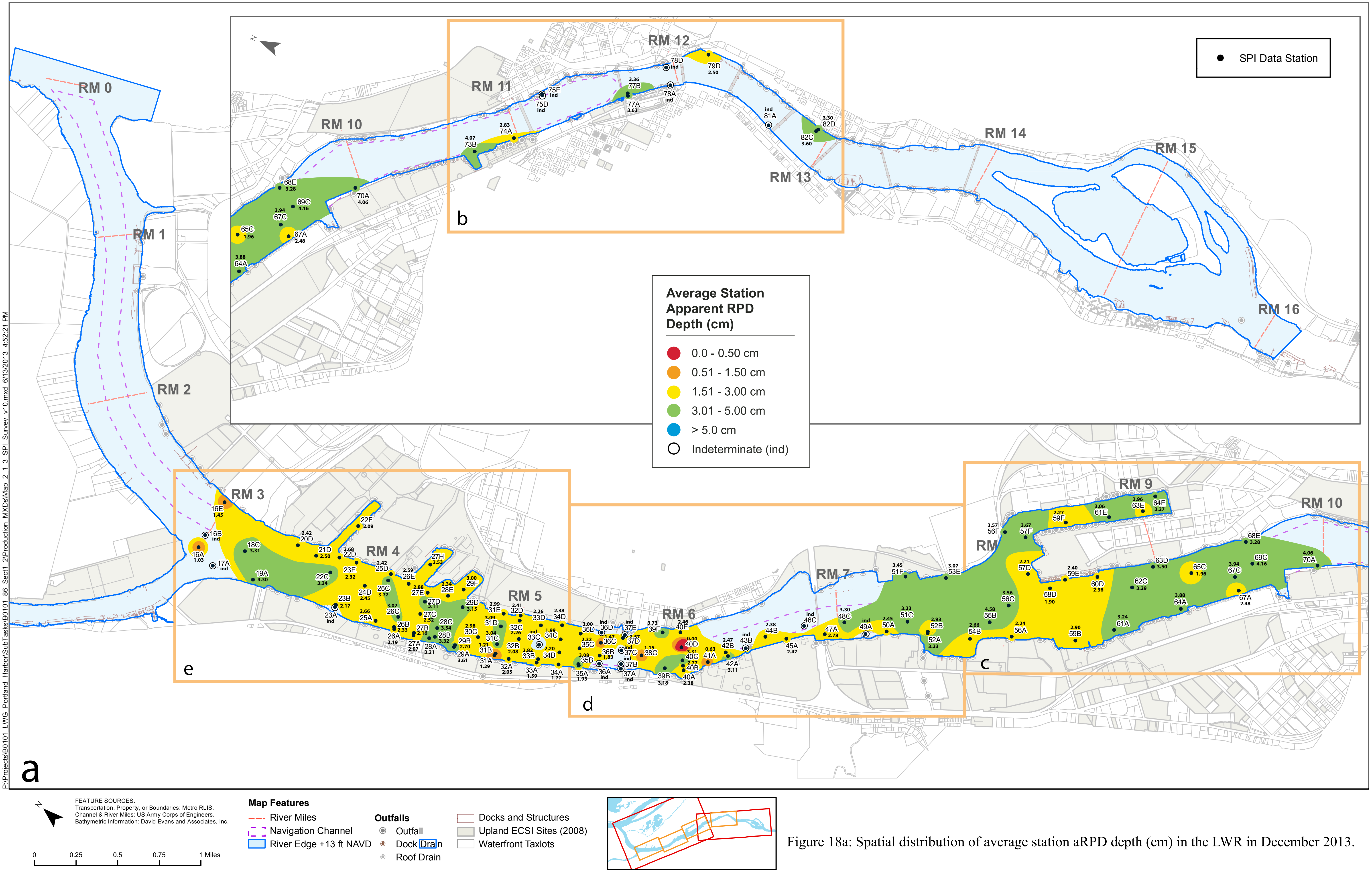

Figure 18a: Spatial distribution of average station aRPD depth (cm) in the LWR in December 2013.

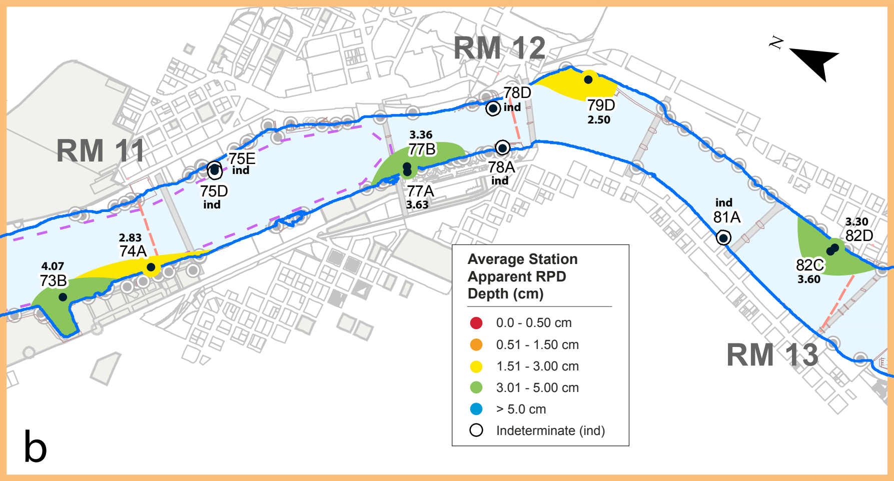

Figure 18b: Spatial distribution of average station aRPD depth (cm) in the LWR in December 2013.

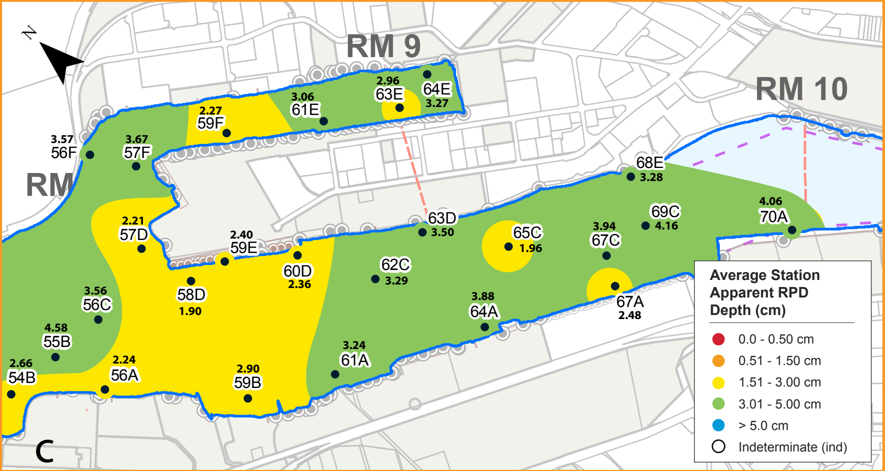

Figure 18c: Spatial distribution of average station aRPD depth (cm) in the LWR in December 2013.

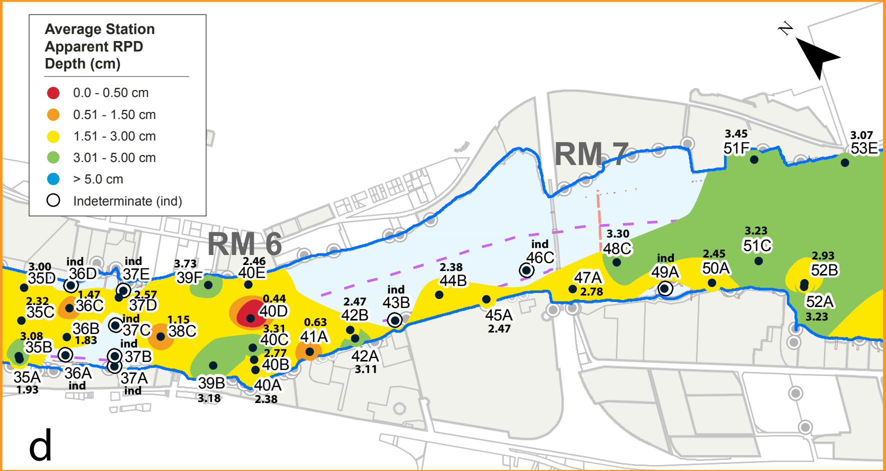

Figure 18d: Spatial distribution of average station aRPD depth (cm) in the LWR in December 2013.

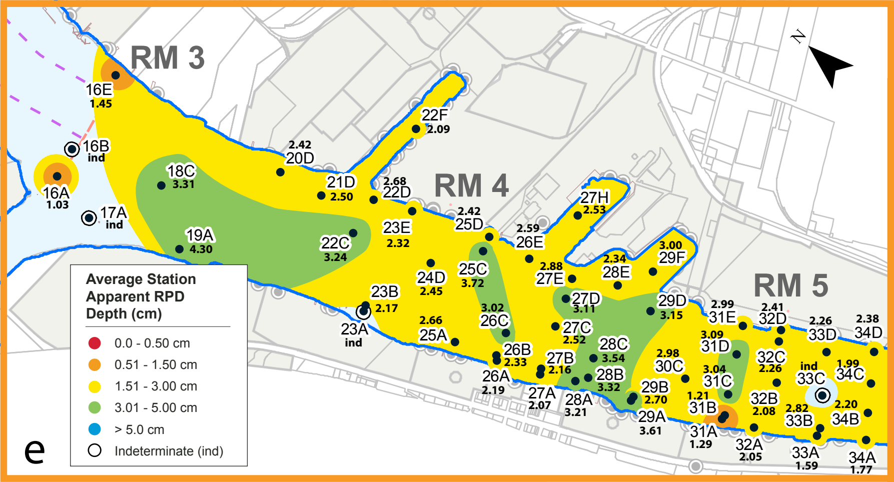

Figure 18e: Spatial distribution of average station aRPD depth (cm) in the LWR in December 2013.

Figure 19: This profile image from Station 73B in the upper reach surveyed shows a large feeding pit at the surface along with subsurface feeding voids and a relatively deep (4.1 cm) aRPD due to the bioturbational activities of the resident infauna.

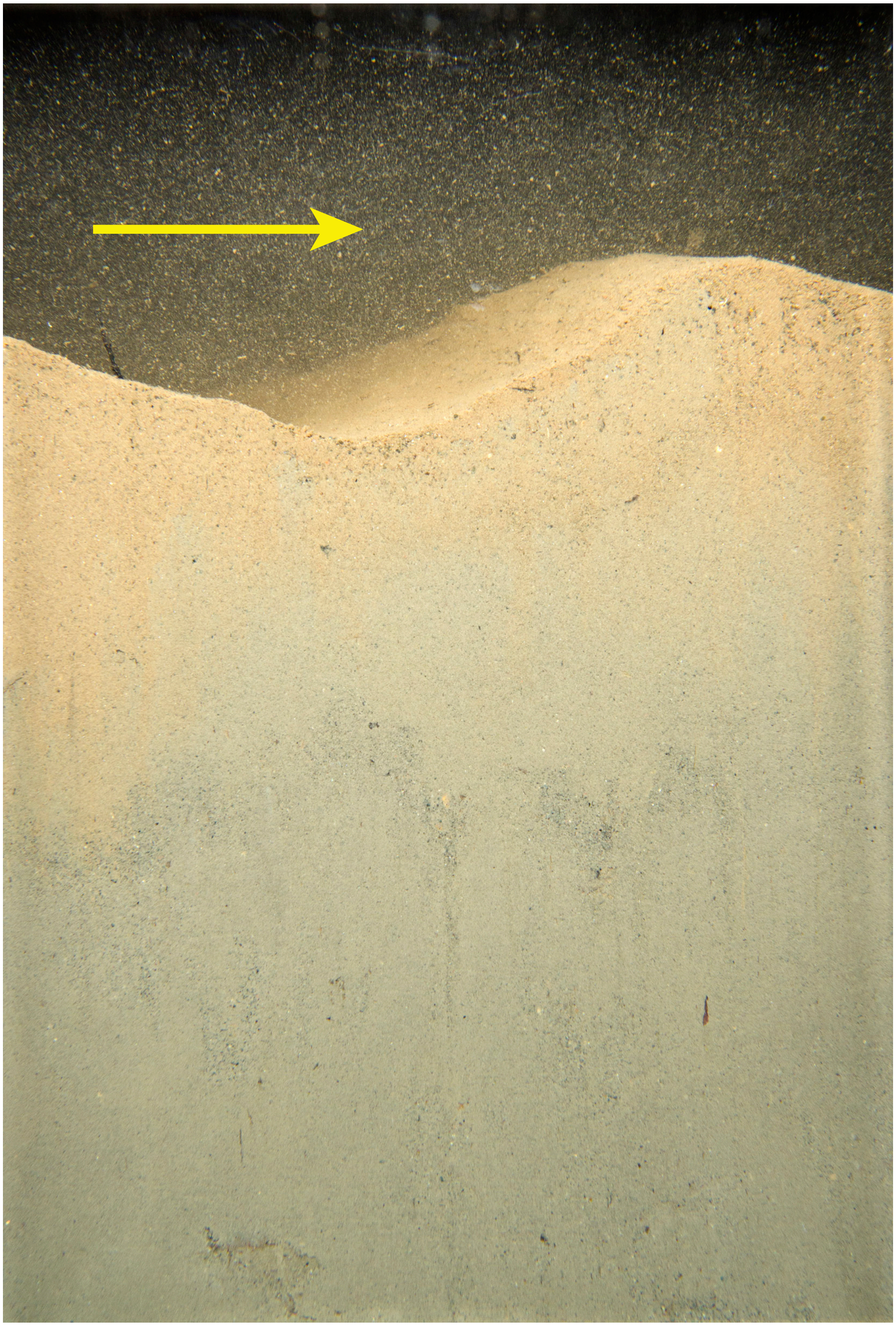

Figure 20: The surface oxidized layer at Station 27C has a slightly enhanced depth due to the surface roughness element of the sand ripple interacting with the bottom current (arrow indicates flow direction). Scale: width of profile image = 14.5 cm.

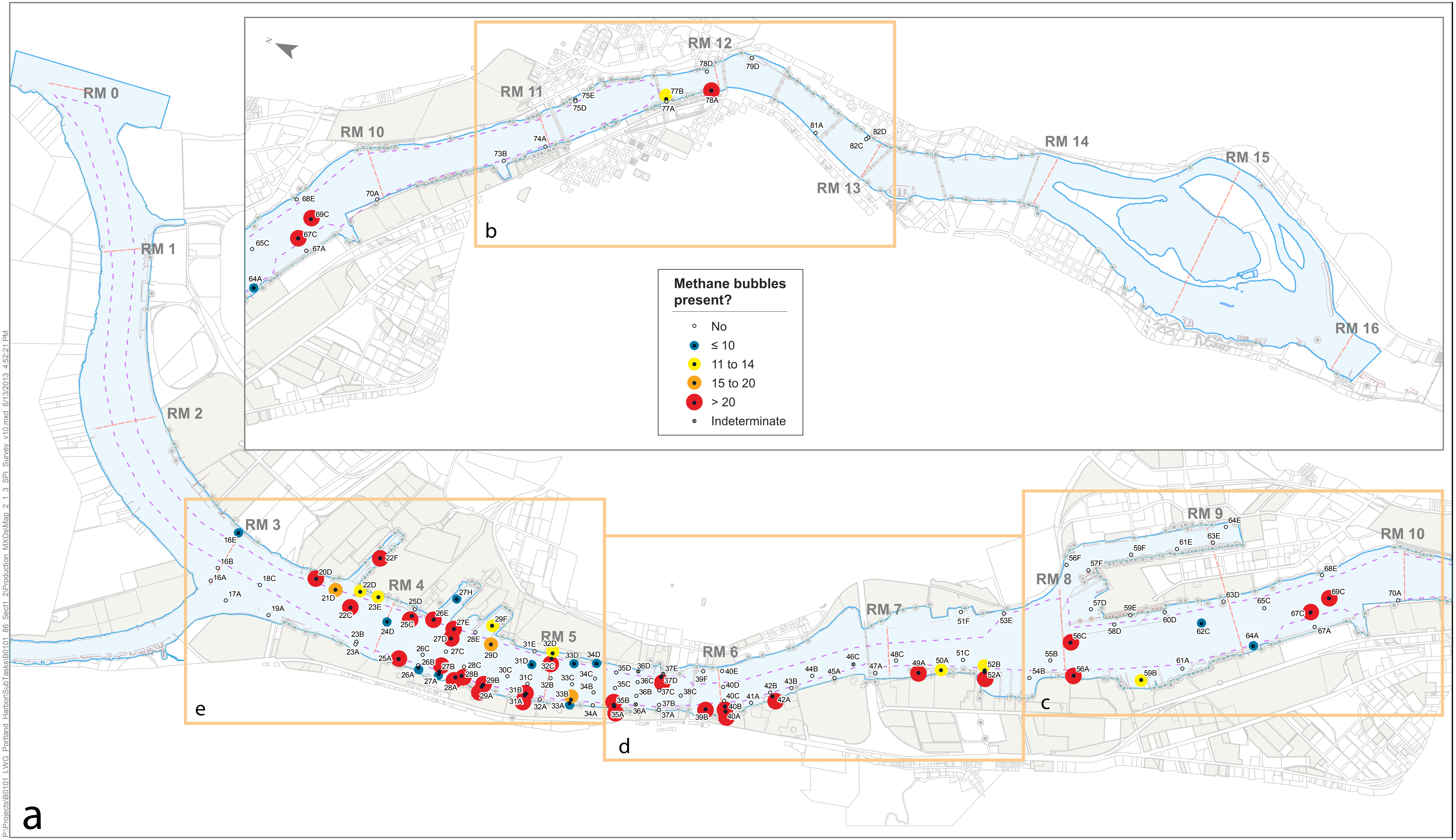

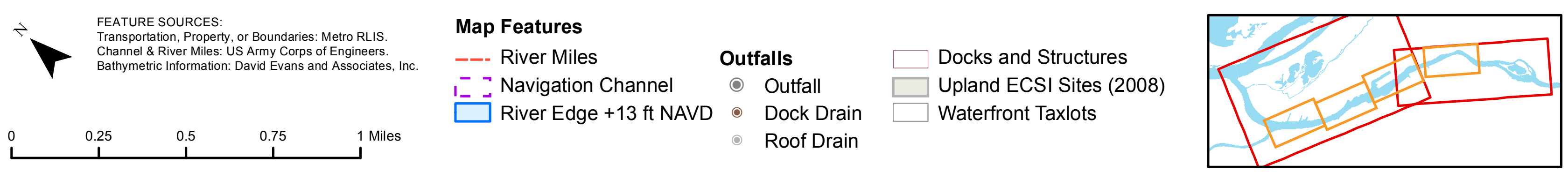

Figure 21a: Spatial distribution and relative amount of subsurface methane at stations surveyed in the LWR, December, 2013.

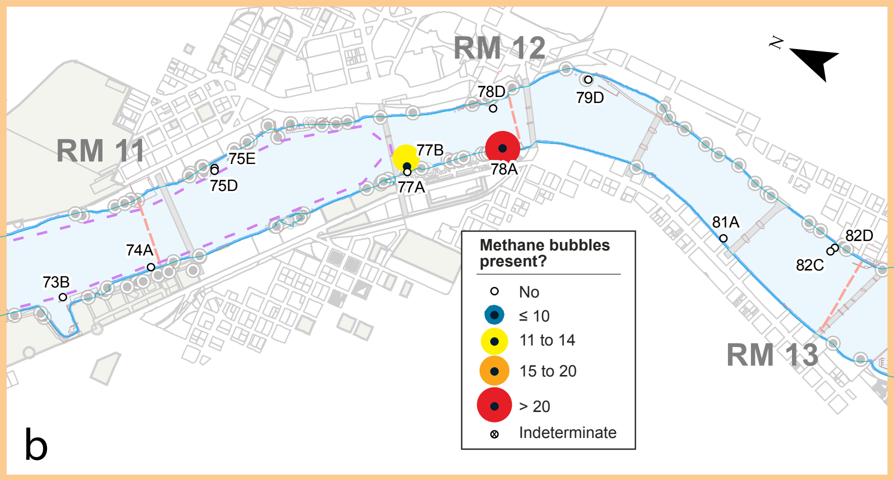

Figure 21b: Spatial distribution and relative amount of subsurface methane at stations surveyed in the LWR, December, 2013.

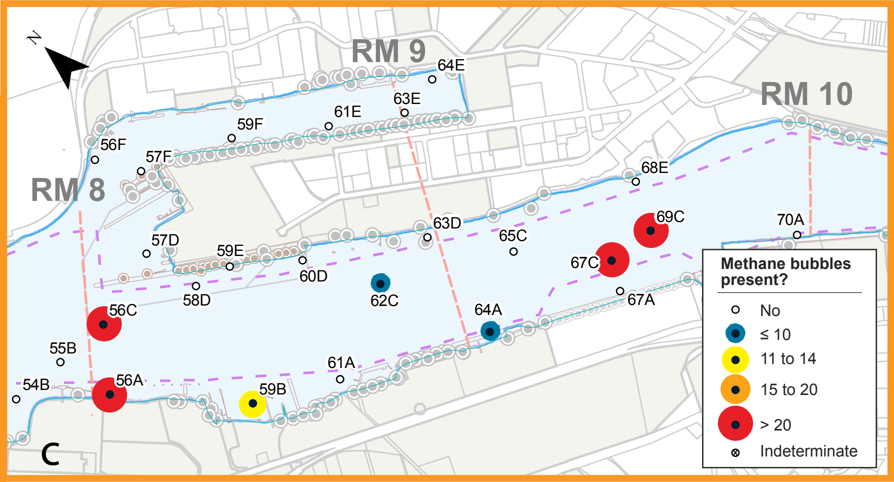

Figure 21c: Spatial distribution and relative amount of subsurface methane at stations surveyed in the LWR, December, 2013.

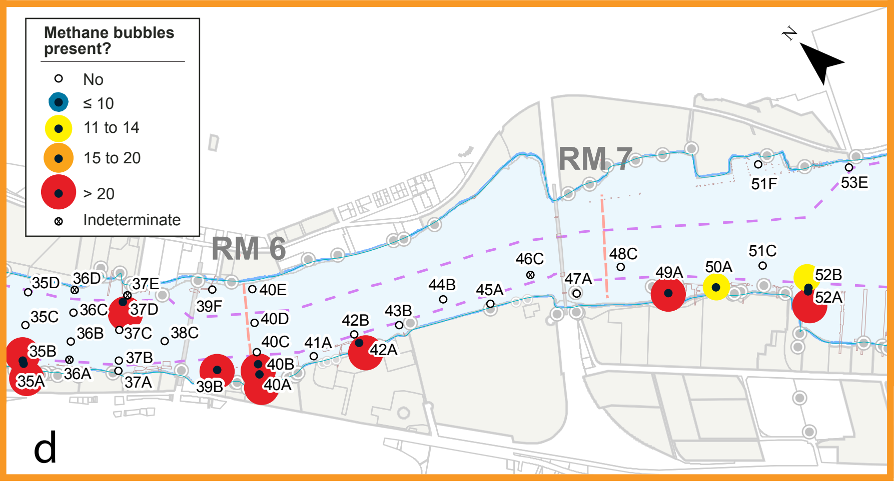

Figure 21d: Spatial distribution and relative amount of subsurface methane at stations surveyed in the LWR, December, 2013.

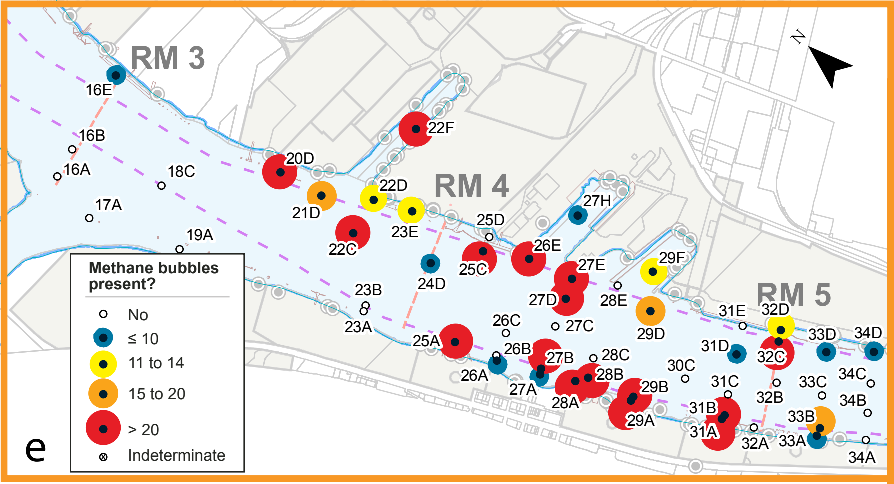

Figure 21e: Spatial distribution and relative amount of subsurface methane at stations surveyed in the LWR, December, 2013.

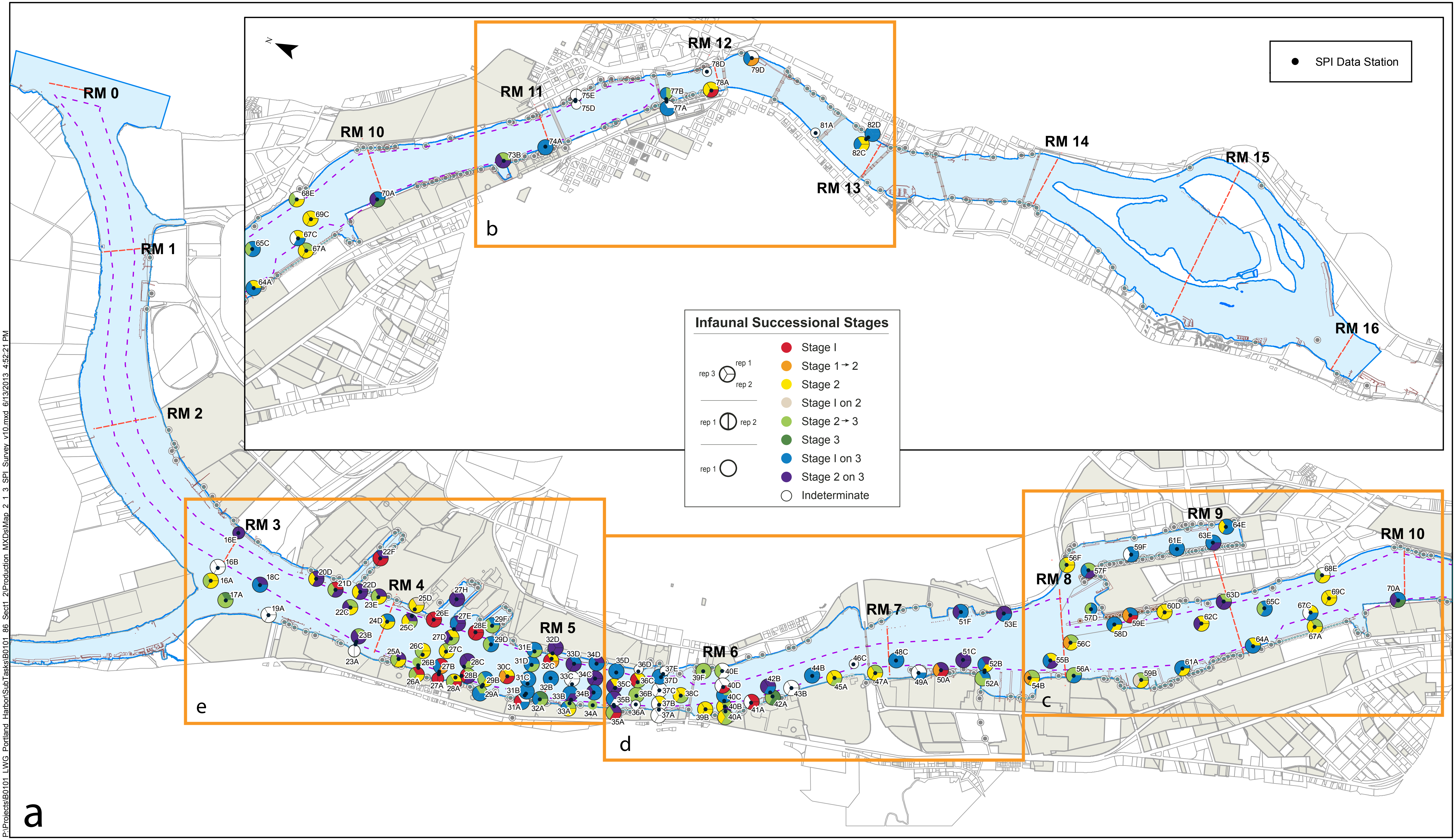

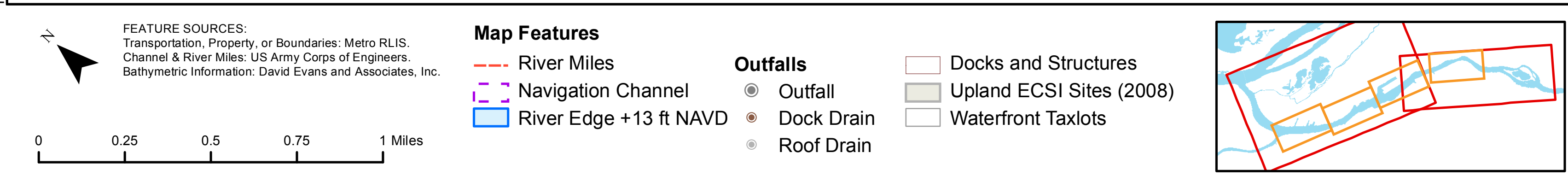

Figure 22a: Spatial distribution of infaunal successional stages at locations surveyed in the LWR, December, 2013.

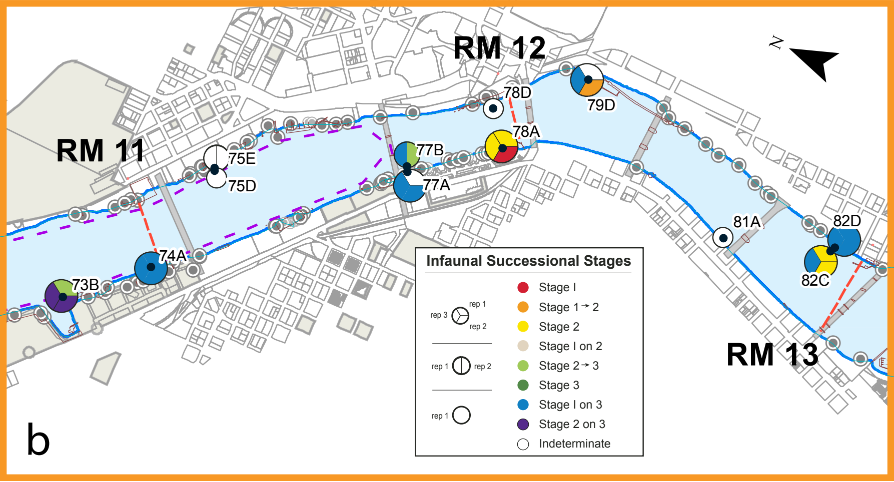

Figure 22b: Spatial distribution of infaunal successional stages at locations surveyed in the LWR, December, 2013.

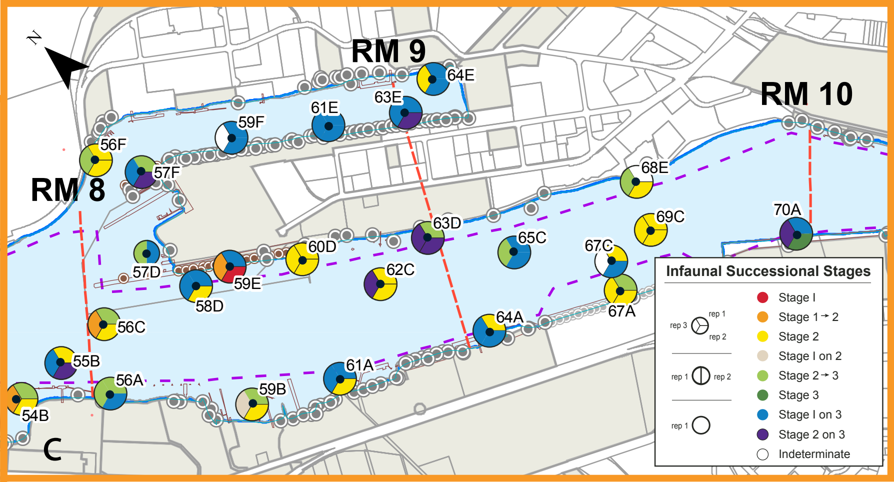

Figure 22: Spatial distribution of infaunal successional stages at locations surveyed in the LWR, December, 2013.

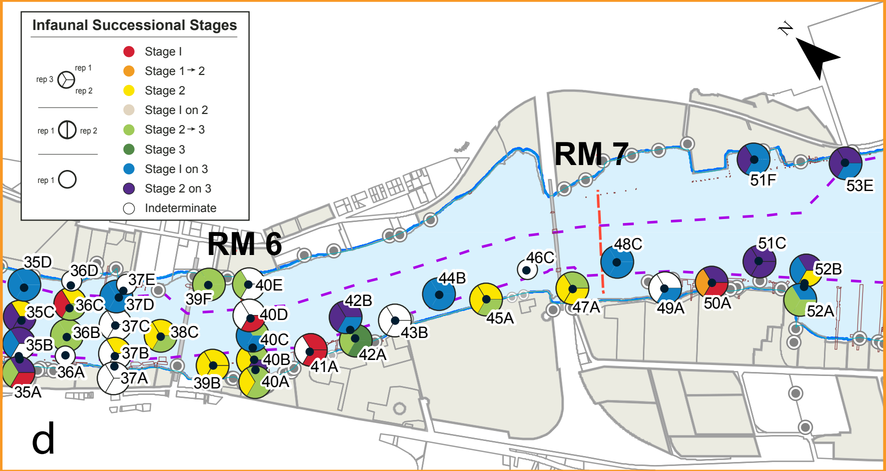

Figure 22d: Spatial distribution of infaunal successional stages at locations surveyed in the LWR, December, 2013.

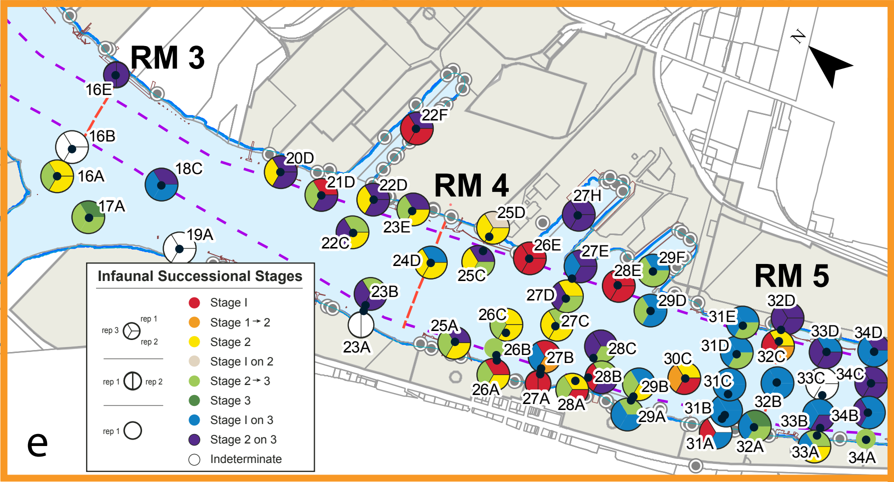

Figure 22e: Spatial distribution of infaunal successional stages at locations surveyed in the LWR, December, 2013.

Figure 23: This profile image from Station 74A in the upper Willamette River shows evidence of Stage 3 taxa in the form of subsurface feeding voids and transected burrows (arrows) as well as a portion of an annelid against the faceplate in the bottom right corner. Scale: width of image =14.5 cm.

Figure 24: This profile image from Station 25A shows evidence of Stage 3 taxa at depth (arrows) despite the obvious accumulation of fine-grained sediment through natural depositional processes at this nearshore location. Scale: width of image = 14.5 cm.

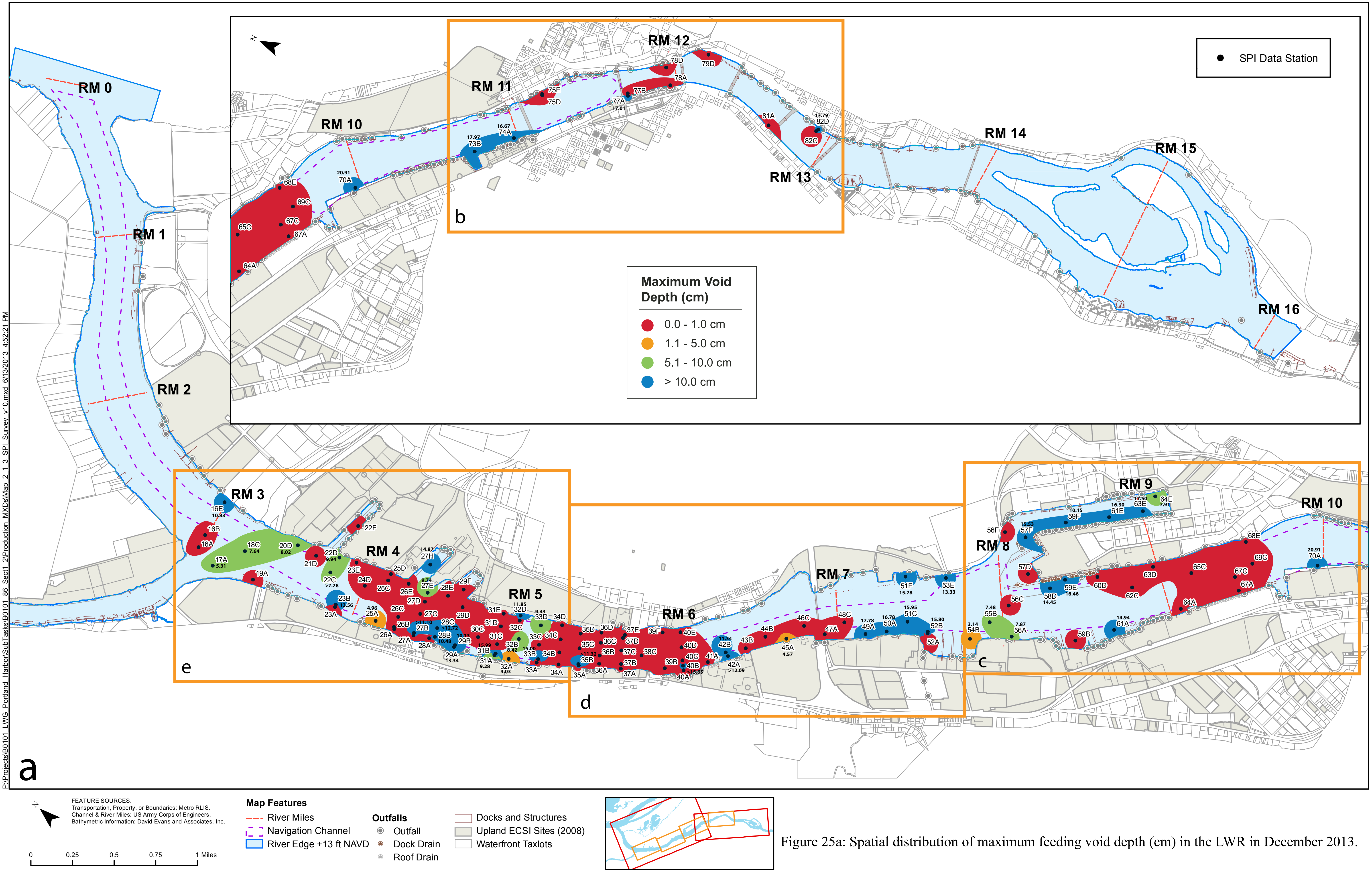

Figure 25a: Spatial distribution of maximum feeding void depth (cm) in the LWR in December 2013.

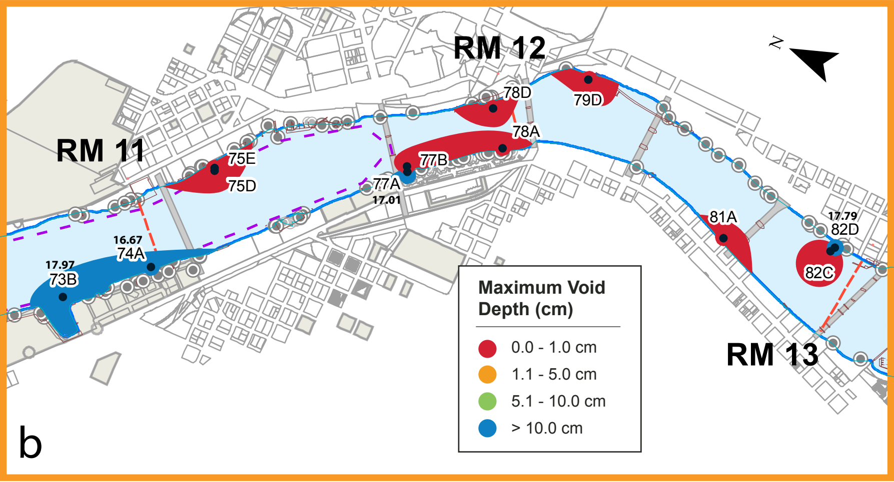

Figure 25b: Spatial distribution of maximum feeding void depth (cm) in the LWR in December 2013.

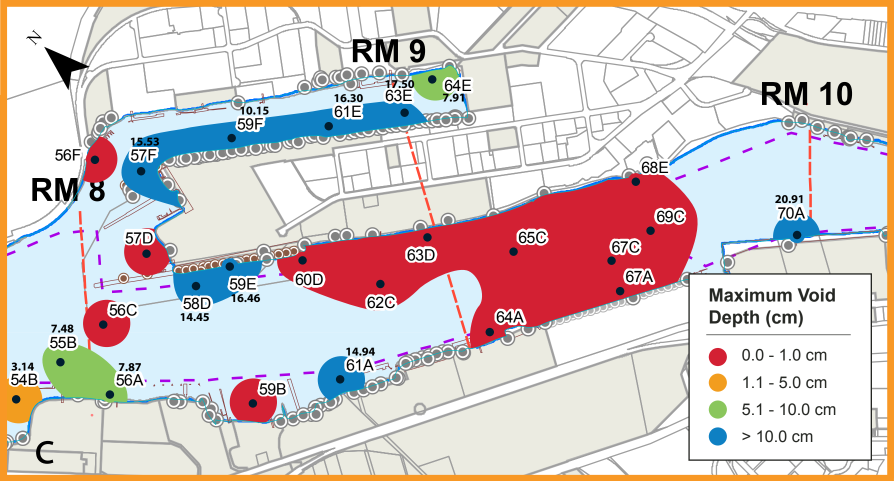

Figure 25c: Spatial distribution of maximum feeding void depth (cm) in the LWR in December 2013.

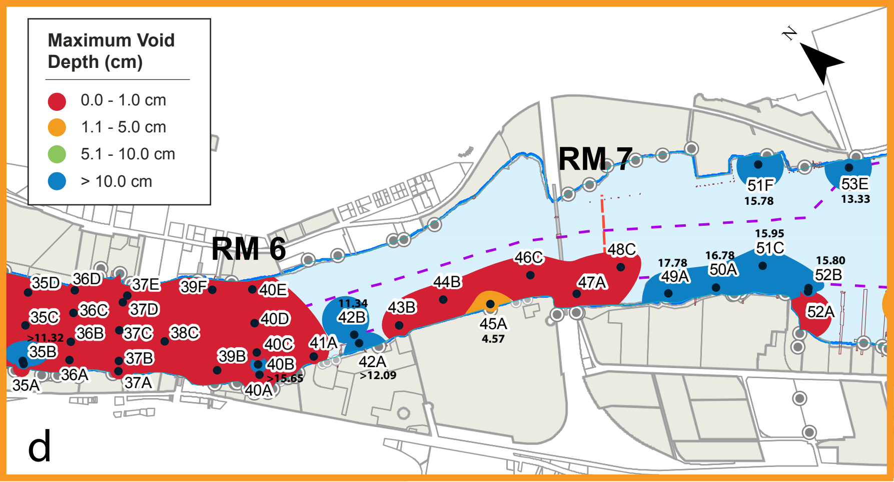

Figure 25d: Spatial distribution of maximum feeding void depth (cm) in the LWR in December 2013.

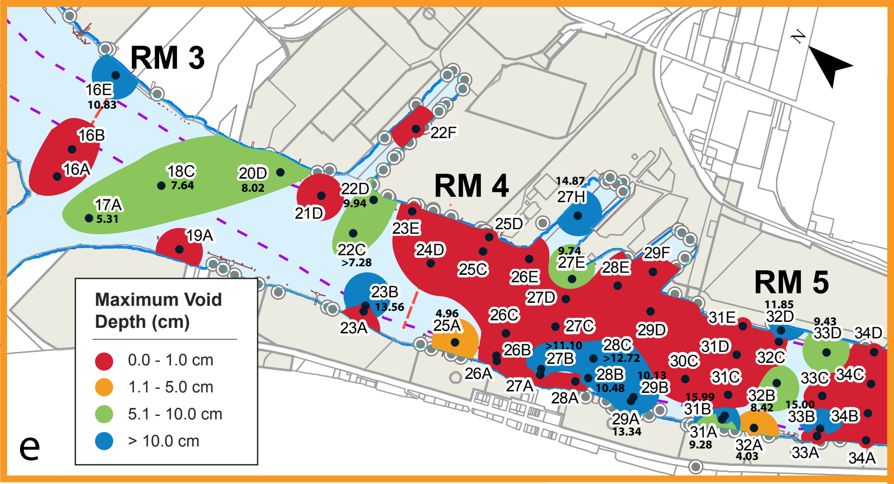

Figure 25e: Spatial distribution of maximum feeding void depth (cm) in the LWR in December 2013.

Figure 26: The sediment in this profile image from Station 67C has relatively low bearing strength and high water content; while subsurface feeding voids are not visible, other evidence (arrows) of Stage 3 taxa are. Scale: width of image = 14.5 cm.

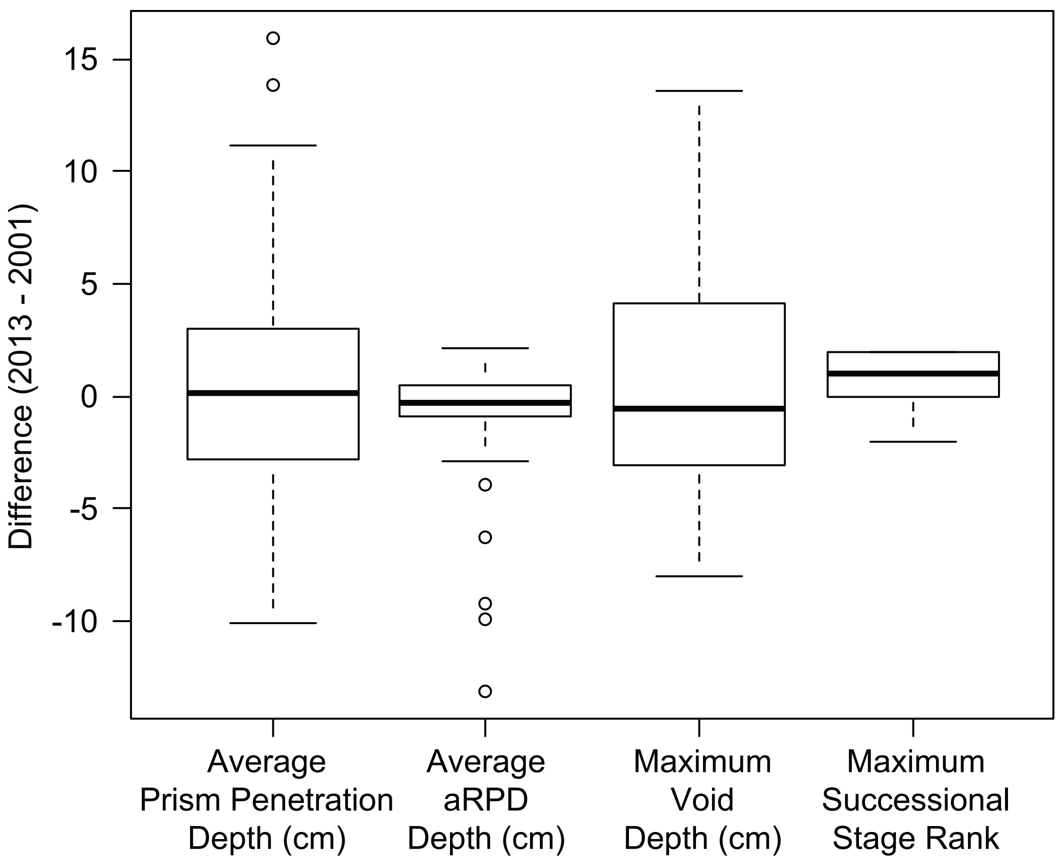

Figure 27: Temporal change at stations surveyed in 2001 and 2013 (n=125) for average camera prism penetration depth, average aRPD depth, maximum void depth, and maximum successional stage rank.

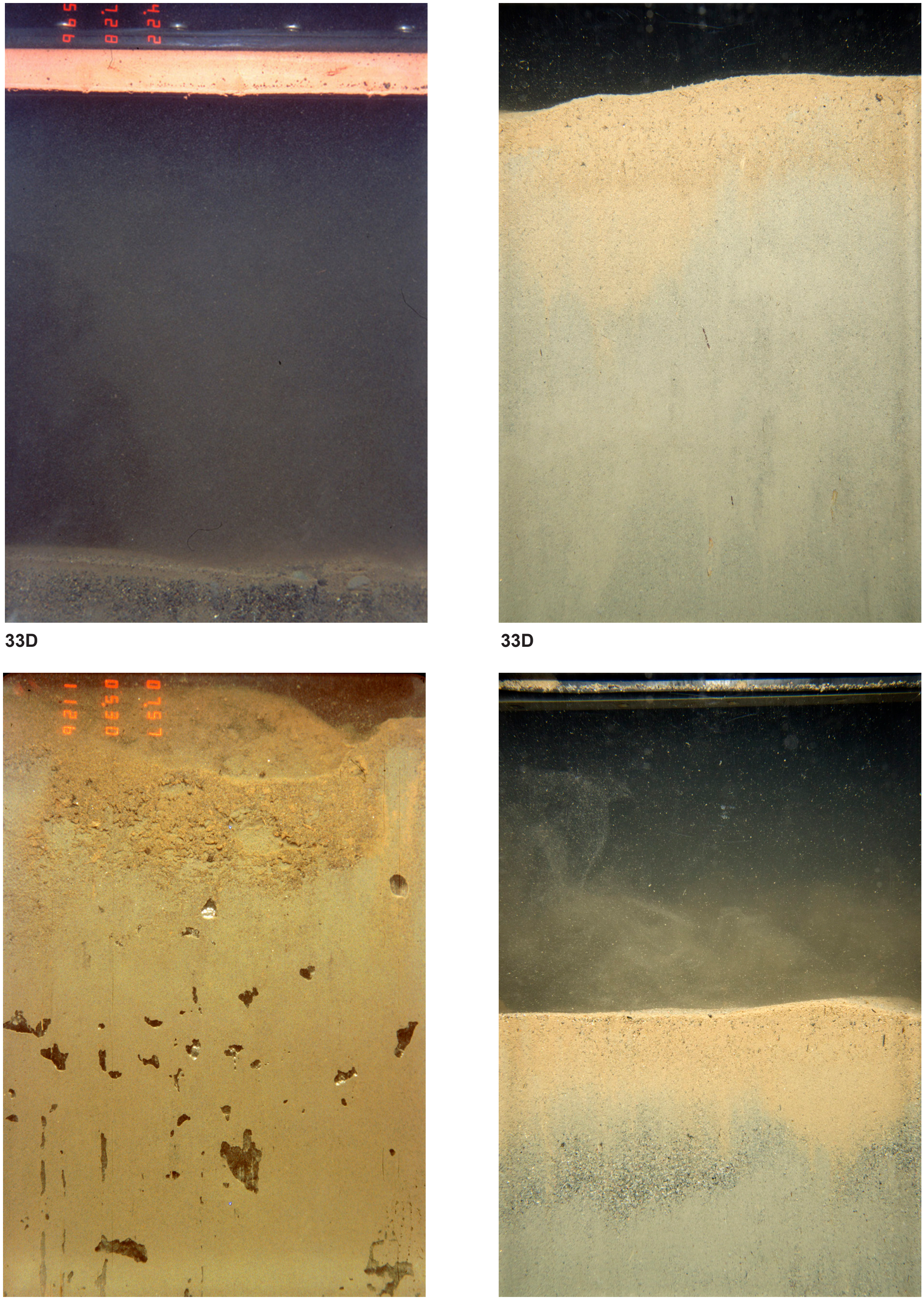

Figure 28: These profile images from Stations 33D (top row) and 42B (bottom row) from 2001 and 2013 show similar variation in sediment type and prism penetration depth in each direction. Scale: width of each profile image = 14.5 cm.

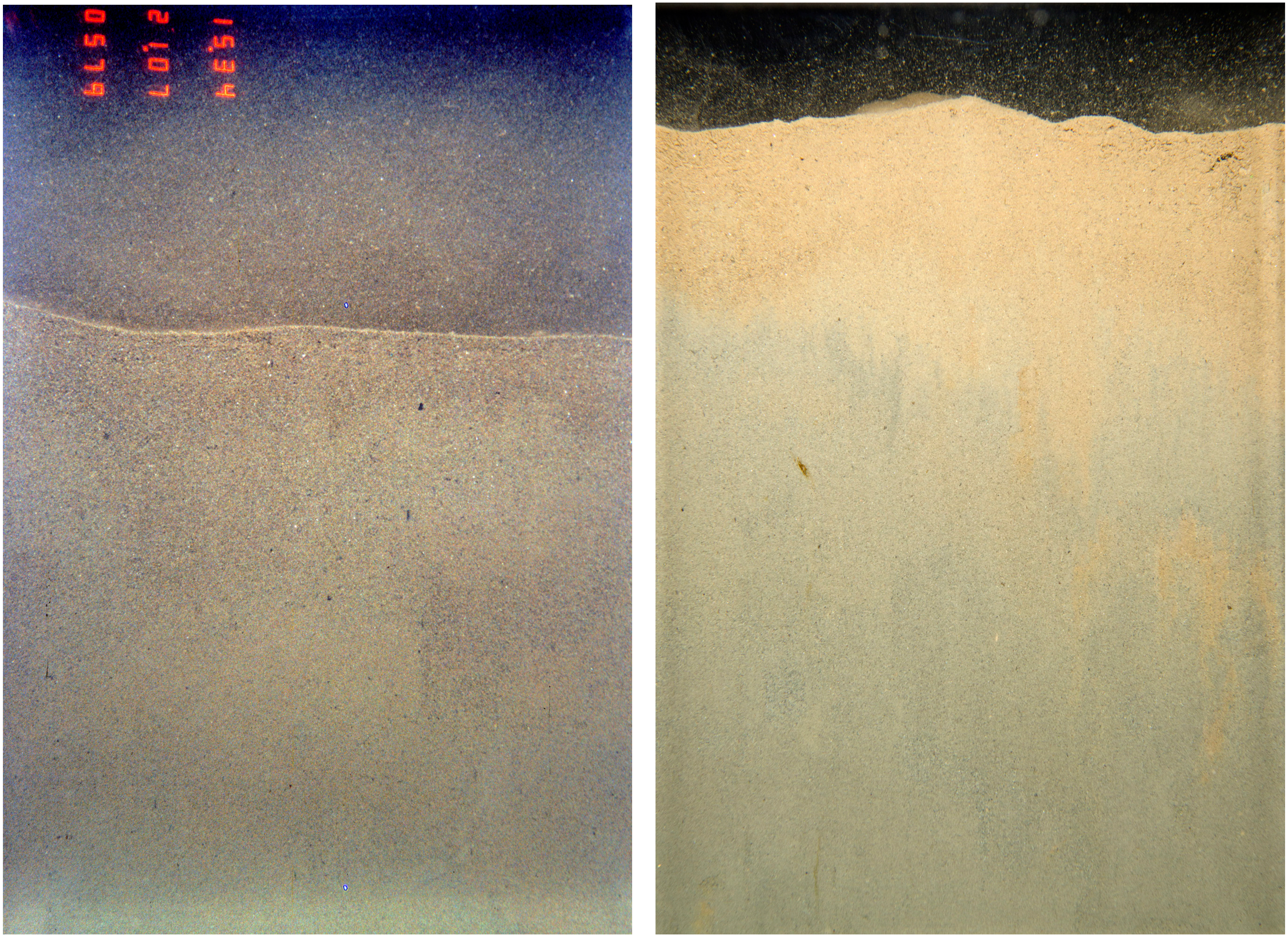

Figure 29: These profile images from Station 73B from 2001 (left) and 2013 (right) show that while a depositional regime still exists at this location, the conditions in 2013 did not result in a rapid accumulation of oxidized fine particles at the surface and an unusually thick aRPD layer, which was the case in 2001. Scale: width of each image = 14.5 cm.

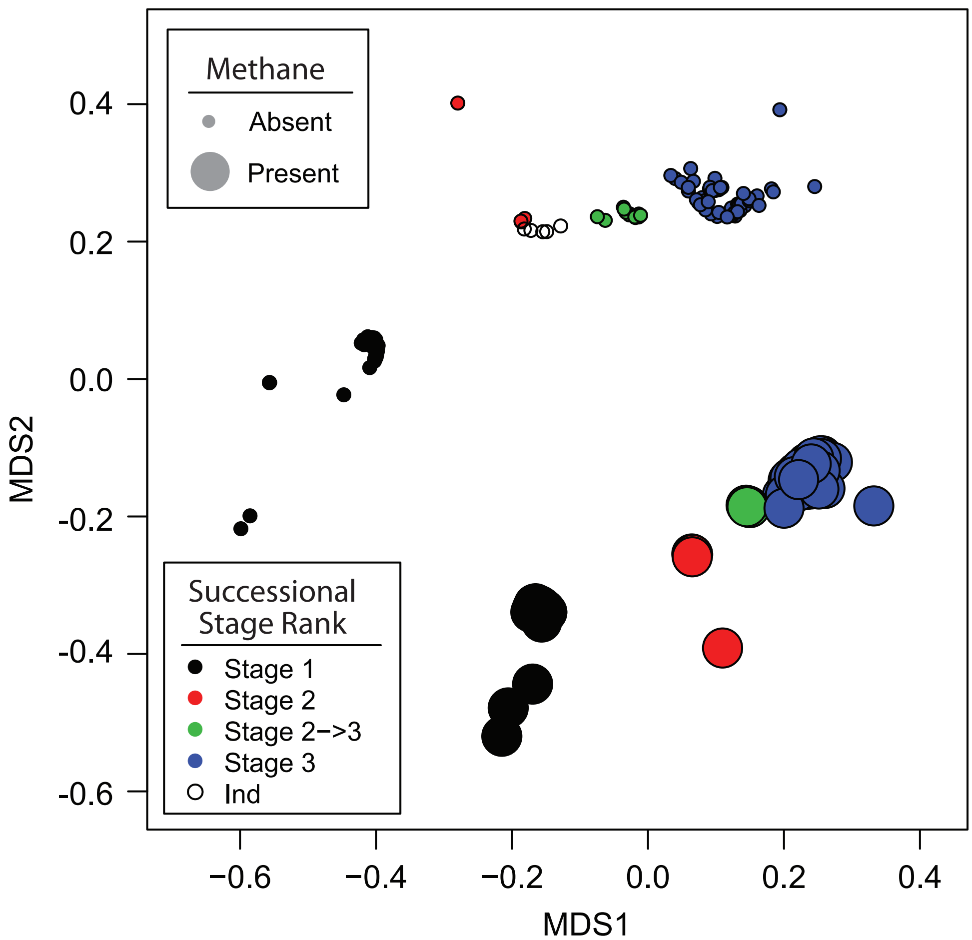

Figure 30. NMDS ordination based on the four response variables (see text). Point size varies by methane, with small circles shown where methane was absent, and large circles shown where methane was present. Point color varies by successional stage (see legend). Stress is 9.8%.

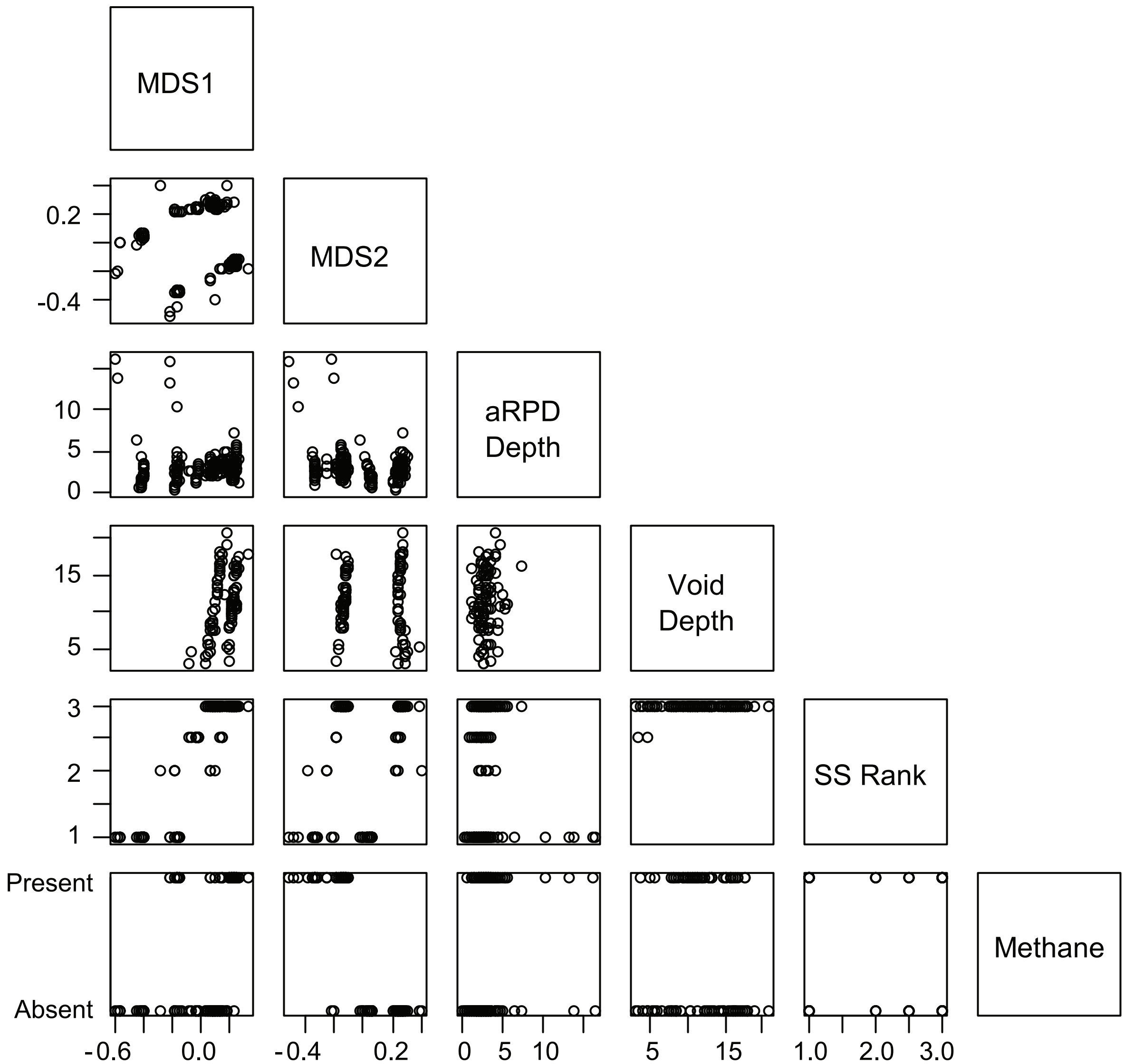

Figure 31. Pairwise scatterplots between the nMDS ordination axes (MDS1 and MDS2 shown in Figure 30) and the response variables on which the ordination was based.

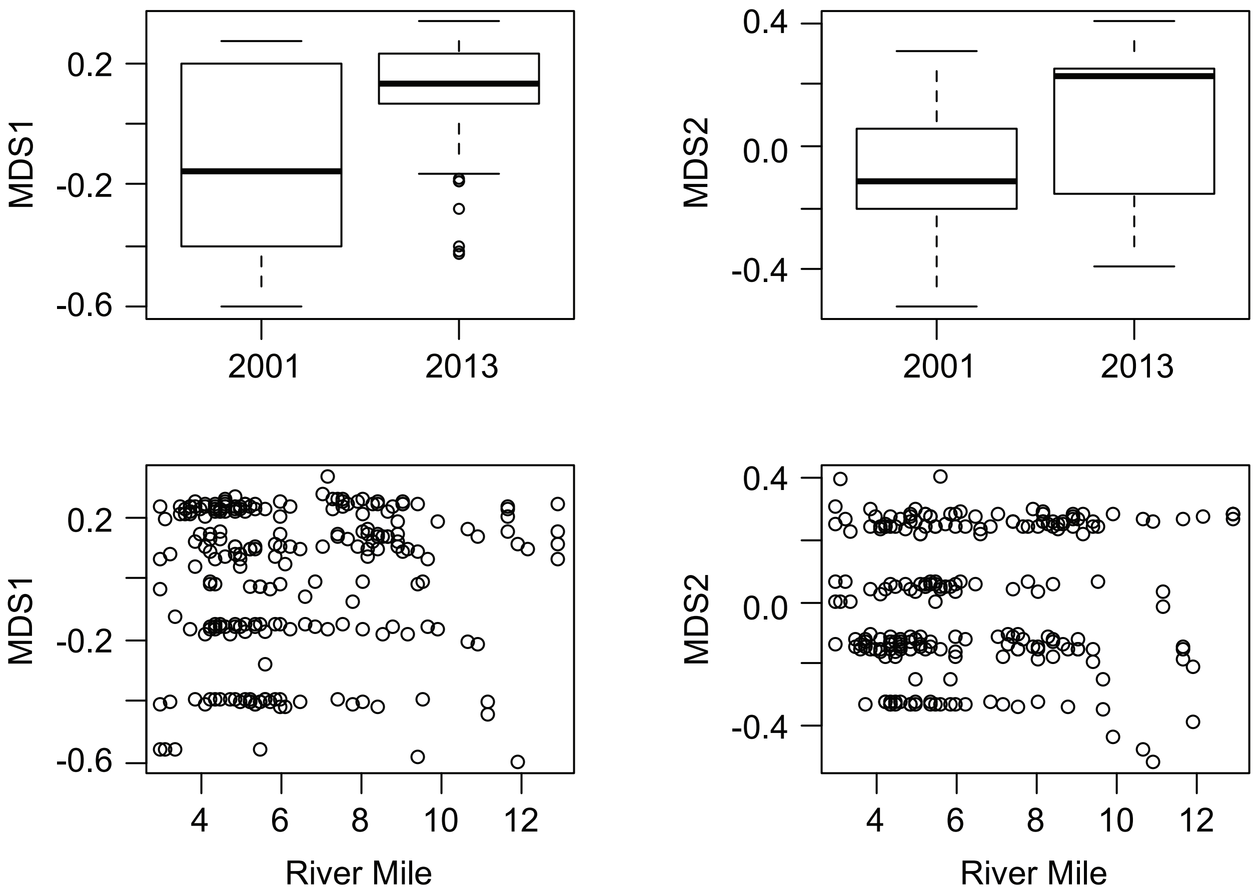

Figure 32. Relationship between the nMDS ordination axes (MDS1 and MDS2 shown in Figure 30) and survey year (top row) or River Mile (bottom row).

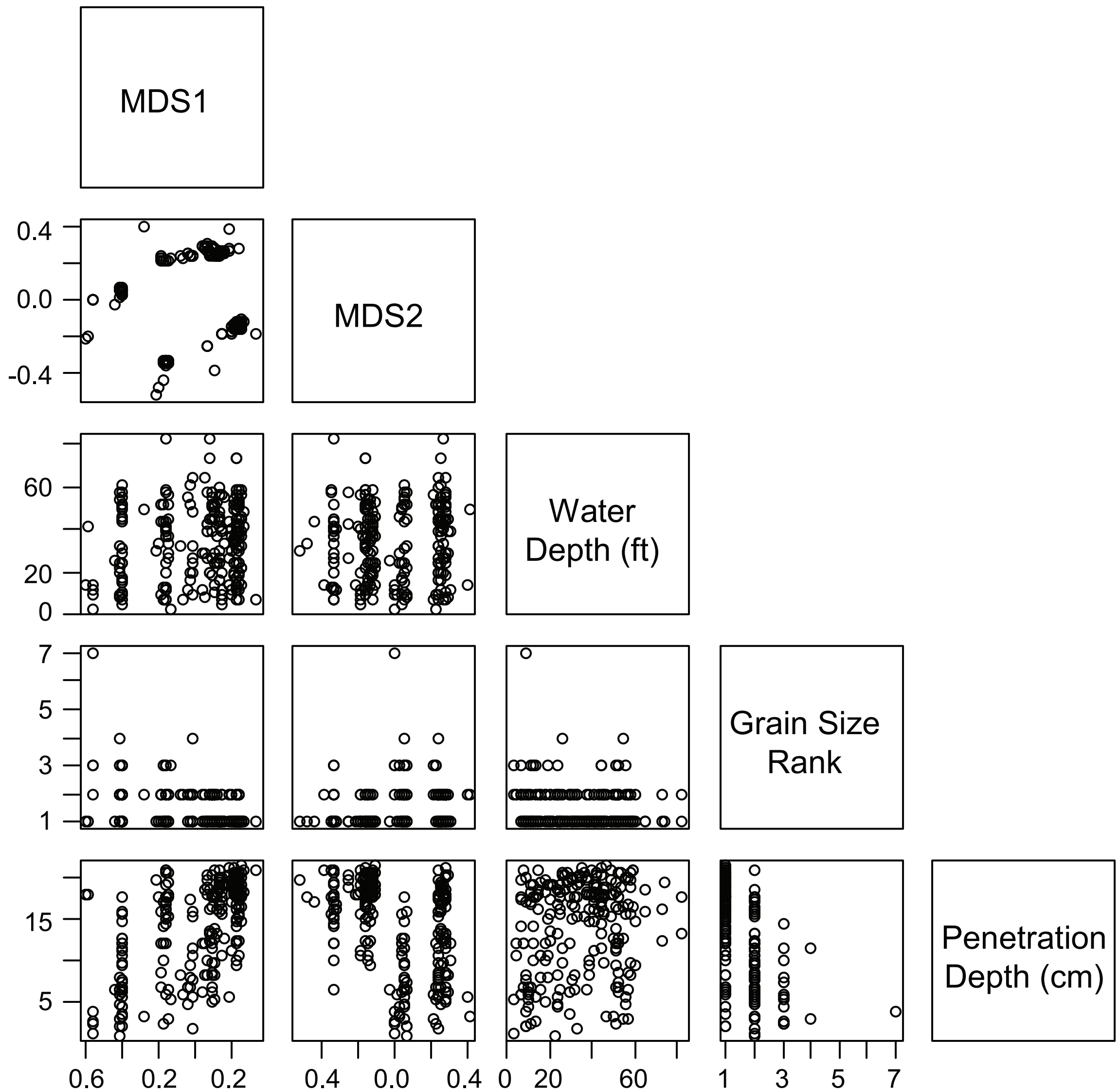

Figure 33. Pairwise scatterplots between the nMDS ordination axes (MDS1 and MDS2 shown in Figure 30) and the physical habitat variables.

APPENDIX A

Sediment Profile Image Analysis Results

Station	Replicate	Date	Time	Stop Collar Setting (in)	# of Weights (per side)	Water Depth (ft)	Calibration Constant	Grain Size Major Mode (phi)	Grain Size Minimum (phi)	Grain Size Maximum (phi)	GrnSize RANGE	Penetration Area (sq.cm)	Penetration Mean (cm)	Penetration Minimum (cm)	Penetration Maximum (cm)	Boundary Roughness (cm)	Boundary Roughness Type	RPD Area (sq.cm)	Mean RPD (cm)	Mud Clast Number	Mud Clast State	Methane ?
16A	E	12/4/2013	14:05:16	15	4	11.2	14.498	>4 / 3 to 2	>4	0	>4 to 0	100.15	6.91	6.80	7.20	0.40	Biological	15.59	1.08	10+	oxidized	n
16A	F	12/4/2013	14:06:21	15	4	12.4	14.498	>4 / 3 to 2	>4	0	>4 to 0	100.67	6.94	6.65	7.21	0.56	Biological	17.15	1.18	8	oxidized	n
16A	H	12/4/2013	14:08:22	15	4	11.6	14.498	>4 / 3 to 2	>4	0	>4 to 0	93.628	6.46	5.80	6.98	1.19	Biological	12.08	0.83	1	oxidized	n
16B	A	12/4/2013	13:53:31	15	4	20.4	14.498	4 to 3	>4	2	>4 to 2	44.83	3.09	2.69	3.40	0.71	Biological	ind	ind	0	-	n
16B	B	12/4/2013	13:54:36	15	4	20.7	14.498	4 to 3	>4	2	>4 to 2	44.424	3.06	2.87	3.30	0.44	Biological	ind	ind	0	-	n
16B	D	12/4/2013	13:57:29	15	4	20.7	14.498	4 to 3	>4	2	>4 to 2	43.928	3.03	2.72	3.33	0.61	Biological	ind	ind	0	-	n
16E	A	12/4/2013	13:08:38	13	1	37	14.498	4 to 3	>4	0	>4 to 0	121.7	8.39	5.99	9.26	3.27	Biological	17.67	1.22	0	-	n
16E	B	12/4/2013	13:09:29	13	1	39	14.498	4 to 3	>4	0	>4 to 0	148.72	10.26	8.14	12.35	4.21	Biological	24.31	1.68	1	reduced	2
17A	D	12/4/2013	13:40:20	13	1	15.2	14.498	4 to 3	>4	0	>4 to 0	81.403	5.61	4.88	6.26	1.39	Biological	ind	ind	0	-	n
17A	G	12/4/2013	14:17:42	15	4	15.2	14.498	4-3 / 3-2	>4	0	>4 to 0	84.628	5.84	5.26	6.25	0.99	Biological	ind	ind	0	-	n
17A	H	12/4/2013	14:18:35	15	4	15.4	14.498	4-3 / 3-2	>4	-1	>4 to -1	80.929	5.58	5.14	6.16	1.01	Biological	ind	ind	0	-	n
18C	A	12/4/2013	14:28:02	15	4	46.2	14.498	4 to 3	>4	2	>4 to 2	294.86	20.34	20.10	20.48	0.37	Biological	47.15	3.25	0	-	n
18C	B	12/4/2013	14:28:58	15	4	46.2	14.498	4 to 3	>4	1	>4 to 1	272.9	18.82	18.57	19.00	0.43	Biological	63.00	4.35	3	oxidized	n
18C	E	12/4/2013	14:42:06	14	2	46.2	14.498	4 to 3	>4	2	>4 to 2	242.71	16.74	16.59	16.99	0.39	Biological	33.71	2.33	0	-	n
19A	B	12/3/2013	16:01:47	13	1	5.6	14.498	3 to 2	>4	0	>4 to 0	91.406	6.30	5.78	6.78	1.00	Physical	91.41	6.30	0	-	n
19A	C	12/3/2013	16:03:14	13	1	5.6	14.498	3 to 2	>4	0	>4 to 0	75.252	5.19	3.94	6.41	2.47	Physical	51.65	3.56	0	-	n
19A	D	12/3/2013	16:04:02	13	1	5.6	14.498	3 to 2	>4	0	>4 to 0	63.204	4.36	3.52	5.00	1.48	Physical	43.95	3.03	0	-	n
20D	A	12/3/2013	16:12:09	13	1	37	14.498	>4	>4	1	>4 to 1	280.71	19.36	18.80	19.76	0.96	Biological	49.54	3.42	0	-	15+
20D	B	12/3/2013	16:13:15	13	1	39.5	14.498	>4	>4	0	>4 to 0	277.15	19.12	18.51	19.88	1.37	Biological	24.09	1.66	0	-	20+
20D	D	12/3/2013	16:14:53	13	1	41.5	14.498	>4	>4	1	>4 to 1	261.29	18.02	17.71	18.39	0.68	Biological	31.81	2.19	0	-	n
21D	A	12/4/2013	15:11:55	14	2	51.1	14.498	4 to 3	>4	0	>4 to 0	241.19	16.64	16.21	17.41	1.20	Biological	17.08	1.18	0	-	trace
21D	C	12/4/2013	15:13:28	14	2	53.9	14.498	>4	>4	0	>4 to 0	273.63	18.87	17.63	19.93	2.31	Biological	44.55	3.07	0	-	15+
21D	D	12/4/2013	15:14:20	14	2	56	14.498	>4	>4	0	>4 to 0	263.72	18.19	17.93	18.37	0.44	Biological	47.32	3.26	0	-	7
22C	B	12/4/2013	15:02:48	14	2	55.3	14.498	>4	>4	0	>4 to 0	299.49	20.66	20.10	21.12	1.01	Biological	44.91	3.10	1	reduced	20+
22C	C	12/4/2013	15:03:59	14	2	53.9	14.498	>4	>4	1	>4 to 1	292.18	20.15	20.01	20.20	0.20	Biological	49.05	3.38	1	oxidized	20+
22C	D	12/4/2013	15:05:07	14	2	56	14.498	>4	>4	1	>4 to 1	>301	21.20	21.20	21.20	ind	ind	ind	ind	ind	ind	15+
22D	B	12/3/2013	16:24:53	13	1	26	14.498	>4	>4	0	>4 to 0	254.73	17.57	16.90	18.10	1.20	Biological	34.70	2.39	0	-	10+
22D	C	12/3/2013	16:25:51	13	1	25.6	14.498	>4	>4	1	>4 to 1	268.31	18.51	17.89	19.04	1.15	Biological	38.97	2.69	0	-	11
22D	D	12/3/2013	16:26:57	13	1	26.8	14.498	>4	>4	1	>4 to 1	276.57	19.08	18.38	19.61	1.23	Biological	42.93	2.96	0	-	20+
22F	A	12/4/2013	15:23:52	12	0	43.2	14.498	>4	>4	1	>4 to 1	228.61	15.77	15.49	16.06	0.57	Biological	34.57	2.38	0	-	11
22F	C	12/4/2013	15:25:41	12	0	43.6	14.498	>4	>4	1	>4 to 1	197.51	13.62	13.17	14.09	0.92	Biological	25.31	1.75	0	-	20+
22F	D	12/4/2013	15:26:33	12	0	42.6	14.498	>4	>4	1	>4 to 1	246.92	17.03	16.65	17.82	1.17	Biological	31.19	2.15	0	-	20+
23A	A	12/3/2013	15:37:42	13	1	8.4	14.498	ind	>4	2	>4 to 2	7.6107	0.52	0.20	0.96	0.76	Physical	ind	ind	0	-	n
23A	B	12/3/2013	15:38:31	13	1	8.6	14.498	4 to 3	>4	2	>4 to 2	39.813	2.75	2.49	3.08	0.60	Biological	ind	ind	ind	-	n

Station	Replicate	Date	Time	Stop Collar Setting (in)	# of Weights (per side)	Water Depth (ft)	Calibration Constant	Grain Size Major Mode (phi)	Grain Size Minimum (phi)	Grain Size Maximum (phi)	GrnSize RANGE	Penetration Area (sq.cm)	Penetration Mean (cm)	Penetration Minimum (cm)	Penetration Maximum (cm)	Boundary Roughness (cm)	Boundary Roughness Type	RPD Area (sq.cm)	Mean RPD (cm)	Mud Clast Number	Mud Clast State	Methane ?
23B	A	12/3/2013	15:43:48	13	1	42	14.498	>4	>4	2	>4 to 2	257.93	17.79	16.68	18.46	1.78	Biological	30.27	2.09	0	-	n
23B	C	12/3/2013	15:45:21	13	1	45.6	14.498	>4	>4	1	>4 to 1	254.6	17.56	16.58	18.94	2.36	Biological	27.65	1.91	1	oxidized	n
23B	D	12/3/2013	15:46:48	13	1	42	14.498	>4	>4	2	>4 to 2	277.51	19.14	18.96	19.46	0.50	Biological	36.54	2.52	0	-	n
23E	A	12/4/2013	12:50:51	13	1	16.8	14.498	>4 / 4 - 3	>4	0	>4 to 0	228.51	15.76	14.84	16.33	1.49	Biological	41.66	2.87	0	-	10+
23E	B	12/4/2013	12:51:42	13	1	16	14.498	4 to 3/3 to 2	>4	0	>4 to 0	198	13.66	13.13	14.33	1.20	Biological	29.44	2.03	3	oxidized	20+
23E	C	12/4/2013	12:52:35	13	1	11.8	14.498	>4 / 3 to 2	>4	0	>4 to 0	189.16	13.05	12.56	13.33	0.77	Biological	29.75	2.05	0	-	n
24D	B	12/5/2013	8:02:56	13	1	60	14.498	>4	>4	0	>4 to 0	237.87	16.41	15.79	16.80	1.01	Biological	27.25	1.88	0	-	n
24D	C	12/5/2013	8:04:00	13	1	59.4	14.498	>4	>4	1	>4 to 1	245.68	16.95	16.44	17.51	1.07	Biological	28.41	1.96	0	-	4
24D	D	12/5/2013	8:04:44	13	1	59.4	14.498	>4	>4	1	>4 to 1	242.53	16.73	16.29	17.18	0.89	Biological	50.72	3.50	0	-	n
25A	A	12/3/2013	15:23:47	13	1	44.5	14.498	>4	>4	1	>4 to 1	276.33	19.06	18.12	20.02	1.90	Biological	32.88	2.27	0	-	20+
25A	C	12/3/2013	15:26:15	13	1	42.6	14.498	>4	>4	1	>4 to 1	279.8	19.30	19.08	19.93	0.85	Biological	37.04	2.55	1	oxidized	20+
25A	D	12/3/2013	15:27:15	13	1	43.2	14.498	>4	>4	1	>4 to 1	294.53	>21.2	19.40	>21.2	ind	Biological	45.64	3.15	0	-	20+
25C	B	12/5/2013	8:14:29	13	1	57.6	14.498	>4	>4	1	>4 to 1	288.92	19.93	19.34	20.18	0.84	Biological	56.03	3.86	0	-	20+
25C	C	12/5/2013	8:15:20	13	1	57.6	14.498	>4	>4	2	>4 to 2	262.77	18.12	17.39	19.76	2.37	Biological	47.43	3.27	0	-	20+
25C	D	12/5/2013	8:16:06	13	1	57.6	14.498	>4	>4	1	>4 to 1	289.7	19.98	19.53	20.24	0.71	Biological	58.55	4.04	0	-	9
25D	A	12/4/2013	12:17:04	13	1	60.3	14.498	4 to 3	>4	0	>4 to 0	104.61	7.22	6.89	7.38	0.49	Biological	37.15	2.56	0	-	n
25D	B	12/4/2013	12:18:00	13	1	60	14.498	4 to 3	>4	0	>4 to 0	88.721	6.12	5.73	6.52	0.79	Biological	25.34	1.75	0	-	n
25D	D	12/4/2013	12:19:43	13	1	59.4	14.498	4 to 3	>4	0	>4 to 0	101.05	6.97	6.34	7.28	0.94	Biological	42.76	2.95	8	oxidized	n
26A	A	12/3/2013	15:06:56	13	1	8.2	14.498	4 to 3	>4	1	>4 to 1	150.22	10.36	9.79	11.14	1.34	Biological	17.92	1.24	0	-	5
26A	C	12/3/2013	15:09:13	13	1	7.2	14.498	4 to 3	>4	1	>4 to 1	160.78	11.09	10.85	11.19	0.34	Biological	48.88	3.37	0	-	n
26A	D	12/3/2013	15:10:04	13	1	6.8	14.498	4 to 3	>4	1	>4 to 1	148.77	10.26	9.87	10.66	0.79	Biological	28.65	1.98	0	-	n
26B	D	12/3/2013	15:15:32	13	1	16.5	14.498	>4	>4	1	>4 to 1	252	17.38	16.08	18.35	2.27	Biological	33.75	2.33	0	-	n
26C	B	12/5/2013	8:25:19	13	1	51.0	14.498	>4	>4	0	>4 to 0	221.39	15.27	15.03	15.55	0.52	Biological	58.41	4.03	0	-	n
26C	C	12/5/2013	8:26:08	13	1	51.2	14.498	>4	>4	0	>4 to 0	231.3	15.95	14.35	17.56	3.21	Biological	16.53	1.14	2	both	n
26C	D	12/5/2013	8:27:00	13	1	51.1	14.498	>4	>4	0	>4 to 0	217.83	15.02	13.90	15.57	1.67	Biological	56.33	3.89	0	-	n
26E	A	12/4/2013	12:03:30	13	1	42.0	14.498	>4	>4	1	>4 to 1	273.09	18.84	18.38	19.30	0.92	Biological	47.56	3.28	0	-	20+
26E	B	12/4/2013	12:04:23	13	1	42.6	14.498	>4	>4	1	>4 to 1	251.09	17.32	17.04	17.69	0.65	Biological	29.22	2.02	0	-	10+
26E	C	12/4/2013	12:05:21	13	1	42.4	14.498	>4	>4	1	>4 to 1	246.24	16.98	16.11	18.16	2.04	Biological	35.69	2.46	0	-	20+
27A	A	12/3/2013	14:30:50	13	1	6.0	14.498	4 to 3	>4	1	>4 to 1	145.89	10.06	9.77	10.29	0.52	Biological	38.05	2.62	0	-	n
27A	E	12/3/2013	14:34:37	13	1	4.8	14.498	>4 / 4-3	>4	1	>4 to 1	202.69	13.98	13.56	14.55	0.99	Biological	21.86	1.51	0	-	3
27B	B	12/3/2013	14:38:46	13	1	25.1	14.498	>4	>4	1	>4 to 1	278.77	19.23	18.44	19.77	1.33	Biological	32.34	2.23	0	-	20+
27B	C	12/3/2013	14:39:42	13	1	25.2	14.498	>4	>4	1	>4 to 1	>304.87	>21.2	>21.2	>21.2	ind	ind	ind	ind	ind	ind	20+
27B	D	12/3/2013	14:40:43	13	1	24.4	14.498	>4	>4	1	>4 to 1	>301.78	>21.2	>21.2	>21.2	ind	Biological	30.18	2.08	0	-	15+
27C	B	12/5/2013	8:33:51	13	1	68.0	14.498	>4	>4	0	>4 to 0	234	16.14	15.84	16.48	0.64	Biological	49.29	3.40	1	reduced	n
27C	C	12/5/2013	8:34:59	13	1	68.0	14.498	>4	>4	0	>4 to 0	227.14	15.67	15.00	16.33	1.33	Biological	29.89	2.06	0	-	n
27C	D	12/5/2013	8:35:51	13	1	68.0	14.498	>4	>4	0	>4 to 0	228.57	15.77	15.12	16.39	1.27	Biological	30.54	2.11	2	reduced	n
27D	A	12/5/2013	9:03:13	13	1	72.9	14.498	>4	>4	1	>4 to 1	281.97	19.45	18.86	19.82	0.96	Biological	29.88	2.06	0	-	15+
27D	C	12/5/2013	9:05:25	13	1	72.9	14.498	>4	>4	1	>4 to 1	277.92	19.17	18.76	19.45	0.69	Biological	57.02	3.93	0	-	20+
27D	D	12/5/2013	9:06:24	13	1	71.1	14.498	>4	>4	0	>4 to 0	286.36	19.75	19.30	20.17	0.87	Biological	48.56	3.35	0	-	20+
27E	A	12/4/2013	11:52:55	13	1	35.0	14.498	>4	>4	1	>4 to 1	>300.61	20.73	19.95	>21.2	>1.17	Biological	52.56	3.63	0	-	20+

Station	Replicate	Date	Time	Stop Collar Setting (in)	# of Weights (per side)	Water Depth (ft)	Calibration Constant	Grain Size Major Mode (phi)	Grain Size Minimum (phi)	Grain Size Maximum (phi)	GrnSize RANGE	Penetration Area (sq.cm)	Penetration Mean (cm)	Penetration Minimum (cm)	Penetration Maximum (cm)	Boundary Roughness (cm)	Boundary Roughness Type	RPD Area (sq.cm)	Mean RPD (cm)	Mud Clast Number	Mud Clast State	Methane ?
27E	B	12/4/2013	11:54:10	13	1	34.5	14.498	>4	>4	1	>4 to 1	297.12	20.49	19.90	21.06	1.16	Biological	43.37	2.99	0	-	20+
27E	D	12/4/2013	11:56:39	13	1	35.5	14.498	>4	>4	1	>4 to 1	292.3	20.16	19.58	20.94	1.36	Biological	29.46	2.03	0	-	20+
27H	A	12/4/2013	15:40:31	12	0	39.6	14.498	>4	>4	2	>4 to 2	264.06	18.21	17.87	18.83	0.96	Biological	28.50	1.97	0	-	10
27H	C	12/4/2013	15:42:29	12	0	41.0	14.498	>4	>4	1	>4 to 1	264	18.21	17.98	18.26	0.28	Biological	46.16	3.18	0	-	0
27H	D	12/4/2013	15:43:21	12	0	41.0	14.498	>4	>4	1	>4 to 1	255.05	17.59	17.08	18.20	1.12	Biological	35.17	2.43	0	-	1
28A	A	12/3/2013	14:11:48	13	1	19.8	14.498	>4	>4	1	>4 to 1	274.64	18.94	17.96	19.72	1.76	Biological	40.28	2.78	0	-	20+
28A	B	12/3/2013	14:12:33	13	1	19.5	14.498	>4	>4	1	>4 to 1	271.65	18.74	17.91	19.74	1.83	Biological	41.18	2.84	2	reduced	20+
28A	C	12/3/2013	14:13:19	13	1	18.3	14.498	>4	>4	0	>4 to 0	251.35	17.34	17.16	17.84	0.68	Biological	58.06	4.00	0	-	20+
28B	A	12/3/2013	14:18:29	13	1	33.4	14.498	>4	>4	1	>4 to 1	280.62	19.36	17.60	20.16	2.55	Biological	43.96	3.03	0	-	20+
28B	B	12/3/2013	14:19:13	13	1	32.4	14.498	>4	>4	1	>4 to 1	295.13	20.36	20.08	20.72	0.64	Biological	45.13	3.11	0	-	20+
28B	C	12/3/2013	14:20:41	13	1	31.6	14.498	>4	>4	1	>4 to 1	292.59	20.18	19.52	20.82	1.31	Biological	55.26	3.81	0	-	20+
28C	A	12/4/2013	16:10:45	14	2	62.4	14.498	>4	>4	0	>4 to 0	300.14	20.70	20.04	21.16	1.12	Biological	50.83	3.51	0	-	n
28C	B	12/4/2013	16:11:38	14	2	61.6	14.498	>4	>4	1	>4 to 1	298.36	20.58	20.10	20.88	0.77	Biological	51.94	3.58	10	reduced	n
28C	C	12/4/2013	16:12:29	14	2	61.6	14.498	>4	>4	1	>4 to 1	>305.24	>21.2	>21.2	>21.2	ind	ind	ind	ind	ind	-	n
28E	B	12/4/2013	11:39:26	13	1	46.8	14.498	3 to 2	>4	0	>4 to 0	150.19	10.36	10.00	10.55	0.55	Biological	24.87	1.72	0	-	n
28E	C	12/4/2013	11:41:49	13	1	46.8	14.498	3 to 2	>4	0	>4 to 0	182.19	12.57	12.12	13.16	1.04	Biological	46.21	3.19	6	oxidized	n
28E	D	12/4/2013	11:42:52	13	1	46.8	14.498	3 to 2	>4	0	>4 to 0	173.03	11.93	11.71	12.21	0.51	Biological	30.81	2.12	0	-	n
29A	B	12/3/2013	13:52:00	13	1	12.3	14.498	>4	>4	1	>4 to 1	283.05	19.52	18.84	20.37	1.53	Biological	45.33	3.13	0	-	20+
29A	C	12/3/2013	13:53:14	13	1	11.7	14.498	>4	>4	1	>4 to 1	281.02	19.38	18.88	19.89	1.01	Biological	56.18	3.87	0	-	1
29A	D	12/3/2013	13:53:14	13	1	11.7	14.498	>4	>4	1	>4 to 1	274.27	18.92	18.46	19.76	1.30	Biological	55.33	3.82	9	oxidized	10+
29B	A	12/3/2013	13:57:50	13	1	18.3	14.498	>4	>4	1	>4 to 1	283.13	19.53	18.13	20.06	1.93	Biological	34.57	2.38	0	-	20+
29B	B	12/3/2013	13:58:44	13	1	16.8	14.498	>4	>4	1	>4 to 1	285.41	19.69	19.41	19.92	0.51	Biological	44.29	3.05	0	-	10+
29B	C	12/3/2013	13:59:54	13	1	15.6	14.498	>4	>4	1	>4 to 1	263.43	18.17	18.05	18.28	0.23	Biological	38.63	2.66	0	-	20+
29D	A	12/5/2013	8:44:34	13	1	57.4	14.498	>4	>4	1	>4 to 1	276.88	19.10	18.57	19.53	0.96	Biological	39.30	2.71	0	-	7
29D	B	12/5/2013	8:45:32	13	1	57.4	14.498	>4	>4	1	>4 to 1	274.79	18.95	18.49	19.17	0.68	Biological	45.99	3.17	4	reduced	10+
29D	C	12/5/2013	8:46:34	13	1	57.4	14.498	>4	>4	1	>4 to 1	273.62	18.87	17.88	19.42	1.55	Biological	51.55	3.56	0	-	15+
29F	E	12/4/2013	15:53:26	12	0	45.6	14.498	>4	>4	0	>4 to 0	254.14	17.53	17.18	17.87	0.69	Biological	35.27	2.43	0	-	n
29F	G	12/4/2013	15:55:36	12	0	44.4	14.498	>4	>4	0	>4 to 0	254.53	17.56	17.11	18.21	1.10	Biological	42.58	2.94	0	-	10+
29F	H	12/4/2013	15:56:41	12	0	44.4	14.498	>4	>4	0	>4 to 0	259.43	17.89	16.81	18.43	1.62	Biological	52.55	3.62	0	-	n
30C	A	12/5/2013	9:16:01	13	1	55.3	14.498	>4	>4	0	>4 to 0	155.29	10.71	10.34	11.46	1.12	Biological	48.93	3.38	0	-	n
30C	C	12/5/2013	9:17:35	13	1	55.3	14.498	4 to 3/3 to 2	>4	0	>4 to 0	110.07	7.59	7.13	8.57	1.44	Biological	46.21	3.19	0	-	n
30C	D	12/5/2013	9:18:28	13	1	55.3	14.498	4 to 3	>4	0	>4 to 0	106.41	7.34	6.82	8.12	1.30	Physical	34.52	2.38	4	oxidized	n
31A	B	12/3/2013	11:46:30	14	2	31.5	14.498	>4	>4	1	>4 to 1	>305.82	>21.2	>21.2	>21.2	ind	ind	ind	ind	ind	ind	20+
31A	C	12/3/2013	11:47:44	14	2	31.5	14.498	>4	>4	1	>4 to 1	271.51	18.73	18.39	19.38	0.99	Biological	31.01	2.14	2	oxidized	20+
31A	D	12/3/2013	11:48:39	14	2	22	14.498	>4	>4	1	>4 to 1	287.47	19.83	19.44	20.36	0.92	Biological	6.30	0.43	0	-	20+
31B	A	12/3/2013	11:34:23	14	2	40	14.498	>4	>4	1	>4 to 1	260.45	17.96	17.17	18.32	1.15	Biological	14.93	1.03	0	-	10
31B	B	12/3/2013	11:35:13	14	2	41	14.498	>4	>4	1	>4 to 1	260.31	17.95	17.71	18.43	0.72	Biological	15.68	1.08	0	-	20+
31B	C	12/3/2013	11:36:11	14	2	41.5	14.498	>4	>4	1	>4 to 1	268.28	18.50	18.27	18.80	0.53	Biological	22.00	1.52	8	both	20+
31C	A	12/5/2013	9:25:10	13	1	52.5	14.498	4 to 3	>4	0	>4 to 0	155.43	10.72	10.38	10.90	0.52	Biological	45.98	3.17	0	-	n
31C	B	12/5/2013	9:26:09	13	1	51.8	14.498	4 to 3	>4	0	>4 to 0	179.78	12.40	12.06	12.49	0.43	Biological	37.42	2.58	3	oxidized	n

Station	Replicate	Date	Time	Stop Collar Setting (in)	# of Weights (per side)	Water Depth (ft)	Calibration Constant	Grain Size Major Mode (phi)	Grain Size Minimum (phi)	Grain Size Maximum (phi)	GrnSize RANGE	Penetration Area (sq.cm)	Penetration Mean (cm)	Penetration Minimum (cm)	Penetration Maximum (cm)	Boundary Roughness (cm)	Boundary Roughness Type	RPD Area (sq.cm)	Mean RPD (cm)	Mud Clast Number	Mud Clast State	Methane ?
31C	C	12/5/2013	9:27:02	13	1	51.8	14.498	4 to 3	>4	0	>4 to 0	166.18	11.46	10.86	11.90	1.05	Biological	48.84	3.37	1	oxidized	n
31D	A	12/5/2013	9:34:50	13	1	73.8	14.498	4 to 3	>4	0	>4 to 0	207.33	14.30	13.42	14.70	1.27	Biological	48.54	3.35	0	-	n
31D	C	12/5/2013	9:36:23	13	1	73.8	14.498	4 to 3	>4	0	>4 to 0	172.31	11.88	10.44	13.16	2.72	Biological	38.50	2.66	8	both	2
31D	D	12/5/2013	9:37:05	13	1	73.8	14.498	4 to 3	>4	0	>4 to 0	164.89	11.37	10.46	12.24	1.78	Biological	47.35	3.27	9	both	n
31E	A	12/4/2013	10:52:41	13	1	46.8	14.498	4 to 3	>4	0	>4 to 0	179.4	12.37	11.96	12.94	0.99	Biological	52.70	3.64	0	-	n
31E	B	12/4/2013	10:53:27	13	1	46.8	14.498	4 to 3	>4	0	>4 to 0	194.53	13.42	13.13	13.87	0.74	Biological	37.59	2.59	0	-	n
31E	C	12/4/2013	10:54:13	13	1	46.8	14.498	4 to 3	>4	0	>4 to 0	196.59	13.56	12.89	14.51	1.62	Biological	39.83	2.75	0	-	n
32A	A	12/3/2013	11:57:19	13	1	19.8	14.498	4 to 3/ 1 to 0	>4	-2	>4 to -2	109.96	7.58	6.80	8.65	1.85	Physical	16.83	1.16	0	-	n
32A	B	12/3/2013	12:02:25	14	2	18.6	14.498	4 to 3	>4	0	>4 to 0	69.34	4.78	3.49	5.64	2.15	Biological	36.94	2.55	0	-	n
32A	E	12/3/2013	12:05:46	14	2	16.8	14.498	4 to 3/ 2 to 1	>4	0	>4 to 0	93.378	6.44	5.61	7.37	1.76	Physical	35.25	2.43	0	-	n
32B	A	12/5/2013	9:56:46	13	1	83.0	14.498	4 to 3/3 to 2	>4	0	>4 to 0	195.43	13.48	13.27	13.83	0.56	Biological	37.56	2.59	0	-	n
32B	C	12/5/2013	9:58:27	13	1	83.0	14.498	4 to 3/3 to 2	>4	0	>4 to 0	180.21	12.43	11.90	12.81	0.91	Biological	27.49	1.90	0	-	n
32B	D	12/5/2013	9:59:20	13	1	83.0	14.498	4 to 3	>4	0	>4 to 0	194.79	13.44	13.19	13.92	0.73	Biological	25.34	1.75	0	-	n
32C	A	12/5/2013	9:43:17	13	1	40.6	14.498	>4	>4	1	>4 to 1	275.4	19.00	18.38	20.00	1.62	Biological	47.45	3.27	0	-	20+
32C	B	12/5/2013	9:43:58	13	1	40.6	14.498	>4	>4	1	>4 to 1	274.03	18.90	18.54	19.41	0.88	Biological	29.80	2.06	8	red	20+
32C	C	12/5/2013	9:44:52	13	1	40.6	14.498	>4	>4	1	>4 to 1	273.48	18.86	18.00	19.38	1.38	Biological	21.15	1.46	0	-	20+
32D	A	12/4/2013	10:41:08	13	1	21.6	14.498	>4	>4	1	>4 to 1	253.21	17.47	16.83	18.67	1.84	Biological	31.09	2.14	0	-	10+
32D	B	12/4/2013	10:41:55	13	1	20.8	14.498	>4	>4	1	>4 to 1	274.04	18.90	18.19	19.33	1.14	Biological	35.68	2.46	0	-	3
32D	C	12/4/2013	10:42:51	13	1	21.2	14.498	>4	>4	1	>4 to 1	265.22	18.29	17.87	18.78	0.91	Biological	37.95	2.62	0	-	1
33A	B	12/3/2013	12:15:40	13	1	9.6	14.498	4 to 3	>4	0	>4 to 0	137.94	9.51	9.22	9.67	0.44	Biological	16.59	1.14	0	-	3
33A	C	12/3/2013	12:16:42	13	1	12.6	14.498	4 to 3	>4	1	>4 to 1	77.332	5.33	4.94	5.81	0.87	Biological	15.83	1.09	0	-	n
33A	D	12/3/2013	12:19:21	13	1	16.2	14.498	4 to 3	>4	0	>4 to 0	243.7	16.81	16.30	17.50	1.20	Biological	36.93	2.55	0	-	7
33B	E	12/4/2013	10:18:23	13	1	41.0	14.498	>4	>4	2	>4 to 2	277.08	19.11	17.26	19.73	2.47	Biological	45.32	3.13	1	reduced	15+
33B	F	12/4/2013	10:19:08	13	1	40.5	14.498	>4	>4	1	>4 to 1	272.53	18.80	18.24	19.14	0.90	Biological	52.08	3.59	0	-	9
33B	G	12/4/2013	10:19:56	13	1	41.0	14.498	>4	>4	1	>4 to 1	280.41	19.34	18.34	20.97	2.63	Biological	25.16	1.74	6	reduced	10+
33C	A	12/5/2013	10:06:08	13	1	55.3	14.498	2 to 1	>4	0	>4 to 0	69.384	4.79	4.70	4.86	0.16	Physical	ind	ind	0	-	n
33C	B	12/5/2013	10:06:49	13	1	55.3	14.498	2 to 1	>4	-1	>4 to -1	83.155	5.74	3.29	7.20	3.91	Physical	ind	ind	0	-	n
33C	C	12/5/2013	10:07:31	13	1	55.3	14.498	2 to 1	>4	-2	>4 to -2	55.755	3.85	3.18	4.61	1.43	Physical	ind	ind	0	-	n
33D	A	12/5/2013	10:14:48	13	1	52.5	14.498	>4	>4	1	>4 to 1	266.14	18.36	17.23	18.86	1.63	Biological	33.27	2.29	0	-	n
33D	B	12/5/2013	10:15:43	13	1	53.2	14.498	>4	>4	1	>4 to 1	272.5	18.80	18.40	19.73	1.33	Biological	42.99	2.97	1	oxidized	1
33D	C	12/5/2013	10:16:31	13	1	53.2	14.498	>4	>4	1	>4 to 1	260.39	17.96	17.55	18.67	1.12	Biological	21.92	1.51	0	-	n
34A	B	12/3/2013	13:35:19	15	3	23.2	14.498	4 to 3	>4	0	>4 to 0	114.21	7.88	7.38	8.26	0.88	Biological	25.61	1.77	0	-	n
34B	A	12/5/2013	10:33:39	13	1	51.8	14.498	4 to 3	>4	0	>4 to 0	121.17	8.36	8.12	8.66	0.55	Biological	37.39	2.58	0	-	n
34B	B	12/5/2013	10:34:50	13	1	51.8	14.498	4 to 3	>4	0	>4 to 0	99.946	6.89	6.22	7.44	1.21	Biological	26.60	1.83	0	-	n
34B	D	12/5/2013	10:36:35	13	1	51.8	14.498	4 to 3	>4	0	>4 to 0	72.419	5.00	4.40	5.30	0.91	Biological	31.52	2.17	0	-	n

Station	Replicate	Date	Time	Stop Collar Setting (in)	# of Weights (per side)	Water Depth (ft)	Calibration Constant	Grain Size Major Mode (phi)	Grain Size Minimum (phi)	Grain Size Maximum (phi)	GrnSize RANGE	Penetration Area (sq.cm)	Penetration Mean (cm)	Penetration Minimum (cm)	Penetration Maximum (cm)	Boundary Roughness (cm)	Boundary Roughness Type	RPD Area (sq.cm)	Mean RPD (cm)	Mud Clast Number	Mud Clast State	Methane ?
34C	A	12/5/2013	10:24:19	13	1	56.7	14.498	4 to 3	>4	0	>4 to 0	134.53	9.28	9.03	9.61	0.57	Biological	38.95	2.69	0	-	n
34C	B	12/5/2013	10:25:25	13	1	56.7	14.498	>4/3 to 2	>4	0	>4 to 0	105.45	7.27	5.94	8.85	2.90	Physical	12.82	0.88	10	both	n
34C	D	12/5/2013	10:26:59	13	1	56.7	14.498	4 to 3	>4	0	>4 to 0	120.33	8.30	8.13	8.46	0.33	Biological	34.71	2.39	0	-	n
34D	A	12/4/2013	10:28:45	13	1	16.8	14.498	4 to 3/ 2 to 1	>4	0	>4 to 0	146.92	10.13	8.67	10.51	1.84	Physical	30.80	2.12	0	-	n
34D	B	12/4/2013	10:29:39	13	1	15.6	14.498	4 to 3/ 2 to 1	>4	-1	>4 to -1	138.57	9.56	8.63	10.86	2.23	Biological	24.94	1.72	0	-	n
34D	D	12/4/2013	10:31:19	13	1	18.0	14.498	4 to 3/ 2 to 1	>4	-1	>4 to -1	149.7	10.33	9.43	11.11	1.67	Biological	47.98	3.31	0	-	5
35A	C	12/3/2013	10:20:19	15	3	18	14.498	>4	>4	1	>4 to 1	300.83	20.75	20.56	>20.98	ind	Biological	41.30	2.85	0	-	20+
35A	E	12/3/2013	10:59:14	14	2	17	14.498	>4	>4	1	>4 to 1	289.03	19.94	18.32	21.09	2.77	Biological	14.81	1.02	0	-	20+
35A	G	12/3/2013	11:01:51	14	2	20.5	14.498	4 to 3/>4	>4	0	>4 to 0	215.08	14.84	13.56	15.58	2.02	Physical	ind	ind	0	-	n
35B	B	12/3/2013	11:13:07	14	2	35	14.498	>4	>4	1	>4 to 1	304.91	21.03	>21.03	>21.03	ind	ind	ind	ind	ind	ind	15+
35B	F	12/4/2013	10:07:33	13	1	39.5	14.498	>4	>4	1	>4 to 1	64.218	4.43	3.40	5.62	2.23	Biological	56.32	3.88	4	both	n
35B	G	12/4/2013	10:08:42	13	1	40.0	14.498	>4	>4	1	>4 to 1	273.82	18.89	17.58	19.68	2.10	Biological	32.88	2.27	0	-	10+
35C	B	12/5/2013	10:43:37	13	1	58.1	14.498	4 to 3	>4	0	>4 to 0	121.53	8.38	7.96	8.85	0.89	Physical	26.28	1.81	0	-	n
35C	C	12/5/2013	10:44:26	13	1	58.1	14.498	2 to 1	>4	-1	>4 to -1	118.64	8.18	7.44	8.99	1.56	Biological	25.44	1.75	0	-	n
35C	D	12/5/2013	10:45:07	13	1	58.1	14.498	4 to 3	>4	0	>4 to 0	128.36	8.85	7.91	9.59	1.69	Biological	49.04	3.38	0	-	n
35D	B	12/5/2013	10:51:40	13	1	45.6	14.498	>4	>4	1	>4 to 1	281.51	19.42	18.83	19.97	1.14	Biological	40.23	2.77	0	-	n
35D	C	12/5/2013	10:52:33	13	1	45.6	14.498	>4	>4	1	>4 to 1	267.96	18.48	18.19	18.86	0.67	Biological	56.42	3.89	3	both	n
35D	D	12/5/2013	10:53:30	13	1	45.6	14.498	>4	>4	1	>4 to 1	222.29	15.33	15.07	15.74	0.67	Biological	33.71	2.32	0	-	n
36A	-	12/3/2013	10:08:39	13	1	42	14.498	ind	ind	??	??	0	0.00	-	-	ind	-	-	ind	-	-	-
36B	A	12/5/2013	11:08:36	13	1	53.2	14.498	3 to 2	>4	0	>4 to 0	91.088	6.28	6.04	6.70	0.66	Biological	18.42	1.27	0	-	n
36B	B	12/5/2013	11:09:31	13	1	53.2	14.498	4 to 3	>4	0	>4 to 0	97.95	6.76	6.48	7.08	0.60	Biological	30.11	2.08	0	-	n
36B	D	12/5/2013	11:11:01	13	1	53.2	14.498	4 to 3	>4	0	>4 to 0	103.11	7.11	6.72	7.73	1.01	Biological	30.84	2.13	0	-	n
36C	B	12/5/2013	11:00:16	13	1	58.1	14.498	4 to 3/ 2 to 1	>4	0	>4 to 0	124.44	8.58	8.28	9.01	0.73	Physical	26.31	1.81	0	-	n
36C	C	12/5/2013	11:01:11	13	1	57.4	14.498	4 to 3/ 2 to 1	>4	0	>4 to 0	158.71	10.95	10.38	11.24	0.85	Biological	25.45	1.76	0	-	n
36C	D	12/5/2013	11:01:57	13	1	58.1	14.498	4 to 3/ 1 to 0	>4	0	>4 to 0	130.53	9.00	8.78	9.43	0.66	Biological	12.34	0.85	0	-	n
36D	-	12/4/2013	8:38:58	13	1	9.9	14.498	ind	ind	??	??	0	0.00	-	-	ind	-	-	ind	-	-	-
37A	A	12/3/2013	9:58:34	13	1	12.4	14.498	-4 to -5	>4	-6	>4 to -6	17.896	1.23	0.07	2.05	1.99	Physical	ind	ind	0	-	n
37A	B	12/3/2013	9:59:33	13	1	14.4	14.498	-4 to -5	>4	-6	>4 to -6	16.013	1.10	0.29	2.12	1.83	Physical	ind	ind	0	-	n
37A	C	12/3/2013	10:00:30	13	1	10.4	14.498	ind	>4	-6	>4 to -6	13.795	0.95	0.17	4.22	4.05	Physical	ind	ind	0	-	n
37B	A	12/5/2013	11:17:02	13	1	49.7	14.498	4 to 3	>4	1	>4 to 1	121.19	8.36	8.02	8.75	0.73	Physical	ind	ind	0	-	n
37B	B	12/5/2013	11:17:42	13	1	49.7	14.498	4 to 3	>4	1	>4 to 1	18.189	1.25	0.09	4.26	4.18	Physical	ind	ind	0	-	n
37B	C	12/5/2013	11:18:25	13	1	51.1	14.498	4 to 3	>4	1	>4 to 1	7.2021	0.50	0.00	1.41	1.41	ind	ind	ind	0	-	n
37C	B	12/5/2013	11:31:52	13	1	51.1	14.498	2 to 1	>4	-3	>4 to -3	71.191	4.91	4.68	5.37	0.69	Physical	ind	ind	0	-	n
37C	C	12/5/2013	11:32:40	13	1	51.1	14.498	2 to 1	>4	-1	>4 to -1	72.111	4.97	4.66	5.33	0.67	Physical	ind	ind	0	-	n
37C	D	12/5/2013	11:33:25	13	1	51.1	14.498	2 to 1	>4	-1	>4 to -1	67.049	4.62	4.14	5.58	1.44	Physical	ind	ind	0	-	n
37D	D	12/5/2013	11:42:07	13	1	37.2	14.498	>4	>4	1	>4 to 1	215.73	14.88	14.36	16.13	1.78	Biological	ind	2.62	2	reduced	20+

Station	Replicate	Date	Time	Stop Collar Setting (in)	# of Weights (per side)	Water Depth (ft)	Calibration Constant	Grain Size Major Mode (phi)	Grain Size Minimum (phi)	Grain Size Maximum (phi)	GrnSize RANGE	Penetration Area (sq.cm)	Penetration Mean (cm)	Penetration Minimum (cm)	Penetration Maximum (cm)	Boundary Roughness (cm)	Boundary Roughness Type	RPD Area (sq.cm)	Mean RPD (cm)	Mud Clast Number	Mud Clast State	Methane ?
37D	E	12/5/2013	12:45:37	13	1	40.8	14.498	>4	>4	1	>4 to 1	216.06	14.90	13.69	15.58	1.89	Biological	39.40	2.72	0	-	n
37D	F	12/5/2013	12:46:17	13	1	39.6	14.498	>4	>4	0	>4 to 0	220.99	15.24	14.44	15.78	1.33	Biological	34.61	2.39	0	-	n
37E	A	12/4/2013	8:22:22	13	1	27.6	14.498	ind	>4	??	ind	0	0.00	-	-	ind	-	-	ind	-	-	-
38C	A	12/5/2013	12:53:30	13	1	56.7	14.498	4 to 3	>4	0	>4 to 0	78.046	5.38	4.72	5.86	1.15	Physical	19.06	1.31	0	-	n
38C	B	12/5/2013	12:54:17	13	1	56.7	14.498	4 to 3	>4	0	>4 to 0	62.962	4.34	4.14	4.58	0.44	Biological	15.80	1.09	0	-	n
38C	C	12/5/2013	12:55:01	13	1	56.7	14.498	4 to 3	>4	0	>4 to 0	61.547	4.25	3.97	4.48	0.51	Physical	15.22	1.05	0	-	n
39B	B	12/3/2013	9:23:00	13	1	28.8	14.498	>4	>4	1	>4 to 1	282.52	19.49	15.33	20.05	4.72	Biological	39.56	2.73	0	-	20+
39B	E	12/3/2013	9:31:12	13	1	28.4	14.498	>4	>4	1	>4 to 1	304.36	20.99	>20.99	>20.99	ind	ind	ind	ind	ind	-	20+
39B	F	12/3/2013	9:32:37	13	1	28.4	14.498	>4	>4	1	>4 to 1	293.08	20.22	19.20	21.14	1.95	Biological	52.55	3.62	1	red	20+
39F	A	12/4/2013	8:09:53	13	1	10.5	14.498	4 to 3	>4	1	>4 to 1	78.45	5.41	5.10	5.74	0.64	Biological	38.08	2.63	0	-	n
39F	B	12/4/2013	8:10:34	13	1	9.9	14.498	4 to 3	>4	1	>4 to 1	83.068	5.73	5.18	6.37	1.19	Biological	60.71	4.19	0	-	n
39F	C	12/4/2013	8:11:12	13	1	10.2	14.498	4 to 3	>4	0	>4 to 0	63.631	4.39	2.80	5.82	3.02	Physical	63.63	4.39	0	-	n
40A	E	12/3/2013	8:51:25	14	1	5.4	14.498	>4	>4	1	>4 to 1	290.9	20.06	19.46	21.04	1.57	Biological	35.49	2.45	0	-	20+
40A	F	12/3/2013	8:52:42	14	1	5.4	14.498	>4	>4	1	>4 to 1	295.58	20.39	19.36	21.06	1.71	Biological	33.94	2.34	2	reduced	20+
40A	G	12/3/2013	8:53:59	14	1	5.4	14.498	>4	>4	0	>4 to 0	279.75	19.30	17.70	20.27	2.58	Biological	34.21	2.36	0	-	20+
40B	A	12/3/2013	9:44:52	13	1	23	14.498	>4	>4	0	>4 to 0	299.66	20.67	19.84	>20.97	ind	Biological	40.21	2.77	0	-	20+
40B	B	12/3/2013	9:45:47	13	1	23.2	14.498	>4	>4	1	>4 to 1	304	20.97	>20.97	>20.97	ind	ind	ind	ind	ind	ind	7
40B	D	12/3/2013	9:48:04	13	1	20.4	14.498	>4	>4	1	>4 to 1	225.4	15.55	14.12	18.28	4.16	ind	ind	ind	ind	ind	10+
40C	A	12/5/2013	13:03:30	13	1	51.1	14.498	>4	>4	1	>4 to 1	201.5	13.90	13.52	14.51	0.99	Biological	46.59	3.21	o	-	n
40C	B	12/5/2013	13:04:22	13	1	51.1	14.498	>4	>4	1	>4 to 1	171.66	11.84	10.95	12.51	1.56	Biological	46.94	3.24	9	both	n
40C	D	12/5/2013	13:05:42	13	1	51.1	14.498	>4	>4	0	>4 to 0	179.28	12.37	10.98	13.45	2.48	Biological	50.46	3.48	10+	both	n
40D	B	12/5/2013	13:13:37	13	1	53.9	14.498	2 to 1	>4	0	>4 to 0	27.435	1.89	1.27	2.20	0.93	Physical	ind	ind	0	-	n
40D	C	12/5/2013	13:14:21	13	1	53.9	14.498	2 to 1/ >4	>4	0	>4 to 0	54.731	3.78	3.50	4.36	0.85	Physical	6.37	0.44	5	both	n
40D	D	12/5/2013	13:15:09	13	1	53.9	14.498	3 to 2/>4	>4	0	>4 to 0	50.729	3.50	3.24	3.88	0.64	Physical	ind	ind	0	-	n
40E	B	12/4/2013	7:58:09	13	1	38.0	14.498	ind	>4	ind	ind	0	0.00	0.00	0.00	ind	ind	ind	ind	-	-	-
40E	C	12/4/2013	7:58:49	13	1	36.0	14.498	ind	>4	ind	ind	0	0.00	0.00	0.00	ind	ind	ind	ind	-	-	-
40E	D	12/4/2013	7:59:39	13	1	38.5	14.498	4 to 3	>4	1	>4 to 1	73.347	5.06	4.64	5.61	0.97	Biological	35.70	2.46	n	-	n
41A	A	12/5/2013	13:22:07	13	1	14.0	14.498	>4	>4	2	>4 to 2	31.332	2.16	1.09	3.62	2.53	Physical	9.40	0.65	10+	both	n
41A	B	12/5/2013	12:23:00	13	1	15.2	14.498	>4	>4	2	>4 to 2	53.794	3.71	3.13	4.18	1.05	Biological	8.7861467	0.61	10+	both	n
41A	D	12/5/2013	13:24:57	13	1	14.4	14.498	ind	>4	-5	>4 to -5	0	0.00	0.00	0.00	ind	ind	ind	ind	-	-	-
42A	A	12/5/2013	13:33:44	13	1	28.0	14.498	>4	>4	1	>4 to 1	305.53	21.07	21.07	21.07	ind	ind	ind	ind	ind	ind	8
42A	B	12/5/2013	13:34:40	13	1	26.4	14.498	>4	>4	1	>4 to 1	305.53	21.07	21.07	21.07	ind	ind	ind	ind	ind	ind	20+
42A	C	12/5/2013	13:35:19	13	1	26.0	14.498	>4	>4	1	>4 to 1	253.72	17.50	16.60	18.59	1.99	Biological	45.10	3.11	2	oxidized	15+
42B	A	12/5/2013	13:50:42	13	1	45.0	14.498	4 to 3	>4	0	>4 to 0	114.2	7.88	7.28	8.65	1.38	Physical	27.71	1.91	0	-	n
42B	B	12/5/2013	13:51:37	13	1	45.0	14.498	4 to 3	>4	0	>4 to 0	166.91	11.51	10.94	11.93	0.99	Biological	42.69	2.94	1	oxidized	n
42B	C	12/5/2013	13:52:26	13	1	45.0	14.498	4 to 3	>4	0	>4 to 0	140.16	9.67	9.46	9.99	0.52	Physical	36.91	2.55	0	-	n
43B	A	12/5/2013	14:01:20	13	1	25.2	14.498	-2 to -4	>4	-5	>4 to -5	19.518	1.35	0.21	2.07	1.86	ind	ind	ind	0	-	n

Station	Replicate	Date	Time	Stop Collar Setting (in)	# of Weights (per side)	Water Depth (ft)	Calibration Constant	Grain Size Major Mode (phi)	Grain Size Minimum (phi)	Grain Size Maximum (phi)	GrnSize RANGE	Penetration Area (sq.cm)	Penetration Mean (cm)	Penetration Minimum (cm)	Penetration Maximum (cm)	Boundary Roughness (cm)	Boundary Roughness Type	RPD Area (sq.cm)	Mean RPD (cm)	Mud Clast Number	Mud Clast State	Methane ?
43B	C	12/5/2013	14:03:26	13	1	25.0	14.498	-4 to -5	>4	-5	>4 to -5	32.339	2.23	0.15	4.98	4.84	Physical	ind	ind	0	-	n
43B	D	12/5/2013	14:04:18	13	1	26.0	14.498	-2 to -4	>4	-3	>4 to -3	28.629	1.97	0.61	3.08	2.47	Physical	ind	ind	0	-	n
44B	A	12/5/2013	14:13:50	13	1	49.2	14.498	4 to 3	>4	1	>4 to 1	164.94	11.38	10.62	11.64	1.02	Biological	33.32	2.30	0	-	n
44B	B	12/5/2013	14:14:39	13	1	49.2	14.498	4 to 3	>4	0	>4 to 0	176.1	12.15	11.90	12.70	0.81	Biological	33.82	2.33	0	-	n
44B	C	12/5/2013	14:15:33	13	1	49.2	14.498	4 to 3	>4	0	>4 to 0	182.37	12.58	12.08	13.00	0.92	Biological	36.36	2.51	2	both	n
45A	A	12/5/2013	14:56:05	16	5	7.4	14.498	4 to 3/3 to 2	>4	0	>4 to 0	91.087	6.28	5.91	6.84	0.93	Physical	30.61	2.11	0	-	n
45A	B	12/5/2013	14:56:53	16	5	7.6	14.498	4 to 3/3 to 2	>4	0	>4 to 0	82.664	5.70	5.09	6.63	1.55	Biological	47.57	3.28	0	-	n
45A	C	12/5/2013	14:57:36	16	5	6.8	14.498	3 to 2	>4	-1	>4 to -1	83.223	5.74	5.18	6.15	0.97	Physical	29.40	2.03	0	-	n
46C	-	12/5/2013	14:27:03	13	1	47.4	14.498	ind	>4	-	ind	-	0.00	-	-	ind	-	ind	ind	-	-	-
47A	A	12/5/2013	15:09:57	16	5	18.6	14.498	>4 / 4 to 3	>4	1	>4 to 1	267.97	18.48	17.90	18.86	0.96	Biological	42.93	2.96	0	-	n
47A	C	12/5/2013	15:14:56	16	5	5.0	14.498	>4 / 3 to 2	>4	0	>4 to 0	94.268	6.50	5.89	6.82	0.93	Physical	36.25	2.50	0	-	n
47A	D	12/5/2013	15:15:42	16	5	6.0	14.498	2 to 1	>4	0	>4 to 0	95.174	6.56	4.90	8.04	3.14	Physical	41.88	2.89	0	-	n
48C	A	12/5/2013	14:39:48	13	1	47.4	14.498	>4	>4	1	>4 to 1	259.74	17.92	17.57	18.16	0.59	Biological	48.49	3.34	0	-	n
48C	C	12/5/2013	14:41:27	13	1	47.4	14.498	>4	>4	1	>4 to 1	264.66	18.25	18.08	18.48	0.40	Biological	42.83	2.95	0	-	n
48C	D	12/5/2013	14:42:23	13	1	47.4	14.498	>4	>4	1	>4 to 1	253.54	17.49	16.96	17.95	0.99	Biological	52.35	3.61	3	reduced	n
49A	A	12/5/2013	15:25:31	16	5	6.3	14.498	>4	>4	1	>4 to 1	305.31	21.06	ind	ind	ind	ind	ind	ind	ind	ind	9
49A	B	12/5/2013	15:26:36	16	5	6.0	14.498	>4	>4	1	>4 to 1	305.31	21.06	ind	ind	ind	ind	ind	ind	ind	ind	15+
49A	C	12/5/2013	15:27:29	16	5	6.0	14.498	4 to 3/ >4	>4	1	>4 to 1	305.31	21.06	ind	ind	ind	ind	ind	ind	ind	ind	20+
50A	C	12/5/2013	15:45:19	13	1	11.7	14.498	>4	>4	1	>4 to 1	266.26	18.36	18.11	18.64	0.53	Biological	43.23	2.98	0	-	n
50A	D	12/5/2013	15:46:11	13	1	11.1	14.498	>4	>4	1	>4 to 1	272.56	18.80	18.16	19.60	1.43	Biological	30.43	2.10	5	oxidized	20+
50A	E	12/5/2013	15:47:04	13	1	10.8	14.498	>4	>4	1	>4 to 1	263.82	18.20	17.79	18.43	0.64	Biological	32.88	2.27	0	-	3
51C	B	12/5/2013	15:56:27	13	1	43.2	14.498	>4	>4	1	>4 to 1	276.15	19.05	18.75	19.49	0.74	Biological	42.23	2.91	5	both	n
51C	C	12/5/2013	15:57:13	13	1	43.2	14.498	>4	>4	1	>4 to 1	266.57	18.39	17.66	19.07	1.41	Biological	50.41	3.48	0	-	n
51C	D	12/5/2013	15:58:00	13	1	43.2	14.498	>4	>4	1	>4 to 1	275.97	19.04	18.48	19.81	1.33	Biological	47.84	3.30	0	-	n
51F	A	12/5/2013	16:06:19	13	1	15.7	14.498	>4	>4	1	>4 to 1	296.29	20.44	20.08	20.90	0.83	Biological	50.12	3.46	0	-	n
51F	C	12/5/2013	16:09:08	13	1	15.2	14.498	>4	>4	1	>4 to 1	269.28	18.57	17.26	20.21	2.95	Physical	ind	ind	9	both	n
51F	D	12/5/2013	16:09:54	13	1	15.2	14.498	>4	>4	1	>4 to 1	275.02	18.97	18.70	19.30	0.61	Biological	49.88	3.44	1	oxidized	n
52A	A	12/7/2013	12:28:41	13	1	9.3	14.498	>4	>4	0	>4 to 0	260.4	17.96	17.15	18.40	1.25	Biological	42.24	2.91	0	-	3
52A	B	12/7/2013	12:29:41	13	1	8.7	14.498	>4	>4	1	>4 to 1	259.05	17.87	17.28	18.38	1.09	Biological	51.72	3.57	0	-	20+
52A	C	12/7/2013	12:30:43	13	1	9.0	14.498	>4	>4	0	>4 to 0	248.86	17.16	16.48	17.39	0.91	Physical	46.72	3.22	6	both	10+
52B	A	12/7/2013	12:38:17	13	1	15.3	14.498	>4	>4	1	>4 to 1	288.17	19.88	18.99	21.01	2.02	Biological	47.36	3.27	0	-	4
52B	B	12/7/2013	12:39:11	13	1	15.6	14.498	4 to 3/ >4	>4	0	>4 to 0	253.46	17.48	15.84	19.10	3.25	Physical	34.65	2.39	4	red/oxy	10+
52B	C	12/7/2013	12:40:05	13	1	14.4	14.498	>4	>4	1	>4 to 1	286.61	19.77	19.38	20.53	1.15	Biological	45.23	3.12	0	-	2
53E	A	12/7/2013	12:49:55	13	1	20.5	14.498	>4	>4	1	>4 to 1	252.15	17.39	16.64	17.90	1.25	Biological	33.42	2.30	0	-	n
53E	B	12/7/2013	12:50:58	13	1	21.0	14.498	>4	>4	1	>4 to 1	249.85	17.23	15.95	17.76	1.81	Physical	57.18	3.94	0	-	n
53E	D	12/7/2013	12:52:50	13	1	21.5	14.498	>4	>4	1	>4 to 1	264.02	18.21	17.66	18.59	0.93	Biological	42.87	2.96	0	-	n
54B	A	12/7/2013	12:01:23	13	1	31.0	14.498	4 to 3	>4	1	>4 to 1	95.444	6.58	5.62	7.16	1.55	Biological	37.85	2.61	0	-	n

Station	Replicate	Date	Time	Stop Collar Setting (in)	# of Weights (per side)	Water Depth (ft)	Calibration Constant	Grain Size Major Mode (phi)	Grain Size Minimum (phi)	Grain Size Maximum (phi)	GrnSize RANGE	Penetration Area (sq.cm)	Penetration Mean (cm)	Penetration Minimum (cm)	Penetration Maximum (cm)	Boundary Roughness (cm)	Boundary Roughness Type	RPD Area (sq.cm)	Mean RPD (cm)	Mud Clast Number	Mud Clast State	Methane ?
54B	E	12/7/2013	12:16:28	14	2	31.0	14.498	4 to 3	>4	1	>4 to 1	128.84	8.89	8.55	9.48	0.93	Biological	33.49	2.31	0	-	n
54B	H	12/7/2013	12:19:17	14	2	31.0	14.498	>4	>4	1	>4 to 1	140.37	9.68	9.21	10.28	1.07	Biological	44.30	3.06	0	-	n
55B	A	12/6/2013	15:49:16	13	1	40.8	14.498	>4	>4	1	>4 to 1	295.89	20.41	19.54	21.09	1.55	Biological	93.60	6.46	0	-	n
55B	B	12/6/2013	15:50:16	13	1	40.8	14.498	>4	>4	1	>4 to 1	287.37	19.82	19.10	20.34	1.25	Biological	56.34	3.89	0	-	n
55B	C	12/6/2013	15:51:04	13	1	40.8	14.498	>4	>4	1	>4 to 1	299.04	20.63	20.08	21.12	1.04	Biological	49.33	3.40	0	-	n
56A	B	12/7/2013	11:07:52	13	1	9.5	14.498	>4	>4	0	>4 to 0	273.12	18.84	17.58	20.37	2.79	Biological	34.63	2.39	0	-	20+
56A	C	12/7/2013	11:08:46	13	1	9.5	14.498	>4	>4	1	>4 to 1	281.78	19.44	18.38	20.53	2.15	Biological	25.90	1.79	0	-	10+
56A	E	12/7/2013	11:10:21	13	1	10.0	14.498	>4	>4	0	>4 to 0	275.94	19.03	18.40	19.41	1.01	Biological	37.05	2.56	0	-	15+
56C	A	12/6/2013	15:59:02	13	1	51.0	14.498	>4	>4	1	>4 to 1	228.17	15.74	15.39	15.95	0.56	Biological	63.21	4.36	2	oxidized	n
56C	C	12/6/2013	16:01:20	13	1	51.0	14.498	>4	>4	0	>4 to 0	223.89	15.44	14.62	16.32	1.71	Biological	57.16	3.94	4	both	20+
56C	D	12/6/2013	16:02:22	13	1	51.0	14.498	>4	>4	0	>4 to 0	231.45	15.96	14.78	16.67	1.89	Biological	34.63	2.39	0	-	15+
56F	C	12/7/2013	10:48:47	15	3	23.7	14.498	3 to 2	>4	0	>4 to 0	95.676	6.60	6.10	7.11	1.01	Biological	41.07	2.83	0	-	n
56F	D	12/7/2013	10:49:48	15	3	24.6	14.498	4 to 3	>4	-1	>4 to -1	84.564	5.83	5.57	6.13	0.56	Biological	49.94	3.44	0	-	n
56F	E	12/7/2013	10:50:52	15	3	21.2	14.498	4 to 3	>4	-1	>4 to -1	64.172	4.43	3.83	5.17	1.33	Biological	64.171923	4.43	0	-	n
57D	A	12/7/2013	8:59:55	13	1	51.8	14.498	>4	>4	1	>4 to 1	226.62	15.63	15.10	16.16	1.07	Biological	28.35	1.96	0	-	n
57D	D	12/7/2013	9:02:51	13	1	53.7	14.498	>4	>4	1	>4 to 1	250.02	17.25	16.78	17.90	1.12	Biological	35.84	2.47	0	-	n
57F	A	12/7/2013	9:18:16	12	0	38.5	14.498	>4	>4	1	>4 to 1	227.79	15.71	14.86	16.70	1.84	Biological	53.53	3.69	0	-	n
57F	C	12/7/2013	9:19:49	12	0	38.5	14.498	>4	>4	1	>4 to 1	244.56	16.87	16.54	17.20	0.67	Biological	53.96	3.72	0	-	n
57F	D	12/7/2013	9:20:43	12	0	38.5	14.498	>4	>4	1	>4 to 1	236.13	16.29	14.96	17.92	2.96	Biological	51.95	3.58	10+	both	n
58D	A	12/7/2013	8:38:56	13	1	51.8	14.498	4 to 3	>4	1	>4 to 1	226.7	15.64	14.64	16.46	1.81	Biological	16.53	1.14	0	-	n
58D	B	12/7/2013	8:39:52	13	1	51.8	14.498	4 to 3	>4	1	>4 to 1	244.96	16.90	16.59	17.31	0.72	Biological	29.26	2.02	0	-	n
58D	C	12/7/2013	8:41:16	13	1	51.8	14.498	4 to 3	>4	1	>4 to 1	232.82	16.06	15.50	16.96	1.47	Biological	36.65	2.53	2	both	n
59B	B	12/6/2013	15:32:26	13	1	15.4	14.498	>4	>4	0	>4 to 0	292.35	20.16	19.20	21.01	1.81	Biological	47.09	3.25	1	oxidized	3
59B	C	12/6/2013	15:33:19	13	1	15.4	14.498	>4	>4	1	>4 to 1	269.77	18.61	18.08	19.02	0.93	Biological	43.66	3.01	0	-	6
59B	D	12/6/2013	15:34:17	13	1	15.6	14.498	>4	>4	1	>4 to 1	273.93	18.89	18.41	19.31	0.91	Biological	35.40	2.44	8	oxidized	20+
59E	A	12/7/2013	8:29:19	13	1	40.2	14.498	>4	>4	1	>4 to 1	261.27	18.02	17.59	18.51	0.92	Biological	32.57	2.25	0	-	n
59E	C	12/7/2013	8:31:12	13	1	40.2	14.498	>4	>4	1	>4 to 1	317.35	21.89	15.04	16.99	1.95	Biological	30.59	2.11	0	-	n
59E	D	12/7/2013	8:32:10	13	1	40.2	14.498	>4	>4	1	>4 to 1	243.78	16.81	15.90	17.12	1.23	Biological	41.08	2.83	0	-	n
59F	B	12/7/2013	9:30:59	12	0	40.0	14.498	>4	>4	1	>4 to 1	242.94	16.76	16.40	17.07	0.67	Biological	36.66	2.53	0	-	n
59F	C	12/7/2013	9:32:01	12	0	40.0	14.498	>4	>4	1	>4 to 1	235.69	16.26	15.50	17.44	1.95	Biological	29.18	2.01	0	-	n
59F	D	12/7/2013	9:32:59	12	0	40.0	14.498	4 to 3/ >4	>4	1	>4 to 1	305.22	21.05	21.05	21.05	ind	ind	ind	ind	0	-	n
60D	A	12/7/2013	8:16:01	13	1	43.2	14.498	4 to 3	>4	1	>4 to 1	235	16.21	16.08	16.32	0.24	Biological	31.12	2.15	0	-	n
60D	C	12/7/2013	8:18:16	13	1	43.2	14.498	4 to 3	>4	1	>4 to 1	232.71	16.05	15.68	16.43	0.75	Biological	32.86	2.27	0	-	n
60D	D	12/7/2013	8:19:21	13	1	43.2	14.498	4 to 3	>4	1	>4 to 1	230.58	15.90	15.34	16.16	0.83	Biological	38.57	2.66	0	-	n
61A	E	12/7/2013	11:40:13	12	0	19.2	14.498	>4	>4	1	>4 to 1	257.12	17.73	17.44	18.19	0.75	Biological	44.79	3.09	0	-	n
61A	F	12/7/2013	11:41:32	12	0	19.2	14.498	>4	>4	2	>4 to 2	234.35	16.16	15.42	16.96	1.55	Biological	52.35	3.61	0	-	n

Station	Replicate	Date	Time	Stop Collar Setting (in)	# of Weights (per side)	Water Depth (ft)	Calibration Constant	Grain Size Major Mode (phi)	Grain Size Minimum (phi)	Grain Size Maximum (phi)	GrnSize RANGE	Penetration Area (sq.cm)	Penetration Mean (cm)	Penetration Minimum (cm)	Penetration Maximum (cm)	Boundary Roughness (cm)	Boundary Roughness Type	RPD Area (sq.cm)	Mean RPD (cm)	Mud Clast Number	Mud Clast State	Methane ?
61A	G	12/7/2013	11:42:32	12	0	19.5	14.498	>4	>4	1	>4 to 1	239.23	16.50	15.74	17.15	1.41	Biological	43.63	3.01	0	-	n
61E	A	12/7/2013	9:43:13	12	0	38.5	14.498	>4	>4	2	>4 to 2	282.66	19.50	18.91	19.76	0.85	Biological	49.07	3.38	0	-	n
61E	B	12/7/2013	9:44:09	12	0	38.5	14.498	>4	>4	2	>4 to 2	271.58	18.73	17.98	19.54	1.57	Biological	44.67	3.08	0	-	n
61E	D	12/7/2013	9:46:11	12	0	38.5	14.498	>4	>4	2	>4 to 2	280.59	19.35	18.32	20.45	2.13	Biological	39.52	2.73	1	oxidized	n
62C	B	12/6/2013	15:05:31	13	1	53.8	14.498	>4	>4	1	>4 to 1	244.8	16.89	16.64	17.07	0.43	Biological	45.06	3.11	5	both	8
62C	C	12/6/2013	15:06:50	13	1	53.2	14.498	>4 / 4 to 3	>4	1	>4 to 1	229.1	15.80	15.39	16.03	0.64	Biological	55.76	3.85	0	-	5
62C	D	12/6/2013	15:07:52	13	1	53.2	14.498	>4 / 4 to 3	>4	1	>4 to 1	246.8	17.02	16.06	17.39	1.33	Biological	42.13	2.91	0	-	n
63D	A	12/6/2013	14:52:32	13	1	24.0	14.498	4 to 3	>4	0	>4 to 0	129.98	8.97	8.73	9.08	0.35	Biological	46.57	3.21	4	oxidized	n
63D	B	12/6/2013	14:53:39	13	1	25.0	14.498	4 to 3	>4	0	>4 to 0	101.16	6.98	6.15	8.55	2.39	Physical	53.16	3.67	0	-	n
63D	C	12/6/2013	14:54:41	13	1	24.8	14.498	4 to 3	>4	0	>4 to 0	122.05	8.42	7.22	9.43	2.21	Biological	52.41	3.61	0	-	n
63E	A	12/7/2013	9:57:00	12	0	25.6	14.498	>4	>4	2	>4 to 2	269	18.55	17.92	19.02	1.09	Biological	45.71	3.15	0	-	n
63E	C	12/7/2013	9:58:42	12	0	25.6	14.498	>4	>4	2	>4 to 2	265.96	18.34	18.16	18.54	0.37	Biological	44.97	3.10	3	oxy	n
63E	D	12/7/2013	9:59:35	12	0	25.6	14.498	>4	>4	2	>4 to 2	275.32	18.99	18.56	19.46	0.90	Biological	37.85	2.61	2	reduced	n
64A	E	12/7/2013	11:26:48	12	0	27.2	14.498	>4	>4	1	>4 to 1	256.67	17.70	16.56	18.32	1.76	Biological	38.66	2.67	0	-	n
64A	F	12/7/2013	11:27:34	12	0	27.2	14.498	>4	>4	1	>4 to 1	234.9	16.20	15.47	17.39	1.92	Biological	50.69	3.50	0	-	n
64A	H	12/7/2013	11:29:31	12	0	27.2	14.498	>4	>4	1	>4 to 1	230.58	15.90	14.16	17.52	3.36	Biological	79.39	5.48	0	-	3
64E	A	12/7/2013	10:08:05	12	0	19.5	14.498	4 to 3	>4	1	>4 to 1	188.15	12.98	12.28	13.42	1.15	Biological	36.40	2.51	0	-	n
64E	B	12/7/2013	10:09:02	12	0	19.2	14.498	>4	>4	1	>4 to 1	191.51	13.21	12.70	13.82	1.11	Biological	74.10	5.11	0	-	n
64E	D	12/7/2013	10:11:04	12	0	18.7	14.498	4 to 3	>4	1	>4 to 1	154.95	10.69	10.17	11.93	1.76	Biological	31.82	2.19	0	-	n
65C	A	12/6/2013	14:27:26	13	1	50.4	14.498	4 to 3	>4	0	>4 to 0	93.619	6.46	5.81	7.14	1.33	Biological	35.44	2.44	0	-	n
65C	B	12/6/2013	14:28:23	13	1	50.4	14.498	4 to 3/ 2 to 1	>4	-1	>4 to -1	77.93	5.38	4.98	5.81	0.83	Biological	16.91	1.17	0	-	n
65C	C	12/6/2013	14:29:33	13	1	50.4	14.498	4 to 3/ 2 to 1	>4	-1	>4 to -1	95.456	6.58	6.10	6.98	0.88	Biological	33.02	2.28	0	-	n
67A	A	12/6/2013	14:17:45	13	1	24.0	14.498	2 to 1/ >4	>4	-1	>4 to -1	164.74	11.36	11.08	11.42	0.35	Biological	41.84	2.89	0	-	n
67A	C	12/6/2013	14:19:21	13	1	23.8	14.498	2 to 1/ >4	>4	-1	>4 to -1	175.21	12.08	11.77	12.30	0.53	Biological	34.63	2.39	1	oxidized	n
67A	D	12/6/2013	14:20:12	13	1	24.0	14.498	2 to 1/ >4	>4	-1	>4 to -1	160.27	11.05	10.76	11.24	0.48	Biological	31.42	2.17	0	-	n
67C	A	12/6/2013	14:06:06	13	1	26.4	14.498	>4	>4	1	>4 to 1	291.66	20.12	19.30	21.12	1.81	Biological	57.19	3.94	0	-	20+
67C	B	12/6/2013	14:07:04	13	1	26.4	14.498	>4	>4	1	>4 to 1	301.55	21.17	20.00	>21.17	ind	ind	ind	ind	ind	-	7
67C	D	12/6/2013	14:08:43	13	1	26.4	14.498	>4	>4	1	>4 to 1	304.77	21.02	>21.02	>21.02	ind	ind	ind	ind	ind	-	20+
68E	C	12/6/2013	13:45:19	13	1	15.4	14.498	>4	>4	1	>4 to 1	41.519	2.86	0.91	3.49	2.58	Biological	41.52	2.86	6	oxidized	n
68E	D	12/6/2013	13:46:25	13	1	21.6	14.498	4 to 3 / >4	>4	0	>4 to 0	169.74	11.71	11.18	12.06	0.88	Biological	35.04	2.42	0	-	n
68E	E	12/6/2013	13:47:21	13	1	21.0	14.498	4 to 3	>4	0	>4 to 0	119.18	8.22	7.96	8.60	0.64	Biological	66.05	4.56	10+	oxidized	n
69C	B	12/6/2013	13:56:28	13	1	46.8	14.498	>4	>4	1	>4 to 1	282.92	19.51	19.12	19.89	0.77	Biological	65.83	4.54	0	-	n
69C	C	12/6/2013	13:57:26	13	1	46.8	14.498	>4	>4	1	>4 to 1	284.7	19.64	19.36	19.97	0.61	Biological	62.02	4.28	0	-	12
69C	D	12/6/2013	13:58:14	13	1	47.2	14.498	>4	>4	0	>4 to 0	288.45	19.90	19.62	20.16	0.53	Biological	53.06	3.66	1	reduced	20+
70A	A	12/6/2013	13:25:56	13	1	41.4	14.498	>4	>4	2	>4 to 2	302.57	20.87	20.42	>21.14	ind	Biological	58.80	4.06	0	-	n
70A	B	12/6/2013	13:26:44	13	1	41.4	14.498	>4	>4	1	>4 to 1	>305.22	>21.20	>21.20	>21.20	ind	ind	ind	ind	ind	-	n
70A	C	12/6/2013	13:28:00	13	1	41.4	14.498	>4	>4	1	>4 to 1	>305.22	>21.20	>21.20	>21.20	ind	ind	ind	ind	ind	-	n

Station	Replicate	Date	Time	Stop Collar Setting (in)	# of Weights (per side)	Water Depth (ft)	Calibration Constant	Grain Size Major Mode (phi)	Grain Size Minimum (phi)	Grain Size Maximum (phi)	GrnSize RANGE	Penetration Area (sq.cm)	Penetration Mean (cm)	Penetration Minimum (cm)	Penetration Maximum (cm)	Boundary Roughness (cm)	Boundary Roughness Type	RPD Area (sq.cm)	Mean RPD (cm)	Mud Clast Number	Mud Clast State	Methane ?
73B	A	12/6/2013	13:13:23	13	1	28.2	14.498	>4	>4	1	>4 to 1	270.32	18.65	18.32	19.22	0.90	Biological	46.47	3.21	0	-	n
73B	B	12/6/2013	13:14:19	13	1	28.2	14.498	>4	>4	1	>4 to 1	285.34	19.68	19.46	20.18	0.72	Biological	59.60	4.11	0	-	n
73B	D	12/6/2013	13:15:54	13	1	29.2	14.498	>4	>4	1	>4 to 1	282.01	19.45	19.07	19.81	0.74	Biological	70.76	4.88	0	-	n
74A	A	12/6/2013	12:09:00	13	1	23.5	14.498	>4	>4	1	>4 to 1	225.04	15.52	15.10	16.03	0.93	Biological	39.15	2.70	0	-	n
74A	B	12/6/2013	12:09:50	13	1	27.0	14.498	>4	>4	1	>4 to 1	248.14	17.12	16.70	17.39	0.69	Biological	34.85	2.40	0	-	n
74A	C	12/6/2013	12:11:16	13	1	22.4	14.498	>4	>4	1	>4 to 1	254.76	17.57	15.50	18.40	2.90	Biological	49.16	3.39	0	-	n
75D	B	12/6/2013	11:56:21	13	1	42.7	14.498	ind	>4	ind	ind	1.45	0.10	0.00	0.38	0.38	ind	ind	ind	0	-	n
75E	B	12/6/2013	11:46:43	13	1	30.5	14.498	4 to 3	>4	1	>4 to 1	16.131	1.11	0.59	1.89	1.31	Biological	ind	ind	0	-	n
75E	C	12/6/2013	11:47:29	13	1	30.0	14.498	4 to 3	>4	2	>4 to 2	32.555	2.25	1.73	2.90	1.17	Physical	32.55	ind	0	-	n
77A	A	12/6/2013	11:29:43	14	2	38.2	14.498	>4	>4	1	>4 to 1	305.19	21.05	21.05	21.05	ind	ind	ind	ind	ind	ind	n
77A	B	12/6/2013	11:30:23	14	2	38.2	14.498	>4	>4	1	>4 to 1	180.81	12.47	11.77	12.89	1.12	Biological	49.13	3.39	0	-	n
77A	C	12/6/2013	11:31:05	14	2	38.4	14.498	>4	>4	1	>4 to 1	255.33	17.61	17.26	18.35	1.09	Biological	56.01	3.86	10	both	n
77B	C	12/6/2013	11:22:54	14	2	49.5	14.498	4 to 3	>4	0	>4 to 0	238.72	16.47	15.12	17.66	2.53	Biological	45.10	3.11	6	oxidized	15
77B	D	12/6/2013	11:23:47	14	2	49.5	14.498	4 to 3/3 to 2	>4	0	>4 to 0	243.77	16.81	16.64	17.04	0.40	Biological	52.37	3.61	0	-	n
78A	B	12/6/2013	10:51:30	14	2	9.5	14.498	4 to 3	>4	1	>4 to 1	305.19	21.05	21.05	21.05	ind	ind	ind	ind	ind	ind	20+
78A	C	12/6/2013	10:52:19	14	2	9.5	14.498	3 to 2	>4	1	>4 to 1	>304.98	21.04	20.82	21.05	ind	ind	ind	ind	ind	ind	15+
78A	D	12/6/2013	10:53:27	14	2	9.5	14.498	>4 / 4 to 3	>4	1	>4 to 1	305.19	21.05	21.05	21.05	ind	ind	ind	ind	ind	ind	20+
78D	C	12/6/2013	11:09:42	14	2	83.0	14.498	ind	>4	ind	ind	0	0.00	ind	ind	ind	ind	ind	ind	0	-	n
79D	A	12/6/2013	9:53:54	15	4	24.5	14.498	4 to 3	>4	-4	>4 to -4	34.312	2.37	1.92	3.14	1.22	Physical	ind	ind	0	-	n
79D	B	12/6/2013	9:54:41	15	4	24.5	14.498	>4 / 4 to 3	>4	1	>4 to 1	121.76	8.40	7.43	9.35	1.91	Biological	35.44	2.44	0	-	n
79D	C	12/6/2013	9:55:27	15	4	24.0	14.498	4 to 3	>4	1	>4 to 1	62.938	4.34	4.05	4.69	0.64	Biological	37.05	2.56	0	-	n
81A	F	12/6/2013	10:16:32	14	2	36.0	14.498	-8	>4	-8	>4 to -8	0.00	0.00	0	0.00	ind	-	ind	ind	0	-	n
82C	B	12/6/2013	9:29:18	15	4	35.5	14.498	4 to 3	>4	1	>4 to 1	288.29	19.88	19.76	20.13	0.37	Biological	46.94	3.24	0	-	n
82C	E	12/6/2013	10:24:53	14	2	30.5	14.498	>4 / 4 to 3	>4	1	>4 to 1	264.91	18.27	17.87	18.62	0.75	Biological	53.16	3.67	0	-	n
82C	H	12/6/2013	10:27:53	14	2	28.5	14.498	4 to 3	>4	1	>4 to 1	211.33	14.58	14.27	14.83	0.56	Biological	56.39	3.89	0	-	n
82D	B	12/6/2013	9:20:29	15	4	14.5	14.498	4 to 3 / >4	>4	1	>4 to 1	239	16.48	15.94	16.72	0.79	Biological	33.02	2.28	0	-	n
82D	C	12/6/2013	9:21:22	15	4	19.5	14.498	4 to 3/ >4	>4	1	>4 to 1	276.23	19.05	18.38	19.41	1.03	Biological	59.66	4.11	0	-	n
82D	D	12/6/2013	9:22:19	15	4	19.5	14.498	4 to 3/ >4	>4	1	>4 to 1	249.8	17.23	16.11	18.11	2.00	Biological	50.74	3.50	0	-	n

Station	Replicate	Low DO?	COMMENT	# of Feeding Voids	Void Minimum Depth (cm)	Void Maximum Depth (cm)	Void Average Depth (cm)	Successional Stage
16A	E	n	Silt-clay over silty fine sand; small mud clasts on surface; shallow burrows in upper 2-3 cm; evidence of burrowing throughout profile, portions of thin worms visible against faceplate	0	-	-	-	2
16A	F	n	Silt-clay over silty fine sand; small to med mud clasts on surface and in background; shallow burrowing activity in upper 2-3 cm; evidence of burrowing throughout profile.	0	-	-	-	2
16A	H	n	Silt-clay over fine sand; one larger mud clast in background; shallow burrowing activity in upper 2cm; larger burrow/activity just below SWI at center.	0	-	-	-	2 -> 3
16B	A	n	Consolidated silty, very fine sand; shallow penetration, aRPD indeterminate, extends below penetration depth; evidence of shallow burrowing	0	-	-	-	indeterminate
16B	B	n	Consolidated silty, very fine sand; shallow penetration, aRPD indeterminate, extends below penetration depth; evidence of shallow burrowing	0	-	-	-	indeterminate
16B	D	n	Consolidated silty, very fine sand; shallow penetration, aRPD indeterminate, extends below penetration depth; evidence of shallow burrowing; transected burrow visible.	0	-	-	-	indeterminate
16E	A	n	Silty, very fine sand; coarser grain sand layer <0.5cm at SWI; pit connected to partially filled burrow at depth; bioturbation extends beyond depth of prism penetration.	0	-	-	-	2 on 3
16E	B	n	Silty, very fine sand; uneven surface, lower by a couple cm on right; small methane bubbles at depth on left; void at depth at center, burrowing extends beyond prism penetration depth	1	7.42	10.83	9.13	2 on 3
17A	D	n	Silty, very fine to medium sand; uneven surface, coarser grains at depth on right; wood debris at surface; 3 small voids at depth on left, burrowing extends beyond prism penetration	3	4.34	5.31	4.82	3
17A	G	n	Silty, very fine sand over fine sand, coarser grains at surface and at depth; transected burrows at depth	0	-	-	-	2 -> 3
17A	H	n	Silty, very fine sand mixed with fine sand, extending from surface to depth in 3 places; few granules/pebbles on surface; transected burrows at depth	0	-	-	-	2 -> 3
18C	A	n	Silty, very fine sand; small burrows through aRPD; small burrow/void at depth below aRPD, small annelid near void	1	7.29	7.64	7.46	2 on 3
18C	B	n	Sity very fine sand; v. small and 1 med mud clasts at SWI; small tubes @ SWI, transected burrows at depth	0	-	-	-	1 on 3
18C	E	n	Silty, very fine sand; v. small tubes on surface; small burrows throughout aRPD, transected burrows at depth	0	-	-	-	1 on 3
19A	B	n	Well-sorted fine sand with minor silt fraction; ripples	0	-	-	-	indeterminate
19A	C	n	Well-sorted fine sand; ripples, several tubes in background	0	-	-	-	indeterminate
19A	D	n	Well-sorted fine sand; ripples, several tubes in background	0	-	-	-	indeterminate
20D	A	n	Silt clay with very fine sand; small tube at SWI; small burrows in aRPD; small void a couple cm below aRPD; methane bubbles and evidence of burrowing at depth	1	7.89	8.02	7.96	2 on 3
20D	B	n	Silt-clay with very fine sand; small burrows in aRPD; methane bubbles at depth; small annelid at depth	0	-	-	-	2 on 3
20D	D	n	Silt-clay with very fine sand; small burrows through aRPD; small annelid at depth	0	-	-	-	2
21D	A	n	Silty, very fine sand, with ~0.5 -1 cm layer of fine sand at SWI; few small burrows in aRPD on left, small methane bubbles at depth	0	-	-	-	1
21D	C	n	Silt-clay grading into silty, very fine sand; part of small annelid and evidence of larger burrow few cm below aRPD; methane bubbles at depth	0	-	-	-	2 on 3
21D	D	n	Silt-clay grading into silty, very fine sand; small burrows in aRPD and evidence of burrowing below aRPD; methane bubbles at depth	0	-	-	-	2 -> 3
22C	B	n	Very fine sandy silt-clay; small burrows in aRPD; methane bubbles at depth, evidence of burrowing at depth	0	-	-	-	2 -> 3
22C	C	n	Silt-clay grading into silty, very fine sand at depth; small burrows in aRPD; most methane bubbles at depth	0	-	-	-	2
22C	D	n	Over-penetration. Silt-clay with small wood fibers in surface grading to silty, very fine sand; burrows in aRPD; small void just below aRPD on left; small annelid at depth on right; methane bubbles at depth	1	>6.80	>7.28	7.28	2 on 3
22D	B	n	Silt clay with silty very fine sand at depth; small burrowing in aRPD; small void at depth; methane bubbles at depth; thin annelid at depth on right	1	9.66	9.94	9.80	2 on 3
22D	C	n	Silt-clay with silty very fine sand at depth; small burrows in aRPD; thin annelid a couple cm below aRPD on left, signs of larger burrowers to right; methane bubbles at depth	0	-	-	-	2 on 3
22D	D	n	Silt-clay grading to silty, very fine sand; small burrows through aRPD; methane bubbles at depth	0	-	-	-	2
22F	A	n	Silt-clay admixed with silty, very fine sand; shallow burrows in upper cm; annelid at depth on right; methane bubbles at depth	0	-	-	-	2 on 3
22F	C	n	Silt-clay admixed with silty, very fine sand; small shallow burrows; v thin annelid at depth at center; methane bubbles at depth	0	-	-	-	1
22F	D	n	Silt-clay with small shallow burrows; small annelid at depth; methane bubbles from ~6cm to depth	0	-	-	-	1
23A	A	n	Almost no penetration; silty very fine sand on left with wood debris on right	0	-	-	-	indeterminate
23A	B	n	Silty, very fine sand, evidence of shallow burrowing	0	-	-	-	indeterminate

Station	Replicate	Low DO?	COMMENT	# of Feeding Voids	Void Minimum Depth (cm)	Void Maximum Depth (cm)	Void Average Depth (cm)	Successional Stage
23B	A	n	Silt-clay with very fine sand; transected deeper burrow ~1-2 cm below aRPD on left	0	-	-	-	2 -> 3
23B	C	n	Silt-clay with fraction of very fine sand; shallow burrowing; two small voids, one below aRPD and one at depth	2	5.24	13.56	9.40	2 on 3
23B	D	n	Silt-clay with very fine sand; shallow burrowing and near base of aRPD; evidence of deeper burrowing below aRPD on left and at depth; thin annelid on right at ~9.5cm	0	-	-	-	2 on 3
23E	A	n	Silt-clay over silty very fine sand, coarser sed mixed in; short shallow burrows; methane bubbles and burrowing at depth.	0	-	-	-	2 on 3
23E	B	n	Very fine sand mixed with fine sand, patches of coarser sed throughout and at SWI; few small burrows visible in aRPD	0	-	-	-	2
23E	C	n	Silt-clay over silty fine sand, patches of coarser sed throughout; shallow burroing; v thin small annelid just below aRPD to right of center	0	-	-	-	2 -> 3
24D	B	n	Silt-clay admixed with very fine sand; some evidence of deeper burrows- former burrow end, possible bits of annelids	0	-	-	-	1 on 3
24D	C	n	Silt-clay with wood fibers & very fine sand; possible small annelid at depth; bits of debris and methane bubbles at depth	0	-	-	-	2
24D	D	n	Silt-clay with very fine sand; shallow burrowing in upper cm and through aRPD; possible wood chip debris at depth	0	-	-	-	2
25A	A	n	Silt-clay with minor fraction of very fine sand; shallow burrowing; small void just below aRPD on right; methane bubbles at depth	1	3.74	4.96	4.35	2 on 3
25A	C	n	Silt-clay with large mud clast in background; evidence of subsurface burrowing	0	-	-	-	2
25A	D	n	Silt-clay with large biogenic pit at SWI; short burrows visible in aRPD; methane @ depth	0	-	-	-	1 on 3
25C	B	n	Silt-clay with minor fraction of very fine sand; small burrows through aRPD; evidence of burrowing & methane bubbles at depth	0	-	-	-	2 on 3
25C	C	n	Silt clay with minor fraction of very fine sand; very shallow burrows; annelids at 11.2 and 12.2 cm; methane bubbles at depth	0	-	-	-	2 -> 3
25C	D	n	Silt clay with some very fine sand; small burrows in upper 2 cm; methane bubbles at depth	0	-	-	-	2
25D	A	n	Poorly sorted silty very fine sand; dense assemblage of small tubes on surface; burrowing @ depth	0	-	-	-	1 on 2
25D	B	n	Silty, very fine sand mixed with fine sand, some coarser grains at SWI; burrowing extends beyond prism penetration depth.	0	-	-	-	2
25D	D	n	Silty very fine sand; small to med mud clasts on surface and in background(camera artifact); small burrows in aRPD	0	-	-	-	2
26A	A	n	Silty very fine sand; phytodetritus on surface with algal debris with methane escape burrow; worms visible at depth	0	-	-	-	1
26A	C	n	Silty very fine sand; few bits of algal debris on surface; few tubes and organic debris in background	0	-	-	-	2
26A	D	n	Silty very fine sand; organic debris on surface; bits of annelids visible at depth	0	-	-	-	2 -> 3
26B	D	n	Silt-clay with very fine sand, small annelids and burrows in aRPD	0	-	-	-	2 -> 3
26C	B	n	Silt-clay with minor fraction of very fine sand; short tubes at SWI; small burrows throughout aRPD	0	-	-	-	2
26C	C	n	Silt-clay with minor fraction of very fine sand, clast artifact from camera base in center	0	-	-	-	2
26C	D	n	Silt-clay with minor fraction of very fine sand; short tubes at SWI; small burrows throughout aRPD & large feeding pit at left	0	-	-	-	2 -> 3
26E	A	n	Silt-clay with very fine sand, small annelids and burrows in aRPD, methane at depth	0	-	-	-	1
26E	B	n	Silt-clay with very fine sand, small burrows in aRPD, methane at depth	0	-	-	-	1
26E	C	n	Silt-clay with very fine sand, small burrows in aRPD, methane and annelids (appears to be Capitellids) at depth	0	-	-	-	1
27A	A	n	Silty very fine to fine sand, organic and bit of algal debris on surface; short burrows in aRPD	0	-	-	-	1
27A	E	n	Silt-clay over silty very fine and fine sand; short burrows in aRPD; methane bubble at depth	0	-	-	-	1
27B	B	n	Silt-clay with minor fraction of very fine sand; short burrows in aRPD; long annelid- capitellid- at depth; methane bubbles from 9cm to depth	0	-	-	-	1
27B	C	n	Over-penetration. Silt-clay admixed with very fine sand; short burrows in aRPD, parts of annelids against faceplate at depth, methane bubbles from~7-8cm to depth, evidence of subsurface burrowing.	0	-	-	-	1 -> 2
27B	D	n	Over-penetration except on right. Silt-clay with very fine sand; short burrows through aRPD; small void at 11 cm; methane at depth	1	>10.66	>11.10	>10.88	1 on 3
27C	B	n	Silt clay admixed with very fine sand, some silt at depth (depositional horizons), large mud clast at SWI on right is from camera wiper blade; burrows through aRPD and at depth	0	-	-	-	2 -> 3
27C	C	n	Silt-clay over silty very fine sand and patch of fine sand at depth, some coarser grains near SWI; short burrows in aRPD, one larger one connected to surface; evidence of burrowing at depth	0	-	-	-	2
27C	D	n	Silt-clay over silty very fine sand, patches of fine sand with some coarser grains at depth, mud clasts at SWI on right are from camera; small annelid below aRPD at center.	0	-	-	-	2
27D	A	n	Silt-clay admixed with very fine sand, bits of wood fibers in upper cm; short burrows in aRPD; 2 short thin annelids just below aRPD on right; evidence of deeper burrowers left of center; methane bubbles from 9 cm to depth	0	-	-	-	2
27D	C	n	Silt-clay with minor fraction of very fine sand, some small bits of debris and wood fibers in upper cms; small burrows in aRPD and a couple below; annelid at ~10 cm on left; very thin annelid at depth; methane bubbles from 9cm to depth	0	-	-	-	2 -> 3
27D	D	n	Silt-clay with minor fraction of very fine sand; thin polychates & burrowing at depth; methane bubbles from within aRPD to depth	0	-	-	-	2 on 3
27E	A	n	Silt-clay with minor fraction of very fine sand, over-penetration at center; burrowing at depth among trapped methane gas bubbles	1	9.15	9.39	9.27	2 on 3

Station	Replicate	Low DO?	COMMENT	# of Feeding Voids	Void Minimum Depth (cm)	Void Maximum Depth (cm)	Void Average Depth (cm)	Successional Stage
27E	B	n	Silt-clay admixed with some very fine sand; short burrows through aRPD; small voids or burrow openings; one methane bubble in aRPD, rest from 9.5 cm to depth	1	8.81	9.74	9.27	2 on 3
27E	D	n	Silt clay with minor fraction of very fine sand, large methane bubble just below SWI, rest from few cm below aRPD to depth	0	-	-	-	1 on 3
27H	A	n	High reflectance silt-clay with small burrows through aRPD; transected burrow and small annelids at depth.	0	-	-	-	2 on 3
27H	C	n	Silt clay with many small burrows in upper cm, two extending a couple cm into aRPD; burrow with worm tube leading to partial void at depth, transected burrow at depth; part of another annelid visible at depth	2	10.50	14.87	12.69	2 on 3
27H	D	n	Silt-clay with small burrows in upper cm, small annelid below aRPD on right; transected burrows & voids on left	3	8.65	14.48	11.57	2 on 3
28A	A	n	Silt-clay with minor fraction of very fine sand, small bits of debris in upper 1-2cm; methane bubbles from 6.5 cm to depth.	0	-	-	-	2
28A	B	n	Silt-clay with mud clast artifact from camera wiper blade on surface; short burrows in aRPD; methane bubbles at depth	0	-	-	-	1
28A	C	n	Silt-clay with small bits of debris in upper 2cm; tube at SWI and extending 1cm below,short burrows in aRPD; methane at depth	0	-	-	-	2 -> 3
28B	A	n	Silt-clay; escaping methane at SWI in center; transected burrow at depth, homogeneous profile from methane ebuillition	0	-	-	-	2 -> 3
28B	B	n	Silt-clay with shallow burrowing in aRPD; small void at left at 10 cm, some other indicators of deeper burrowing 6-10cm.	1	10.40	10.48	10.44	2 on 3
28B	C	n	Silt-clay with methane bubbles from just below aRPD to depth; ebullition tracks visible	0	-	-	-	1
28C	A	n	Silt-clay with very fine sand at depth, small burrows through aRPD; indications of deeper burrowing activity from 5-9 cm	1	8.46	8.65	8.55	2 on 3
28C	B	n	Silt-clay with very fine sand at depth; shallow burrowing in aRPD; small void at depth	1	10.29	10.93	10.61	2 -> 3
28C	C	n	Over-penetration. Silt clay with minor fraction of very fine sand; indications of larger burrows at depth; small void at depth	1	>12.29	>12.72	>12.51	2 on 3
28E	B	n	Silty fine and very fine sand, coarser grains at SWI and another patch at depth; small burrows in aRPD; long thin annelid at 6cm	0	-	-	-	1
28E	C	n	Silty fine and very fine sand, band of medium sand at depth and ~1 cm layer of fine to medium grain at SWI; small annelid at depth	0	-	-	-	1
28E	D	n	Silty fine and very fine sand, ~1 cm layer of medium sand at SWI.	0	-	-	-	1
29A	B	n	Silt-clay with shallow burrows in upper cms; small thin annelids at depth; methane bubbles from 9 cm to depth	0	-	-	-	2 -> 3
29A	C	n	Silt-clay with minor fraction of very fine sand, voids and small thin annelids at depth	2	11.42	13.34	12.38	1 on 3
29A	D	n	Silt-clay with mud clast artifacts on surface, small burrows in aRPD; indications of deeper burrowers- former voids, burrow openings, etc.; methane bubbles from 10cm to depth	0	-	-	-	1 on 3
29B	A	n	Silt-clay with minor fraction of very fine sand with small burrows in upper 2 cm; transected burrows & annelid at depth	1	9.90	10.13	10.01	1 on 3
29B	B	n	Silt-clay with minor fraction of very fine sand, methane bubbles at depth; shallow burrows.	0	-	-	-	2
29B	C	n	Silt-clay with some very fine sand; small burrows through aRPD; methane bubbles from 5.5 cm to depth	0	-	-	-	2 -> 3
29D	A	n	Silt-clay with minor fraction of very fine sand, thin annelid at 10.5cm at right; methane & burrowing evidence at depth	0	-	-	-	1 on 3
29D	B	n	Silt clay with some very fine sand, mud clast camera artifacts at surface; long burrow extending at angle and then horizontal from SWI, small thin annelids at depth; methane bubbles at depth	0	-	-	-	1 on 3
29D	C	n	Silt clay with minor fraction of very fine sand, small wood fibers & debris in upper cms; small burrows in aRPD	0	-	-	-	2 -> 3
29F	E	n	Silt-clay with some very fine sand, some coarser grains at SWI at center; small burrows in aRPD; transected burrow at depth on right	0	-	-	-	1 on 3
29F	G	n	Silt clay with some very fine sand; couple small patches of coarser grains near SWI; few tubes at SWI on right; short burrows in aRPD; long thin annelid below aRPD on right; methane bubbles at depth	0	-	-	-	2 -> 3
29F	H	n	Silt clay with some very fine sand; evidence of burrowing at depth	0	-	-	-	2 -> 3
30C	A	n	Silt-clay grading to silty very fine and fine sand at depth, small tubes in background; shallow burrowing in aRPD	0	-	-	-	2
30C	C	n	Silty very fine and fine sand over fine to medium sand at depth;	0	-	-	-	1
30C	D	n	Silty very fine sand mixed with coarser sand, patch of coarse sand at depth; lumpy surface, few small burrows in upper 1-1.5cm	0	-	-	-	1 -> 2
31A	B	n	Over-penetration. Silt-clay with methane bubbles from just below aRPD to depth	0	-	-	-	indeterminate
31A	C	n	Silt clay with minor fraction of very fine sand, small burrows in aRPD; small annelid ~5cm at right; transected burrows at depth	1	9.12	9.28	9.20	1 on 3
31A	D	n	Silt clay with some very fine sand; homogeneous texture above methane gas zone.	0	-	-	-	1
31B	A	n	Silt-clay with some very fine sand; short burrows in aRPD; small voids; methane bubbles and burrowing at depth	4	3.45	15.99	9.72	1 on 3
31B	B	n	Silt-clay with minor fraction of very fine sand; small tubes on surface in background; short burrows in aRPD; small annelid just below aRPD on left, part of a larger one at ~ 6cm; methane bubbles from 6 cm to depth	0	-	-	-	1 on 3
31B	C	n	Silt clay with some very fine sand; mud clast camera artifacts on surface; small void within aRPD on left, small annelid just below; small annelid and part of a large one at depth ~ 8cm; methane bubbles from 4 cm to depth	1	1.28	1.49	1.39	1 on 3
31C	A	n	Silty very fine sand, small patch of fine sand at depth on right, some coarser grains near surface; tube in background; shallow burrowing, couple v small thin annelids in aRPD; appears to be clay clast in bottom right corner, transected burrows @ depth	0	-	-	-	1 on 3
31C	B	n	Silty very fine sand, some coarser grains in aRPD; few patches of coarser fine sand at depth; small to med mud clasts on surface; small tubes @ SWI, evidence of burrowing at depth	0	-	-	-	1 on 3

Station	Replicate	Low DO?	COMMENT	# of Feeding Voids	Void Minimum Depth (cm)	Void Maximum Depth (cm)	Void Average Depth (cm)	Successional Stage
31C	C	n	Silty very fine sand over layer of silty medium sand, some coarse grains throughout; large biogenic mounds, transected burrows at depth	0	-	-	-	1 on 3
31D	A	n	Silty very fine sand over fine to medium sand, burrowing through aRD; annelid at depth	0	-	-	-	1 on 3
31D	C	n	Silty very fine sand over fine to medium sand layer, evidence of transected burrows at depth	0	-	-	-	2 -> 3
31D	D	n	Silty very fine sand, small tubes on surface; transected burrows at depth and bioturbation exceeds prism penetration depth	0	-	-	-	1 on 3
31E	A	n	Silty very fine sand, some coarser grains near surface; tubes in background; small burrows in upper 1-2 cm; aRPD much deeper on right, with tunnelling from 5.5-10.5 cm	0	-	-	-	1 on 3
31E	B	n	Silty very fine sand, patch of coarser grains on left below aRPD, small bits of debris; small burrows in aRPD; small thin annelids below aRPD -3.5cm	0	-	-	-	2 -> 3
31E	C	n	Silty fine sand mixed and overlaying silty very fine sand; SWI; shallow burrowing, small annelid just below aRPD on left	0	-	-	-	1 on 3
32A	A	n	Poorly-sorted very fine sand mixed with coarse sand; large rocks on surface; aRPD is patch to left of center with tunneling burrows and small void	1	3.54	3.96	3.75	3
32A	B	n	Silty very fine sand, patch of coarser grains in center; burrowing throughout depth of profile; most likely Stage 3 present	0	-	-	-	2 -> 3
32A	E	n	Poorly sorted silty very fine sand overlaying medium sand; pebbles on surface; small void at image edge on left	1	3.42	4.03	3.73	1 on 3
32B	A	n	Silty very fine sand over medium to coarse sand at depth; some coarser grains near SWI; transected burrows; void at depth below aRPD at center	1	7.99	8.42	8.20	1 on 3
32B	C	n	Silty very fine sand over coarser sand at depth, worms against faceplate & transected burrows throughout profile	0	-	-	-	1 on 3
32B	D	n	Silty very fine sand, lens of fine sand at mid-depth; coarser grains near surface; small tube lying on surface; transected burrows and portions of annelids visible against faceplate at depth	0	-	-	-	1 on 3
32C	A	n	Very fine sandy silt; few bits of debris near SWI; shallow burrowing, small annelid at 6.5 cm on left; methane bubbles at depth	0	-	-	-	2
32C	B	n	Very fine sandy silt; small to med reduced mud clasts at surface (camera artifacts); shallow burrowing; methane bubbles at depth	0	-	-	-	1 -> 2
32C	C	n	Very fine sandy silt; small bits of debris near surface; evidence of Stage 1 burrowing throughout profile; methane bubbles at depth	0	-	-	-	1
32D	A	n	Very fine sandy silt; small burrows through aRPD; small annelid at ~ 4cm; small void at depth on left; methane bubbles at depth	1	8.79	9.16	8.98	2 on 3
32D	B	n	Very fine sandy silt; small burrows in aRPD; annelid with fecal pellets in burrow at 7.3 cm; void on left; methane bubbles at depth	1	10.60	11.85	11.22	2 on 3
32D	C	n	Very fine sandy silt; few bits of debris just below SWI; small burrows in aRPD; small annelid at 7.7cm; 1 small methane bubble at depth on left, evidence of transected burrows at depth.	0	-	-	-	2 on 3
33A	B	n	Silty very fine sand, patch/band of coarser sand at ~2cm; shallow burrowing; methane bubbles & transected burrows at depth	0	-	-	-	2 -> 3
33A	C	n	Silty very fine sand; small tubes on surface; shallow burrowing	0	-	-	-	2
33A	D	n	Silty very fine sand over fine to medium sand at depth; transected burrows throughout profile; small - med-large annelids at depth; methane bubbles at depth	0	-	-	-	1 on 3
33B	E	n	Very fine sandy silt, evidence of burrowing throughout profile; small void with methane bubble in it at depth; methane bubbles at depth	1	12.36	12.84	12.60	1 on 3
33B	F	n	Very fine sandy silt; small burrows through aRPD; small void, annelid, and methane bubbles at depth	1	13.18	13.58	13.38	2 on 3
33B	G	n	Very fine sandy silt; small to med-large mud clasts on surface (camera artifacts); small void just below aRPD, another at depth; part of annelid at 8cm on left; methane bubbles at depth	1	4.26	15.00	9.63	1 on 3
33C	A	n	Poorly sorted medium to coarse sand, shallow penetration; lack of fines precludes aRPD assessment	0	-	-	-	indeterminate
33C	B	n	Medium to coarse sand, ripple on surface; shallow penetration; lack of fines precludes aRPD assessment	0	-	-	-	indeterminate
33C	C	n	Poorly sorted medium to coarse sand, shallow penetration; lack of fines precludes aRPD assessment	0	-	-	-	indeterminate
33D	A	n	Very fine sandy silt; short burrows in aRPD; deeper burrowing annelids and transected burrows at depth	0	-	-	-	1 on 3
33D	B	n	Very fine sandy silt;shallow burrowing and through aRPD ~3-4cm; narrow tunnel/void in aRPD on right; relict aRPD; small void at depth	1	8.84	9.43	9.14	2 on 3
33D	C	n	Very fine sandy silt; shallow burrowing; uneven aRPD, transected burrows at depth	0	-	-	-	2 on 3
34A	B	n	Poorly sorterd silty very fine sand, patch of coarse sand at depth on left; sharp contact horizon with underlying consolidated clay, burrowing throughout profile.	0	-	-	-	2 -> 3
34B	A	n	Silty very fine sand, coarser grains throughout, patch at bottom on right and below SWI; small tube in background on right; small burrows in aRPD; aRPD deeper on left; transected burrow at depth on left	0	-	-	-	1 on 3
34B	B	n	Silty very fine sand mixed with fine to medium sand, with small patches of coarser grains at depth; void at depth, bioturbation exceeds prism penetration depth	0	-	-	-	1 on 3
34B	D	n	Silty very fine sand, coarser grains throughout with patches at depth and just below SWI; shallow burrows; shallow penetration	0	-	-	-	2 on 3

Station	Replicate	Low DO?	COMMENT	# of Feeding Voids	Void Minimum Depth (cm)	Void Maximum Depth (cm)	Void Average Depth (cm)	Successional Stage
34C	A	n	Silty very fine sand over medium to fine sand at depth, coarse grains in upper 1-2 cm; shallow burrows; small thin annelid as well as transected burrows at depth	0	-	-	-	2 on 3
34C	B	n	Silty very fine sand mixed and over coarser fine sand; surface disturbed by camera sampling of previous rep, small to med-large mud clasts are sampling artifacts; however, evidence of burrowing throughout profile, infauna similar to previous rep	0	-	-	-	2 on 3
34C	D	n	Silty very fine sand over coarser sand at depth, small burrows down to 3 cm and transected burrows at depth	0	-	-	-	2 on 3
34D	A	n	Silty very fine sand over medium to coarse sand, transected burrows at depth; clay on left side of image is smear artifact	0	-	-	-	2 on 3
34D	B	n	Siltyvery fine sand over coarser sand below aRPD; med-large pit at surface; transected burrows at depth	0	-	-	-	1 on 3
34D	D	n	Sitly very fine sand over coarser sand; small methane bubbles at depth, transected burrows throughout profile	0	-	-	-	1 on 3
35A	C	n	Very fine sandy silt; over-penetration on left half of image; small burrows through aRPD; small annelid at 8.25 cm, another slightly larger one at 17cm; methane bubbles at depth, transected burrow lower right hand corner	0	-	-	-	2 on 3
35A	E	n	Very fine sandy silt; uneven surface, possibly disturbed by camera sampling of previous reps; few old small tubes at SWI and methane bubbles at depth.	0	-	-	-	1
35A	G	n	Silty very fine sand over silt; small thin annelid below aRPD on left, transected burrows at depth; light colored clay appears to be smear by camera prism, disturbed upper part of profile.	0	-	-	-	2 -> 3
35B	B	n	Over-penetration. Silt with minor fraction of very fine sand; short burrows in aRPD; void at 11 cm; methane bubbles from 10 cms to depth	1	>10.62	>11.32	11.00	2 on 3
35B	F	n	Shallow penetration with camera mud clast artifacts. Silt with minor fraction of very fine sand; suc. Stage Ind because of shallow penetration	0	-	-	-	indeterminate
35B	G	n	Silt-clay with some very fine sand; small bits of debris near surface; shallow burrowing; methane bubbles from ~8 cm to depth	1	10.49	10.81	10.65	1 on 3
35C	B	n	Poorly sorted silty very fine sand, lots of coarser grains in 1-2cm below SWI, some at depth; small tubes & ripples on surface; few tubes to right of center at SWI	0	-	-	-	2
35C	C	n	Poorly sorted silty medium sand mixed with fine and very fine sand; burrowing throughout depth of profile	0	-	-	-	2 on 3
35C	D	n	Silty very fine sand with substantial fraction of medium sand , some coarser grains at depth; some burrows through aRPD, transected burrows at depth	0	-	-	-	2 on 3
35D	B	n	Silty-clay with minor fraction of very fine sand, few bits of debris near surface; shallow burrowing; small annelid at 8.5cm on right, transected burrows at depth.	0	-	-	-	1 on 3
35D	C	n	Silt clay with some very fine sand; bits of debris in upper 2 cms; aRPD deeper at center; small burrows in aRPD, evidence of burrowing at depth	0	-	-	-	1 on 3
35D	D	n	Silty-clay with some very fine sand; bits of debris in upper 2 cm; indications of deeper burrowers, burrow/tunnel opening at right ~8cm	0	-	-	-	1 on 3
36A	-	-	No images with penetration or view of sediment surface; hard bottom	-	-	-	-	indeterminate
36B	A	n	Silty very fine and fine sand, coarser sed in patches; tube lying on surface in background; thin aRPD; small annelid at depth on left	0	-	-	-	2 -> 3
36B	B	n	Silty very fine sand and fine sand, coarser at depth, small patches of coarse sand near SWI; burrowing throughout profile	0	-	-	-	2 -> 3
36B	D	n	Silty very fine sand and fine sand, coarser patch of sand at center; tubed on surface in background; burrowing throughout profile	0	-	-	-	2 -> 3
36C	B	n	Poorly sorted silty sand over medium sand; shallow bedforms	0	-	-	-	2
36C	C	n	Poorly sorted silty sand over medium sand;; small burrows through aRPD to 2.5 cm; evidence of burrowing throughout profile	0	-	-	-	2 -> 3
36C	D	n	Very fine sand over coarse sand at depth and in layer in 2cm below SWI; thin aRPD	0	-	-	-	1
36D	-	-	No images with penetration or view of sediment surface; hard bottom	-	-	-	-	indeterminate
37A	A	n	Very shallow penetration; poorly-sorted silty sand with pebbles and cobble on surface	0	-	-	-	indeterminate
37A	B	n	Very shallow penetration; poorly-sorted silty sand with pebbles and cobble on surface	0	-	-	-	indeterminate
37A	C	n	Very shallow penetration, medium sand underneath layer of silty very fine sand at surface	0	-	-	-	indeterminate
37B	A	n	Silty very fine sand; surface appears disturbed by sampling, aRPD impossible to measure accurately	0	-	-	-	2
37B	B	n	Silty very fine sand; surface appears disturbed by sampling and mud clasts are artifacts from camera, aRPD impossible to measure accurately	0	-	-	-	indeterminate
37B	C	n	Very little penetration, just on right side, limited info available	0	-	-	-	indeterminate
37C	B	n	Medium sand with low fine fraction so no distinct aRPD; few pebbles/cobbes on surface	0	-	-	-	indeterminate
37C	C	n	Medium sand with low fine fraction so no aRPD measurement possible	0	-	-	-	indeterminate
37C	D	n	Medium sand with low fine fraction so no aRPD measurement possible	0	-	-	-	indeterminate
37D	D	n	Very fine sandy silt, bits of debris below SWI; two mounds on surface in background are artifacts from previous sampling; possible tubes on surface in background; aRPD linear measurement from left, the rest of surface disturbed; burrowing in aRPD; methane bubbles at depth; annelids visible at depth	0	-	-	-	1 on 3

Station	Replicate	Low DO?	COMMENT	# of Feeding Voids	Void Minimum Depth (cm)	Void Maximum Depth (cm)	Void Average Depth (cm)	Successional Stage
37D	E	n	Very fine sandy silt, short burrows through aRPD and below; multiple annelids visible against faceplate at depth	0	-	-	-	1 on 3
37D	F	n	Very fine sandy silt; transected burrows throughout profile and multiple annelids visible at depth against faceplate	0	-	-	-	1 on 3
37E	A	-	rock/hard bottom....no penetration in any replicate	-	-	-	-	indeterminate
38C	A	n	Silty very fine and fine sand, patch of coarser sand at base in center; shallow penetration	0	-	-	-	2
38C	B	n	Silty very fine and fine sand, couple small patches of coarser grains at base and on surface; shallow penetration; few small burrows	0	-	-	-	2 -> 3
38C	C	n	Silty very fine and fine sand, patch of coarser sand at right and base; shallow penetration, transected burrows at depth	0	-	-	-	2
39B	B	n	Very fine sandy silt; bits of debris in upper cms; shallow burrows and evidence of burrowing just below aRPD at center; methane bubbles from ~1.5 cm below SWI to depth	0	-	-	-	2
39B	E	n	Over-penetration. Silt-clay with bits of debris near surface; methane bubbles from ~9cm to depth	0	-	-	-	2
39B	F	n	Silt-clay with some very fine sand; few small burrows in aRPD; methane bubbles from 10cm to depth	0	-	-	-	2
39F	A	n	Silty very fine sand; small burrows in aRPD; short tubes in background, transected burrows throughout depth	0	-	-	-	1 on 3
39F	B	n	Silty very fine sand; small bits of debris on surface; edge of piece of wood projecting out of bottom on right; bioturbation exceeds prism penetration depth	0	-	-	-	1 on 3
39F	C	n	Silty very fine sand, uneven surface disturbed by imprint of base sled of camera from previous replicate; aRPD exceeds penetration depth	0	-	-	-	1 on 3
40A	E	n	Silt-clay with some very fine sand; small bits of debris in upper cms; small tubes on surface to right; burrowing throughout profile; methane bubbles at depth	0	-	-	-	2 -> 3
40A	F	n	Silt-clay with some very fine sand; small tubes on left; small bits of debris in upper cm; burrowing in aRPD and below; methane bubbles from 7.5cm to depth	0	-	-	-	2 -> 3
40A	G	n	Silt-clay with some very fine sand, burrows in upper cms; small thin annelid at center near methane bubble; methane bubbles from 5.5cm to depth, portions of annelids visible against faceplate throughout entire profile	0	-	-	-	2
40B	A	n	Silt-clay with some very fine sand, over-penetration on left; narrow burrow from surface to 2.2 cm revealing portion of bivalve against faceplate; short burrows in upper cm; small thin annelids at 5cm at center; methane bubbles at depth	0	-	-	-	2 -> 3
40B	B	n	Silt-clay with over-penetration; connected narrow void through much of aRPD; void at depth is small; annelid at 15cm	2	>1.12	>15.65	ind	2 on 3
40B	D	n	Camera disturbance of surface and sed smeared on faceplate above SWI, precluding aRPD measurement ,	0	-	-	-	2
40C	A	n	Silt clay with some very fine sand; shallow burrows through aRPD and portions of annelids visible against faceplate at depth	0	-	-	-	2 -> 3
40C	B	n	Silt clay with some very fine sand, small to med-large mud clasts (camera artifacts) on surface, one in drag-down; couple tubes on surface; burrowing throughout profile	0	-	-	-	1 on 3
40C	D	n	Silt clay with some very fine sand, camera artifact mud clasts in background; multiple short tubes on surface; burrowing through aRPD and at depth	0	-	-	-	1 on 3
40D	B	n	Silty medium sand with small patch of very fine sand; penetration too shallow to determine stage	0	-	-	-	indeterminate
40D	C	n	Thin layer of silty medium sand over silty sediment; uneven surface; thin aRPD; basement clays appear consolidated	0	-	-	-	1
40D	D	n	Silty medium to fine sand overlaying silt clay; penetration too shallow to determine stage	0	-	-	-	indeterminate
40E	B	-	No penetration; large debris on surface- wood, pipe, small dead fish at center near base; slight patch of sandy sed surface visible	-	-	-	-	indeterminate
40E	C	-	No penetration; silty/sandy detrital mantle covering a hard surface (rock? Log?)	-	-	-	-	indeterminate
40E	D	n	Silty very fine sand; pieces of wood debris at surface; small burrows within aRPD and transected burrow at lower right corner	0	-	-	-	2 -> 3
41A	A	n	Shallow penetration, surface at diagonal- camera not level (edge of base sled on rock or other debris); fairly consolidated silt-clay; many small to med mud clasts at SWI and in background.	0	-	-	-	1
41A	B	n	Shallow penetration; consolidated silt-clay; many small to med-large mud clasts at SWI; few old old tubes; sediment below aRPD is mix of light and very dark grays; extremely low albedo at depth, check location	0	-	-	-	1
41A	D	-	No penetration; surface covered with small rocks and cobbles	-	-	-	-	indeterminate
42A	A	n	Over-penetration; silt-clay with some very fine sand, small bits of debris throughout; two small voids; methane bubbles at depth, transected burrows with worms visible	2	>9.24	>12.09	ind	3
42A	B	n	Over-penetration; very fine sand, small bits of debris; methane bubbles from 6.8cm to depth	0	-	-	-	3
42A	C	n	Very fine sandy silt;old tubes and debris on surface, mud clast artifacts, shallow burrowing and to 3-4 cm on right; evidence of burrowing throughout profile	1	9.78	10.10	9.94	1 on 3
42B	A	n	Silty very fine and fine sand mixed, small patch of coarse sed at SWI in center; evidence of burrowing throughout profile	0	-	-	-	2 on 3
42B	B	n	Silty very fine sand with few patches of fine sand and small patch at SWI; small tubes on surface; shallow burrows in aRPD; void at depth	1	10.95	11.34	11.14	1 on 3
42B	C	n	Silty very fine sand with larger particles at mid-depth; few bits of debris in upper cms; evidence of burrowing throughout profile	0	-	-	-	2 on 3
43B	A	n	Very shallow penetration, surface covered with pebbles, oxidized silt detrital mantle; episodic depositional	0	-	-	-	indeterminate

Station	Replicate	Low DO?	COMMENT	# of Feeding Voids	Void Minimum Depth (cm)	Void Maximum Depth (cm)	Void Average Depth (cm)	Successional Stage
43B	C	n	Very shallow penetration, silt-covered pebbles, possible bedform	0	-	-	-	indeterminate
43B	D	n	Very shallow penetration, surface covered with pebbles, oxidized silt detrital mantle; episodic depositional	0	-	-	-	indeterminate
44B	A	n	Silty very fine sand, small patches of fine sand at depth; v small to small mud clasts on surface; bit of wood debris on right at SWI; evidence of burrowing throughout profile	0	-	-	-	1 on 3
44B	B	n	Silty very fine sand, medium sand at depth, few coarser grains near surface; few small tubes on right; episodic depositional, burrowing at depth	0	-	-	-	1 on 3
44B	C	n	Silty very fine sand, coarser grains across surface and in patches at depth; small to med mud clasts; small tube on left; short burrows in aRPD, burrowing at depth and portions of worms against faceplate at depth	0	-	-	-	1 on 3
45A	A	n	Silty very fine and fine sand; short burrows in upper cm on left, shallow bedform, sand over mud; periodic bedload transport	0	-	-	-	2
45A	B	n	Silty very fine sand over fine to medium sand, small-scale ripples, thin algae filaments at SWI at center; aRPD deeper on right; small void, evidence of burrowing at depth.	1	3.75	4.57	4.16	2 -> 3
45A	C	n	Silty fine sand mixed with medium and coarse sand, small patch of oxy very fine sand on right at SWI; sand ripples	0	-	-	-	2
46C	-	-	No images with penetration; large rock visible in two	-	-	-	-	indeterminate
47A	A	n	Very fine sandy silt over silty fine sand; evidence of burrowing throughout depth of profile	0	-	-	-	2 -> 3
47A	C	n	Silty very fine and fine sand, small-scale ripples, alternating depositional and transport intervals	0	-	-	-	2
47A	D	n	Silty medium sand, hydraulically-driven aRPD, some burrowing evident at depth	0	-	-	-	2
48C	A	n	Very fine sandy silt, indication of deeper burrower (annelid) at depth on right	0	-	-	-	1 on 3
48C	C	n	Very fine sandy silt, episodically depositional, evidence of burrowing throughout profile	0	-	-	-	1 on 3
48C	D	n	Very fine sandy silt, wiper blade artifact mud clasts on surface; burrowing throughout profile	0	-	-	-	1 on 3
49A	A	n	Over-penetration; silty very fine sand; bit of a annelid visble at ~5cm; methane bubbles at depth	0	-	-	-	indeterminate
49A	B	n	Over-penetration; silty very fine sand; small methane bubbles at depth; void at depth	1	16.99	17.78	17.39	1 on 3
49A	C	n	Over-penetration; silty very fine sand over silt-clay; methane bubbles from ~10cm to depth; low reflectance reduced sediment at depth	0	-	-	-	indeterminate
50A	C	n	Silty clay with very fine sand admixed; small burrows through aRPD; part of annelid and transected burrows at depth; 2 of voids are v small	3	7.86	16.78	12.32	2 on 3
50A	D	n	Very fine sandy silt; small to med med clasts at surface; shallow burrowing; methane bubbles from ~9.5cm to depth	0	-	-	-	1
50A	E	n	Very fine sandy silt; small burrows transected mid-profile, smal methane bubbles bottom right	0	-	-	-	1 -> 2
51C	B	n	Very fine sandy silt; transected burrow just below SWI, shallow burrowing in upper cm and through aRPD, small void and transected burrow at depth	1	0.76	8.79	4.77	2 on 3
51C	C	n	Silt clay with admixed very fine sand ; small void at base of aRPD; aRPD deeper on left; large and medium-small annelids at ~13cm on left	1	2.90	3.14	3.02	2 on 3
51C	D	n	Silt clay with some very fine sand ; small burrows in aRPD; indications of deeper burrowers at base of aRPD; small thin annelid below aRPD on left; small void and transected burrow at depth	1	15.58	15.95	15.77	2 on 3
51F	A	n	Silt-clay with some very fine sand; transected burrows at depth	1	10.27	10.62	10.45	1 on 3
51F	C	n	Silt-clay with some very fine sand, surface disturbed by previous replicate, aRPD indeterminate; transected burrows at depth	1	14.01	15.78	14.89	1 on 3
51F	D	n	Silt-clay with some very fine sand; small shallow burrows and in aRPD, med burrow at base of aRPD on left; bits of annelid visible at depth	0	-	-	-	2 on 3
52A	A	n	Silt-clay over very fine sandy silt; bits of debris throughough most of depth besides aRPD; shallow burrowing; large worm tube extending from below SWI to on top of surface; small methane bubbles at depth, transected small burrows at depth	0	-	-	-	1 on 3
52A	B	n	Silt-clay over very fine sandy silt, coarser below aRPD; shallow burrowing; methane bubbles from 7cm to depth	0	-	-	-	2 -> 3
52A	C	n	Very fine sandy silt; small to med mud clasts on surface in background; shallow burrowing, small bits of debris throughout; methane bubbles at depth	0	-	-	-	2 -> 3
52B	A	n	Very fine sandy silt; small burrows throughout aRPD; tube remnants and small thin annelid at ~9-10 cm; methane bubbles at depth	0	-	-	-	2 on 3
52B	B	n	Silty very fine sand over silt; med-large mud clasts at surface, which is disturbed from sampling during previous replicate - surface features are artifact; methane bubbles at depth	0	-	-	-	2
52B	C	n	Very fine sandy silt; small tubes at surface; burrowing through aRPD; small voids at depth; methane bubbles at depth	2	14.91	15.80	15.35	1 on 3
53E	A	n	Silt-clay with minor fraction of very fine sand; short burrows through aRPD; transected burrow at mid-depth; part of large tube at depth at center	2	9.35	12.06	10.70	2 on 3
53E	B	n	Silt clay with minor fraction of very fine sand; divot on left from base sled artifact of previous replicate image; transected burrows and voids at depth.	4	8.44	13.33	10.88	1 on 3
53E	D	n	Silt clay admixed with very fine sand; short thin burrows through aRPD, transected burrows at depth	0	-	-	-	2 on 3
54B	A	n	Silty very fine sand; shallow burrowing; void is small at base of aRPD	1	2.99	3.14	3.07	2 -> 3

Station	Replicate	Low DO?	COMMENT	# of Feeding Voids	Void Minimum Depth (cm)	Void Maximum Depth (cm)	Void Average Depth (cm)	Successional Stage
54B	E	n	Silty very fine sand; surface has a bit of a ripple; small tubes in background; shallow burrowing	0	-	-	-	2
54B	H	n	Very fine sandy silt; small tubes laying on surface in background; bits of thin algae filaments below aRPD dragged down by prism	0	-	-	-	1 -> 2
55B	A	n	Silt-clay with minor fraction of very fine sand; short burrows through aRPD to at least 5cm	0	-	-	-	2
55B	B	n	Silt-clay with minor fraction of very fine sand; short burrows through aRPD, Large annelid against faceplate at depth	0	-	-	-	2 on 3
55B	C	n	Silt clay with less than 30% very fine sand; small tubes at surface; small void a couple cms below aRPD; med annelid at 13 cm	1	7.22	7.48	7.35	1 on 3
56A	B	n	Very fine sandy silt; two annelids at 12-13 cm; methane bubbles from ~9cm to depth	0	-	-	-	2 -> 3
56A	C	n	Very fine sandy silt-clay, shallow burrowing and one larger burrow at base of aRPD; annelid at 13.5 cm; methane bubble at 7cm, rest at depth	1	7.58	7.87	7.73	1 on 3
56A	E	n	Very fine sandy silt, small bits of debris in upper cms; shallow burrowing; methane bubbles & oxygenated burrow halos at depth	0	-	-	-	2 -> 3
56C	A	n	Very fine sandy silt; transected burrow and portion of annelid visible in lower right corner	0	-	-	-	2 -> 3
56C	C	n	Very fine sandy silt; bits of debris on surface; tubes on surface and in background; shallow burrowing; aRPD thinner on left; methane bubbles at depth	0	-	-	-	2
56C	D	n	Very fine sandy silt; small divot on surface at left; shallow burrowing; methane bubbles at depth	0	-	-	-	1 -> 2
56F	C	n	Very poorly sorted medium to coarse sand with high silt fraction; evidence of burrowing throughout profile	0	-	-	-	2
56F	D	n	Poorly sorted medium to coarse sand with high silt fraction; aRPD extends beyond penetration depth on left; shallow burrowing; small tubes on surface in background	0	-	-	-	2
56F	E	n	Poorly sorted medium to coarse sand with high silt fraction; aRPD extends beyond penetration depth; small tubes on surface in background, large rock on surface, transected burrow on left	0	-	-	-	2 -> 3
57D	A	n	Silt-clay with minor fraction of very fine sand; shalllow burrowing; evidence of deeper burrowing and a couple small annelids a couple cm below aRPD at right	0	-	-	-	2 -> 3
57D	D	n	Silt clay with admixed very fine sand; shallow burrowing; evidence of deeper burrowing and a couple small annelids at ~10cm	0	-	-	-	1 on 3
57F	A	n	Silt clay with admixed very fine sand, couple long tubes in background; burrowing through aRPD; relict aRPD; small annelid at 10.5cm	0	-	-	-	2 -> 3
57F	C	n	Silt-clay with minor fraction of very fine sand; burrowing through aRPD, evidence of deeper burrowers at base of aRPD; voids are small; some sloughing against faceplate	2	7.72	15.53	11.63	2 on 3
57F	D	n	Silt-clay with some very fine sand; surface covered with small to medium mud clasts, artfifact from camera base sled; a couple long tube on surface; voids are small and narrow, annelid against faceplate at bottom of image	2	11.34	13.72	12.53	1 on 3
58D	A	n	Silty very fine sand; surface on left covered with tubes; shallow burrowing; transected void at depth	1	14.01	14.45	14.23	1 on 3
58D	B	n	Silty very fine sand; shallow burrowing; a few transected burrows at depth	0	-	-	-	2
58D	C	n	Silty very fine sand; bit of debris on surface; few tubes at surface; surface disturbed by camera frame, artifact mud clasts;transected burrows at depth (center and bottom left)	0	-	-	-	1 on 3
59B	B	n	Silty clay with some admixed very fine sand; bits of debris in upper 2 cm; short tubes on surface; small burrows through aRPD; annelid at 9.5 cms; methane bubbles at depth	0	-	-	-	2 -> 3
59B	C	n	Silty clay with minor fraction of very fine sand; bits of debris and coarser grains in upper cms; small burrows down to at least 3cm; methane bubbles at depth	0	-	-	-	2
59B	D	n	Silt-clay with admixed very fine sand, small bits of debris/coarser grains in upper cm; short tubes on surface; shalllow burrowing in aRPD; small thin annelid at 12.5cm; methane bubbles from 12.8cm to depth	0	-	-	-	1 on 2
59E	A	n	Silt-clay with admixed very fine sand; short thick tube at SWI; shallow burrowing; small void at depth	1	16.14	16.46	16.30	1 on 3
59E	C	n	Silt-clay with admixed very fine sand; surface appears disturbed by previous camera replicate, but homogeneous profile at depth	0	-	-	-	1
59E	D	n	Silt-clay wth admixed very fine sand; small stick on surface, sticking straight up ; shallow burrowing; depositional	0	-	-	-	1 -> 2
59F	B	n	Silt-clay with noticeable decrease in proportion of fine sand compared to previous locations; burrowing in aRPD; void a couple cm below aRPD; transect large tube at depth on right	1	6.18	6.46	6.32	1 on 3
59F	C	n	Homogeneous silt-clay, shallow transected burrow; voids & transected burrows at depth	2	2.79	10.15	6.47	1 on 3
59F	D	n	Over-penetration; silty sand; homogeneous silt-clay; couple indications of deeper burrowers/former voids at depth	0	-	-	-	indeterminate
60D	A	n	Silty very fine sand, shallow burrowing through aRPD, homogeneous sedimentary fabric	0	-	-	-	2
60D	C	n	Silty very fine sand, shallow burrowing through aRPD, homogeneous sedimentary fabric	0	-	-	-	2
60D	D	n	Silty very fine sand, shallow burrowing through aRPD, homogeneous sedimentary fabric -- all reps very similar	0	-	-	-	2
61A	E	n	Silt clay with minor fraction of very fine sand; burrow at base of aRPD on right; other voids below aRPD to depth; small thin annelid at 10.3 cm; larger annelid at 14.5cm	3	2.48	11.05	6.76	1 on 3
61A	F	n	Silt clay with some admixed very fine sand; rippled surface; small tubes at SWI; homogeneous fabric	0	-	-	-	2

Station	Replicate	Low DO?	COMMENT	# of Feeding Voids	Void Minimum Depth (cm)	Void Maximum Depth (cm)	Void Average Depth (cm)	Successional Stage
61A	G	n	Silt clay with minor fraction of very fine sand; one void a couple cm below aRPD on right, other 2 at depth; transected burrows at depth	3	4.87	14.94	9.91	1 on 3
61E	A	n	Well-sorted silt-clay, burrowing in aRPD, transected burrow just below SWI; voids a few cm below aRPD and at depth	4	7.84	15.76	11.80	1 on 3
61E	B	n	Wll-sorted silt-clay, burrowing throughout profile, voids are small; bioturbation exceeds prism penetration depth	3	10.66	13.66	12.16	1 on 3
61E	D	n	Silt-clay, burrowing throughout profile, transected voids and burrows at depth -- all 3 reps very similar	4	12.27	16.30	14.28	1 on 3
62C	B	n	Very fine sandy silt, some coarser sand at mid-depth; thin small annelids in aRPD; methane bubbles at depth	0	-	-	-	2
62C	C	n	Very fine sandy silt over fine sand small burrows in aRPD; relict aRPD; methane bubbles at depth	0	-	-	-	2
62C	D	n	Very fine sandy silt with band of fine sand at ~12 cm; few bits of debris in aRPD; small burrows through aRPD; relict aRPD; annelids at 8 - 9 cm at center	0	-	-	-	2 on 3
63D	A	n	Silty very fine sand, small patches of coarser grains at depth and near SWI; small mud clasts on surface; evidence of burrowing at depth	0	-	-	-	2 -> 3
63D	B	n	Silty very fine sand, patches of coarse grains near SWI and at depth on right; small tubes in background, bioturbation exceeds prism penetration depth	0	-	-	-	2 on 3
63D	C	n	Silty very fine sand, some coarser sed; bits of debris on surface; aRPD is deeper on left; evidence of burrowing throughout profile	0	-	-	-	2 on 3
63E	A	n	Well-sorted silt-clay, few bits of debris in aRPD; small burrows through aRPD; burrows and voids transected at depth	0	-	-	-	1 on 3
63E	C	n	Well-sorted silt-clay, burrowing through aRPD; annelid at ~7.5 cm; transected burrow & voids at depth	3	8.49	17.50	13.00	2 on 3
63E	D	n	Well-sorted silt-clay, indications of deeper burrows at base of aRPD; small voids at depth	3	7.16	15.33	11.25	1 on 3
64A	E	n	Silt-clay with admixed very fine sand; small tubes at SWI; shallow burrowing; annelid at 12.5cm	0	-	-	-	2
64A	F	n	Very fine sandy silt; larger burrow at base of aRPD; bioturbation exceeds prism penetration depth	0	-	-	-	1 on 3
64A	H	n	Silt-clay with admixed very fine sand; small bits of debris in upper cms; few small thin annelids at depth; small methane bubbles, evidence of burrowing at depth	0	-	-	-	1 on 3
64E	A	n	Silty very fine sand; small void a few cm below relict aRPD at center	1	7.68	7.91	7.79	1 on 3
64E	B	n	Very fine sandy silt;voids are small; few thin annelids at depth, recently deposited fecal pellets in void on left	2	4.30	7.47	5.89	1 on 3
64E	D	n	Silty very fine sand; large leaf on surface in background; bits of debris on surface; shallow burrowing	0	-	-	-	2
65C	A	n	Poorly sorted silty very fine sand; patch of coarse sand at depth at center; scattered coarse grains near surface; tube in background at surface; bioturbation exceeds prism penetration depth	0	-	-	-	1 on 3
65C	B	n	Silty very fine sand and coarse sand, coarse sand is on left at surface and at depth; evidence of burrowing throughout profile	0	-	-	-	1 on 3
65C	C	n	Silty very fine sand over medium sand at depth, some coarse grains near surface as well; few bits of debris; bioturbation exceeds prism penetration depth	0	-	-	-	2 -> 3
67A	A	n	Silty medium to coarse sand mixed over silt-clay; small tubes in background, transected burrow on right	0	-	-	-	2 -> 3
67A	C	n	Silty medium to coarse sand mixed over silt-clay; small tubes in background, homogeneous fabric at depth	0	-	-	-	2
67A	D	n	Silty medium to coarse sand mixed over silt-clay; bioturbation largely confined to upper sandy layer	0	-	-	-	2
67C	A	n	Silt-clay with layer of silty very fine sand at depth;small burrows through aRPD; methane bubbles from 11.5cm to depth, small worms at depth	0	-	-	-	2
67C	B	n	Over-penetration except on left; silt clay with layer of silty very fine sand at depth, similar to last replicate; small burrows in aRPD; small thin annelid at 12cm; methane bubbles and larger annelid at depth	0	-	-	-	1 on 3
67C	D	n	Over-penetration; silt clay with some silty very fine sand at depth; bit of burrowing visible;methane bubbles at depth	0	-	-	-	indeterminate
68E	C	n	Shallow penetration; compact silt-clay; sediment with orangish hue behind lighter oxy sed; pit at center, transected burrow at right edge	0	-	-	-	indeterminate
68E	D	n	Silty very fine sand, band of coarser sand at mid-depth; shallow burrowing appears to be confined to upper 2 depositional intervals	0	-	-	-	2
68E	E	n	Silty very fine sand, coarser grain at mid-depth; sediment with orangish hue behind lighter oxidized sed in upper cms -- appears similar to tracer particles	0	-	-	-	2 -> 3
69C	B	n	Silt-clay with admixed very fine sand, burrowing through aRPD; some transected small burrows at depth	0	-	-	-	2
69C	C	n	Silt clay with some very fine sand mixed at depth; small burrows through aRPD; methane bubbles at depth	0	-	-	-	2
69C	D	n	Silt clay with deep layer of silty very fine sand with methane; burrowing through aRPD; deep relict aRPD; methane bubbles from 12cm to depth	0	-	-	-	2
70A	A	n	Silt-clay with admixed very fine sand at depth; over-penetration on left; burrowing through aRPD and at depth.	1	10.81	10.98	10.90	1 on 3
70A	B	n	Over-penetration; silty clay with minor fraction of very fine sand; small bits of debris in aRPD; small burrows in aRPD; small annelid at ~11cm; voids and burrows at depth	3	7.70	20.91	14.31	3
70A	C	n	Over-penetration; silt-clay with some very fine sand at depth; two med burrows near presumed surface; transected deeper burrow on left	0	-	-	-	2 on 3

Station	Replicate	Low DO?	COMMENT	# of Feeding Voids	Void Minimum Depth (cm)	Void Maximum Depth (cm)	Void Average Depth (cm)	Successional Stage
73B	A	n	Silt clay with some admixed very fine sand at depth; shallow burrowing including one larger burrow just below SWI on right; oxygenated halos at depth	0	-	-	-	2 -> 3
73B	B	n	Silt clay with admixed very fine sand; burrowing through aRPD; burrows and void at depth	0	-	-	-	2 on 3
73B	D	n	Silt-clay with admixed very fine sand; small burrows through aRPD; small void at depth	1	17.84	17.97	17.90	2 on 3
74A	A	n	Silt-clay with some very fine sand couple small annelids at ~ 7-9 cm; evidence of burrowing throughout profile	0	-	-	-	1 on 3
74A	B	n	silt-clay over a layer of silty very fine sand at depth; void at depth	1	16.19	16.67	16.43	1 on 3
74A	C	n	silt-clay over a layer of silty very fine sand at depth; void at depth, burrowing throughout profile	3	9.88	16.11	13.00	1 on 3
75D	B	n	hard bottom, no penetration	0	-	-	-	indeterminate
75E	B	n	Very shallow penetration; silty very fine sand	0	-	-	-	indeterminate
75E	C	n	Very shallow penetration; very fine sand; only oxy sediment visible; shallow burrowing	0	-	-	-	indeterminate
77A	A	n	Over-penetration; bits of debris near surface and in depth; deep aRPD	0	-	-	-	indeterminate
77A	B	n	Silt-clay over silty very fine sand at depth; small burrows in aRPD;	0	-	-	-	1 on 3
77A	C	n	Silt clay with silty very fine sand at depth; small to med mud clasts on surface, camera artifacts; some burrows in aRPD; few bits of debris in aRPD and at depth; voids at depth & bioturbation exceeds prism penetration depth	4	12.60	17.01	14.80	1 on 3
77B	C	n	Silty very fine and fine sand; patch of coarser sand in depression on left at SWI; burrowing throughout profile; bits of larger debris (maybe wood chips) at depth on right; methane bubbles at depth	0	-	-	-	1 on 3
77B	D	n	Silty very fine and fine sand; small burrows through aRPD; bits of debris at mid-depth and at depth; evidence of burrowing throughout profile	0	-	-	-	2 -> 3
78A	B	n	Over-penetration; silty very fine sand over silty fine sand over silt; relict aRPD; methane bubbles from >8cm to depth	0	-	-	-	2
78A	C	n	Over-penetration; silty fine and very fine sand; few burrows visible in aRPD; grayish sand on left near surface; methane bubbles at depth	0	-	-	-	1
78A	D	n	Over-penetration; silt-clay over silty fine sand; deep aRPD; methane bubbles from > 5cm to depth; shallow burrows and annelid at depth	0	-	-	-	2
78D	C	n	No penetration; surface is coarse sand with small cobbles	-	-	-	-	indeterminate
79D	A	n	Very shallow penetration; silt-covered cobble; aRPD extends beyond penetration depth	0	-	-	-	indeterminate
79D	B	n	Silt clay over silty very fine sand; shallow burrowing	0	-	-	-	1 -> 2
79D	C	n	Silty very fine sand; shallow penetration; organism against faceplate at depth, bioturbation extends beyond prism penetration depth, small tubes @ SWI in background	0	-	-	-	1 on 3
81A	F	n	No penetration; visible surface is large rock covered with layer of silt	-	-	-	-	indeterminate
82C	B	n	Silty very fine sand; small tubes on surface, small burrows through aRPD	0	-	-	-	2
82C	E	n	Silt-clay over silty very fine sand; small burrows through aRPD; bivalve at ~1cm to left of center; some small burrows at depth	0	-	-	-	2
82C	H	n	Silty very fine sand, reduced fecal pellets in feeding pit left of center, burrowing evident throughout profile, small tubes at surface	0	-	-	-	1 on 3
82D	B	n	Silt-clay over silty very fine sand over silt; alternating transport & depositional regime; shallow burrowing; void is very small	1	12.08	12.28	12.18	1 on 3
82D	C	n	Silty very fine sand over silt; burrowing through aRPD; voids at depth	2	16.08	17.79	16.93	1 on 3
82D	D	n	Silty very fine sand over silt; evidence of burrowing at depth - alternating transport/depositional banding evident at all 3 reps from location.	0	-	-	-	1 on 3

APPENDIX B

Navigation Log File

Station	Raw_Depth_ft	Predicted_Tide_ft	Depth_MLLW_ft	Easting	Northing	Long	Lat
16A	12.4	1.6	10.8	7615070.63	720398.39	-122.7946389	45.61978356
16A	12	0.5	11.5	7615158.25	720391.78	-122.7942958	45.61977226
16B	24.4	1.5	22.9	7615583.67	720490.33	-122.7926447	45.62007555
16B	21.5	0.5	21	7615580.1	720490.6	-122.7926587	45.62007601
16E	40.2	1.2	39	7616781.69	720734.95	-122.7879914	45.62083931
17A	14.8	0.9	13.9	7615023.89	719658.19	-122.7947393	45.61775067
18C	45.7	0.7	45	7616057.6	719217.1	122.790652	45.616622
19A	3.5	0.7	2.8	7615574.32	718413.61	-122.792451	45.61438151
20D	30.9	0.6	30.3	7617332.92	718102.25	-122.7855467	45.61366455
21D	49.9	0.6	49.3	7617473.62	717451.66	-122.7849252	45.61189187
22C	55	1.5	53.5	7617385.46	716772.05	-122.7851944	45.61002187
22D	19.9	1.5	18.4	7617936.1	716872.31	-122.7830546	45.61033943
22F	37.7	1.3	36.4	7619065.83	717101.55	-122.778667	45.61105535
23A	11.6	1.8	9.8	7616655.68	715913.82	-122.7879501	45.60761239
23B	39	1.9	37.1	7616744.86	715945.47	-122.7876053	45.60770609
23E	14	2.1	11.9	7618187.1	716353.38	-122.7820169	45.60893622
24D	58.8	2.2	56.6	7617804.01	715670.06	-122.7834378	45.60703321
25A	39.1	2.3	36.8	7617220.31	714677.57	-122.785608	45.60426703
25C	53.1	2.3	50.8	7618481.65	715245.97	-122.7807442	45.60592305
25D	12.1	2.3	9.8	7618635.89	715310.99	-122.780149	45.60611325
26A	6.8	2.3	4.5	7617420.32	714055.89	-122.7847582	45.6025782
26B	22	2.3	19.7	7617476.17	714100.5	-122.784545	45.60270483
26C	50.5	2.3	48.2	7617794.3	714237.8	122.783318	45.603106
26E	42.6	2.3	40.3	7618782.01	714699.63	-122.7795109	45.6044485
27A	9.4	2.3	7.1	7617711.32	713481.66	-122.7835582	45.6010265
27B	30.8	2.3	28.5	7617771.39	713510.02	-122.7833267	45.6011089
27C	66.7	2.3	64.4	7618335.6	713769	122.781152	45.601862
27D	74.6	1.3	73.3	7618730.86	713935.79	-122.7796264	45.60235046
27E	36.1	2.2	33.9	7618990.33	714051.24	-122.7786258	45.60268704
27H	40.3	1.1	39.2	7619707.8	714605.96	-122.7758846	45.60426327
28A	12.5	0.9	11.6	7617934.3	713038.4	122.782638	45.599829
28B	36.3	1	35.3	7618113.8	712941.44	-122.7819267	45.59957666
28C	60.5	1	59.5	7618370.48	713075.34	-122.780939	45.59996363
28E	45	1	44	7619357.4	713523.6	122.777134	45.601269
29A	12.8	0.9	11.9	7618291.68	712275.04	-122.7811585	45.59776349
29B	20.9	0.9	20	7618349.5	712292.6	122.780935	45.597816

Appendix B

Station	Raw_Depth_ft	Predicted_Tide_ft	Depth_MLLW_ft	Easting	Northing	Long	Lat
29D	59	0.8	58.2	7619408.3	712929.4	122.77687	45.599644
29F	43.5	0.7	42.8	7619827.2	713180.3	122.775262	45.600634
30C	52.8	0.7	52.1	7619026.3	711931.2	122.778252	45.596878
31A	33.9	0.6	33.3	7618973.55	711148.81	-122.7783715	45.59472867
31B	41.9	0.7	41.2	7619028.15	711171.58	-122.7781608	45.59479531
31C	51.6	0.7	50.9	7619285.49	711336.76	-122.7771741	45.59526805
31D	73.8	0.7	73.1	7619772.4	711626	122.775304	45.596099
31E	44.9	0.7	44.2	7620128.91	711831.57	-122.7739348	45.59668973
32A	30.1	1	29.1	7619177.3	710751.34	-122.7775321	45.59365475
32B	83	0.9	82.1	7619857.6	710935.1	122.774896	45.594211
32C	43.1	0.8	42.3	7620308.6	711299.7	122.773174	45.595245
32D	25.2	0.8	24.4	7620436.5	711392.3	122.772686	45.595509
33A	16.4	1.1	15.3	7619693.63	709994.65	-122.7754326	45.59162015
33B	43.5	1.2	42.3	7619793.64	710057.18	-122.7750489	45.59179931
33C	57.6	1.2	56.4	7620159.06	710337.68	-122.7736528	45.59259652
33D	52.6	1.4	51.2	7620645.87	710713.87	-122.7717932	45.59366541
34A	17.6	1.8	15.8	7620111.62	709467.25	-122.7737424	45.59020654
34B	53	1.7	51.3	7620410.5	709700.7	122.772601	45.59087
34C	58.9	1.6	57.3	7620756.08	709949.89	-122.7712789	45.59157943
34D	19.1	1.5	17.6	7621107.61	710217.33	-122.7699356	45.59233972
35A	25.8	1.9	23.9	7620499.66	708970.6	-122.7721726	45.5888749
35B	42.9	2.1	40.8	7620544.18	709006.43	-122.7720027	45.58897656
35C	59.2	2.2	57	7620939.12	709314.66	-122.7704944	45.58985203
35D	47.4	2.2	45.2	7621305.5	709601	122.769095	45.590665
36A	39.5	2.4	37.1	7620974.85	708516.5	-122.7702673	45.5876666
36B	54.5	2.4	52.1	7621202.37	708696.8	-122.7693987	45.58817842
36C	63	2.4	60.6	7621525.15	708939.91	-122.768165	45.58886978
36D	11.2	2.4	8.8	7621762.56	709138.82	-122.7672598	45.58943337
37A	14.9	2.4	12.5	7621346.5	707920.9	122.768751	45.586062
37B	51.9	2.4	49.5	7621448.55	708017.29	-122.7683629	45.58633448
37C	52.5	2.4	50.1	7621786.98	708296.48	-122.7670721	45.58712594
37D	32	1.5	30.5	7622107.53	708537.04	-122.7658469	45.58781011
37E	11.5	1.6	9.9	7622217.12	708550.24	-122.7654204	45.58785472
38A	20.3	1.4	18.9	7621821.37	707439.22	-122.7668439	45.58477837
38C	56.9	1.4	55.5	7622092.36	707717.83	-122.7658164	45.58556304
39B	27.7	1.3	26.4	7622293.6	706890	122.76494	45.583309

Fall 2013 Survey

Station	Raw_Depth_ft	Predicted_Tide_ft	Depth_MLLW_ft	Easting	Northing	Long	Lat
39F	11.6	1.2	10.4	7623085.19	707713.43	-122.7619394	45.58562727
40A	10.3	1	9.3	7622645	706413.8	122.763516	45.58203
40B	25.6	1.1	24.5	7622741.89	706522.59	-122.7631495	45.58233615
40C	53	1.1	51.9	7622857.05	706649.24	-122.7627138	45.58269222
40D	55.3	1.1	54.2	7623147.07	706959.05	-122.7616153	45.58356385
40E	33.7	1.1	32.6	7623472.5	707301.8	122.760382	45.584527
41A	9.3	1	8.3	7623352.97	706033.79	-122.7607103	45.581043
42A	8.4	1.8	6.6	7623930.59	705694.87	-122.7584182	45.58015813
42B	46.7	1.8	44.9	7623933.71	705768.76	-122.758414	45.58036095
43A	8.6	0.8	7.8	7624450.45	705340.88	-122.7563499	45.57922748
43B	38.6	0.8	37.8	7624484.27	705441.22	-122.7562289	45.57950516
44B	57.7	0.7	52	7625180.8	705238.3	122.753487	45.579002
45A	7.8	0.8	7	7625583.21	704691.66	-122.7518569	45.57753427
46C	48.8	1.2	47.6	7626259	704547.64	-122.749203	45.57719106
47A	20.6	1.5	19.1	7626528.51	703888.87	-122.7480793	45.57540556
48C	50.6	2.3	48.3	7627192	703680.5	122.745464	45.574885
49A	9.8	2.4	7.4	7627378.9	702931.8	122.744656	45.572846
50A	15.4	1.4	14	7627889.02	702501.24	-122.7426177	45.57170496
51C	47.7	1.3	46.4	7628559.78	702219.78	-122.7399689	45.57098434
51F	16.9	1.3	15.6	7629588.51	703257.12	-122.7360653	45.57390644
52A	14.2	1.1	13.1	7628734.09	701495.24	-122.73921	45.56901121
52B	22.4	1.1	21.3	7628758.91	701518.27	-122.7391156	45.56907623
53E	25.7	1	24.7	7630400.17	702262.8	-122.7327895	45.57124199
54B	32.9	0.8	32.1	7629501.29	700391.88	-122.7360961	45.56604452
55B	45.9	1.2	44.7	7630308.11	700283.87	-122.7329353	45.5658096
56A	12.4	0.8	11.6	763434.3	699457.6	122.732354	45.563554
56C	56.8	0.8	56	7631099.93	700198.35	-122.7298355	45.56563511
56F	24.6	0.8	23.8	7632733.11	701862.35	-122.7236397	45.57032056
57D	55.5	1	54.5	7632237.37	700418.53	-122.7254195	45.56632476
57F	39.7	1.1	38.6	7633043.89	701279.51	-122.722364	45.5687461
58D	53.2	1	52.2	7632370.2	699607.6	122.724814	45.564111
59B	20.5	1.5	19	7631674.76	697914.95	-122.7273461	45.55941842
59E	46.9	1.8	45.1	7633009.75	699346.83	-122.7222897	45.56344489
59F	40.1	1.1	39	7634253.1	700638	122.717575	45.567078
60D	45.2	1.9	43.3	7633504.01	698873.15	-122.7203098	45.56218351
61A	25.9	2.2	23.7	7632781.5	697212.9	122.722951	45.557577

Station	Raw_Depth_ft	Predicted_Tide_ft	Depth_MLLW_ft	Easting	Northing	Long	Lat
61E	42.5	1.2	41.3	7635313.9	699741.5	122.713339	45.5647
62C	60.9	2	58.9	7634164.6	697701.8	122.717606	45.559022
63D	25.9	2	23.9	7635083.39	697667.04	-122.7140165	45.55899568
63E	28	1.2	26.8	7636168.24	699077.92	-122.7099333	45.56294523
64A	33.4	1.3	32.1	7634704.34	696103.26	-122.7153284	45.5546799
64E	21	1.2	19.8	7636770.4	699102.4	122.707585	45.563057
65C	53.7	1.9	51.8	7635747.05	696629.02	-122.7113155	45.55619967
67A	27.9	1.8	26.1	7636367	695131.4	122.708736	45.55214
67C	44.4	1.7	42.7	7636598.86	695510.96	-122.707872	45.55319826
67C	42.1	1.4	40.7	7636613.24	695512.17	-122.707816	45.55320265
68E	11	1.7	9.3	7637668.58	696036.23	-122.7037535	45.55471845
69C	59.2	1.2	57.8	7637284.3	695388.4	122.705184	45.552914
70A	45.7	1.1	44.6	7638623.87	693834.53	-122.6997915	45.54875359
70A	44.4	1.5	42.9	7638625.56	693827.15	-122.6997842	45.54873348
73B	34.4	1	33.4	7641216.69	690865.63	-122.6893602	45.54080706
73B	34.5	1.6	32.9	7641204.27	690868.12	-122.6894089	45.54081296
74A	30.8	0.9	29.9	7642102.47	689888.8	-122.6858012	45.5381947
75D	46.9	1	45.9	7643700.46	689622.01	-122.6795388	45.53758164
75E	26	1.1	24.9	7643768.02	689665.58	-122.6792798	45.53770609
77A	42.3	2	40.3	7644848	687154.9	122.674803	45.530903
77B	53.3	2	51.3	7644886.7	687194.3	122.674656	45.531013
78A	16.2	2	14.2	7645662.8	686071.9	122.671511	45.527993
78D	51.4	2	49.4	7646173.24	686428.74	-122.6695571	45.52900926
79D	20.3	2	18.3	7647060.6	685395.88	-122.6659877	45.52624278
81A	38	1.7	36.3	7645765.05	682709.58	-122.6707595	45.51878243
82C	30.9	1.7	29.2	7646254.9	6811236.3	122.668695	45.514779
82D	8.3	1.7	6.6	7646298	681213.2	122.668524	45.514719